Doc: IEEE 802.4L/88-07

C. A. Rypinski
130 Stewart Drive
Tiburon, CA 94920

Documents
CCIR Study Groups
Period 1986-1990

Document US 8/13-3 Rev. 1
27 January 1987
Original: English

Subject: Input to Document IWP 8/13-27, Rev. 3, Draft Report

United States of America

THE PORTABLE RADIO PROPAGATION ENVIRONMENT

PHIL PORTER, BELLCORE

In Section 3.6 of Draft Report IWP 8/13 Rev. 2, contributions were solicited from administrations on propagation information relevant to future land mobile telecommunications systems. This document summarizes recently available propagation measurements made in and around houses and buildings and proposes models for several characteristics of such radio channels. Future low-power portable radio communications systems may operate in this environment. Further information is needed concerning propagation in this environment, particularly related to delay-spread characterization--experimental data, analysis, and simulation.

Fundamental limitations on portable radio system parameters and on the application of radio link techniques result from the effects of radio propagation within and around houses and buildings. This is a very complex and difficult radio propagation environment because the shortest direct path between any pair of fixed and portable set locations is usually blocked by walls, ceilings or other objects. Often many attenuated propagation paths exist between any pair of locations. The different propagation paths are produced by reflections from walls, ceilings and objects. Each path may have a different time delay and a different attenuation. The overall result is a complex and widely varying multipath transmission channel between fixed radio terminals (henceforth called ports) and portable sets. Because of the complexity and variability, analytical determination of many of the multiple-path propagation parameters is not feasible. It is usually necessary to resort to measurements and to empirically determine statistical distributions of many of the parameters for different locations of ports and portable sets.

Radio transmission over a port-to-portable radio link is reciprocal. That is, the locations of signal transmission and of signal reception can be interchanged without changing the received signal characteristics. This location interchange does not include the interchange of the antennas and requires some specific conditions on antenna, receiver and transmitter impedances. It is sufficient (but not necessary) that these impedances all be real and of the same magnitude. Because of reciprocity, the discussion can proceed on the basis of transmission in either direction without loss of generality.

The portable radio environment is qualitatively similar to the mobile (vehicular) radio environment.[1] [2] [3] [4] [5] [6] [7] [8] [9] That is, propagation is dominated by the effects of shadowing and reflections from walls, objects and the ground. Therefore, some of the small-scale multipath propagation characteristics are the same in both environments. However, in the portable environment, antenna heights will be lower, or antennas will be located within buildings, and distances between transmitters and receivers will be shorter than in the mobile environment. These physical differences cause quantitative differences between some of the large-scale portable and mobile propagation parameters discussed in the following sections. Since there have been more mobile radio propagation measurements made, these will be used to extend the portable radio propagation picture where appropriate.

Most portable and mobile radio measurements have been made at frequencies near 1 GHz. These results can be extrapolated with some confidence over a frequency range of at least 2:1; therefore they are applicable over one of the identified ranges of potential portable communications frequencies.

I. Multipath Time Delay Structure

The multipath time delay structure, i.e., the "echo pattern," of portable radio transmission channels can be measured by transmitting wide-band pulse-like signals between potential port and portable locations. Figure 1 illustrates measurements made at 850 MHz with a 0.025 μ sec. time resolution. The measurements were made between locations within a large building.[10] [11] [12] The graphs show the relative average power received as a function of propagation time delay. A measure of the widths of such averaged power delay profiles or power impulse responses is needed in order to determine limits on the digital transmission rates possible over such radio channels.[1] [2] The zero references for the decibel power level and the time delay scales on the figures are arbitrary.

A. Small Scale Signal Variations

The power level at a particular delay in Figure 1a represents the average of the power level received at that delay for eight different receiver locations within a 4 foot square area.[10] The power values that were averaged were in power units (watts), not in dB. The transmitter location was fixed. The power level at a particular delay fluctuates from receiver location to receiver location within a small area and with motion of people in the aisles of the building. An example of these fluctuating power levels is seen in Figure 2. The figure shows the eight individual measurements of power level versus delay used to perform the averaging operation described above to produce the results of Figure 1a. These fluctuating power levels are indicative of the existence of propagation paths with time delays that differ by less than the resolution of the measurement.[2] [3] For example, the measurement resolution of .025 μ seconds corresponds to a path distance resolution of 25 feet. Many of the walls of rooms and aisles in the building are separated by 5 to 10 feet, much less than the 25 foot resolution. The signals received over unresolved paths have phases that vary many degrees with receiver location changes on the order of an inch, since the wavelength is only 14 inches. These phase changes cause the unresolved multipath signals to add in phase at some locations and out of phase at others, producing the observed fluctuations. The unresolved-path signal fluctuations are similar to the fluctuations of a single-frequency signal illustrated in a later section.

Similar wideband multipath measurements have been made in mobile radio environments.[2] [3] [4] [5] [6] [7] [8] [9] Unresolved-path signal fluctuations are shown in references 2 and 3. The multiplicity of unresolved paths at specific delays was illustrated by simultaneously resolving the paths in delay and in Doppler frequency shift caused by vehicle motion. The Doppler frequency shift of each path is related to its angle of arrival at the receiver location.[2] [3] [7] Reflections from room and hallway walls within buildings are expected to produce wide angle-of-arrival distributions similar to the wide distributions observed from reflections from building walls along streets.

The unresolved paths within a resolved profile peak in Figure 1a probably result from reflections from walls and other objects near the transmitter or the receiver. Angles to these nearby reflectors are distributed throughout 360°. The individual peaks probably result from the attenuated direct path and from walls defining large open areas or located at the ends of hallways. Signals arriving over the longer delayed paths all experience close-in reflections similar to those arriving over the shorter paths. For example, if the receiver is within a room, the unresolved paths probably result from reflections from the room walls and from objects within the room. Signals entering the room after being reflected from a faraway wall (i.e., delayed several tenths of a μ sec.) are still subjected to close-in reflections within the room.

Averaging out the signal fluctuations caused by the phase changes of the unresolved shorter paths yields a picture of the magnitudes of the reflections at various delays. Nearly the same power average results from any set of measurements taken within the same small area. This occurs because the magnitudes of the dominant reflections at the longer delays do not change significantly for small changes in receiver (or transmitter) location of a few wavelengths, that is, for motion over small-scale distances.

The average received power within a small area is the integral of a power delay profile with proper calibration of the power density scale. That is, average power received, $\overline{P_e}$, is

$$\overline{P_e} = K\int_0^\infty P(\tau)d\tau \qquad (1)$$

where $P(\tau)$ is the power delay profile scaled in power units (watts), τ is time delay and K is the overall power scaling factor for the profile.

The time-varying multipath transmission channel represented by a power delay profile (power impulse response) has been called a G[illegible] channel.[14] [15] [2] [3] [4] [5] [6] The word "Gaussian" (G) refers to a Gaussian random process[1] for describing the fluctuations of the unresolved path signals at each delay. A Gaussian process has an envelope that is Rayleigh distributed. It was shown for mobile radio multipath propagation that the envelope fluctuations at a particular delay can usually be approximated well by a Rayleigh distribution.[2] [3] The sum of a large number of signals with random amplitudes and uniformly distributed random phases approximates a Gaussian process. By the central limit theorem,[16] the approximation continues to improve as the number of signals increases. The portable radio multipath channel is similar to the mobile radio channel since both have a large number of unresolved paths resulting in a large number of random signals at each delay. Therefore, the fluctuations at each delay for portable radio channels are also expected to be well approximated by Gaussian random processes.

The term "wide sense stationary" (WSS) refers to the average or means being the same, i.e., statistically stationary, for different collections of samples taken from the same area. The random phase addition process for motions over small-scale distances results in an approximately stationary power average at each delay. Again, in the similar mobile radio environment, it was shown that the power averages were approximately wide sense stationary[2] [3] over small-scale distances.

The term "uncorrelated scattering" (US) refers to the correlation between signal fluctuations at different delays. The uncorrelated property results if the Doppler spectrum is different for different delays, i.e., if the angle-of-arrival spectrum is different. Different Doppler spectra at different delays were also shown for mobile radio channels[2] [3] [7] and again can be expected for the portable radio environment.

The averaged power delay profiles, $P(\tau)$, are then the quantities needed to describe the GWSSUS channels for conditions that are appropriate to digital portable radio multipath channels.[13] [14] [15] [17] These conditions are that 1) the width of the signaling pulses transmitted over the channel is much greater than the delay spread defined later, and 2) the pulse transmission rate (i.e., the baud rate) is much greater than the variation rate of the small scale signal fluctuations (i.e., the Doppler spectrum width). If these conditions are not satisfied, low error rate transmission is not generally possible over the channel. When the conditions are met, the power delay profile is then

$$P(\tau) = \langle |h(\tau)|^2 \rangle = \langle |p(\tau) * g(\tau)| \rangle \qquad (2)$$

where the brackets $\langle\ \rangle$ indicate averaging over an ensemble of small-scale locations, the $*$ indicates convolution, the $h(\tau)$ are samples of complex bandlimited bandpass impulse responses of the random multipath medium, the $g(\tau)$ are samples of the complex bandpass impulse responses of the medium without bandlimiting, and $p(\tau)$ is a function representing the bandlimiting by the equivalent pulse of the wideband signal used to probe the propagation medium.[6] [18] If the width of $p(\tau)$ is much less than the spread of $P(\tau)$, as in Figure 1, the bandlimiting effect of $p(\tau)$ is insignificant.

The error rates for digital transmission through multipath channels, and particularly GWSSUS channels, are most strongly dependent on the delay spread or width of the power delay profile defined as the square root of the second central moment.[13] [14] [15] [17] That is

$$\text{delay spread} = \left[\frac{\int_0^\infty (\tau - D)^2 P(\tau)\, d\tau}{\int_0^\infty P(\tau)\, d\tau} \right]^{\frac{1}{2}} \tag{3}$$

where the average delay D is

$$D = \frac{\int_0^\infty (\tau)\, p(\tau)\, d\tau}{\int_0^\infty P(\tau)\, d\tau} . \tag{4}$$

The delay spread for Figure 1a is about 0.25 μ second.[10] As an example, a non-equalized channel transmitting binary biphase modulation with raised cosine pulses and differential detection (i.e., DPSK) would have an irreducible bit error rate[1] of 10^{-3} for a bit rate of about 300 kilobits/second and the 0.25 μ second delay spread of Figure 1a. The irreducible error rate is the error rate that occurs at high signal-to-noise ratios for which the noise contribution to errors is negligible. The error rate depends somewhat on the shape of the power-delay profile; however, the effect of profile shape is much less than the statistical uncertainty of the knowledge of the delay spread statistics that exists because of the limited number of measurements that are available. Also, different types of digital modulation and different pulse shapings have different susceptibilities to delay spread. Further analysis, computer simulation and laboratory experiments are needed to assess the susceptibilities of the different modulations that are appropriate candidates for portable radio systems.[19] [20]

B. Large-Scale Signal Variations

Moving the receiver (or transmitter) to a different room (or a different street or building) results in different dominant reflecting surfaces at longer delays and in different attenuations of shorter, nearly direct, paths. Therefore, averaged power-delay profiles from different rooms, etc., are qualitatively and quantitatively quite different. Since the reflection magnitudes and the number of reflectors are different, the total average received power is differe in different locations also.

The averaged power delay profile in Figure 1b was measured in a different location from the one in Figure 1a. Comparison of the two figures graphically illustrates the gross differences between profiles measured for different transmitter-receiver locations. The relative power scales (the power levels representing 0 dB) are also different by many dB for Figures 1a and b.

The large differences between power-delay profiles show that the multipath propagation process is only approximately statistically stationary (quasi-stationary) over small areas and is highly non-stationary over large distances, from room to room, from building to building, etc.

Since the single parameter, delay spread, dominates irreducible radio link error rate, two-step modeling of the multipath channels is appropriate.[2] [8] Small areas can be modeled as GWSSUS channels and their power-delay profiles and delay spreads determined. Then distributions of delay spread can be used to determine the highest bit rate providing the desired error performance over a specified fraction of the overall portable radio environment.

Examples of such distributions of delay spread measured at 850 MHz are shown in Figures 3 through 5. Figure 3 shows the cumulative distributions of time delay spread measured in

two office buildings differing in linear dimensions by more than a factor of three.[12] The solid curve (1) shows the delay distribution measured within the larger building, while the dotted curve (2) shows the distribution measured within the smaller building. The distributions are similar, and the worst-case time delays observed for the larger (250 nanoseconds) and smaller (220 nanoseconds) are nearly identical. This could be caused by reflections from a hill immediately behind the smaller building.

Figure 4 shows the cumulative distribution of delay spread (solid curve 1) measured at the smaller office building over paths from locations within the building to simulated port locations within a few hundred feet outside the building.[11] The dotted curve (2) shows the corresponding distribution measured for similar inside-to-outside paths at a two-story residence on a one-acre flat lot. The distributions are similar, with worst-case delay spreads around 320 nanoseconds.

The presence of a strong direct path between the transmitter and receiver can significantly reduce the time delay spread observed. Figure 5 shows cumulative distributions of delay spread in the large office building of Figure 3, when the receiver was in an aisle and the transmitter was in the same aisle or one of its rooms (one aisle coverage), and in the adjacent aisles and rooms as well (three aisle coverage).[12] The maximum delay spread observed drops to under 100 nanoseconds in the former case. This result has been seen consistently in all similar measurements.

The measurements above and all others from references 10,11, and 12, other similar measurements in houses and other buildings, and the mobile radio measurements in residential areas[3] suggest that bit rates of a few hundred kilobits/second should be usable for ports inside buildings and for outside ports having antenna heights less than 30 feet and ranges to portable sets on the order of 1000 feet.

It should be noted that delay spreads are often several microseconds in mobile radio environments with base station antenna heights of a hundred feet or more and distances between base-stations and mobiles of over a mile. The high base station antennas strongly illuminate reflecting surfaces (walls, hills, etc.) several miles away. Buildings between base stations and mobiles sometimes attenuate shorter, more direct, paths more than paths to the farther-away reflectors. Thus, the far-out paths cause propagation delays of many microseconds and can be significant in overall received power delay profiles for such mobile radio channels. The lower antenna heights for ports result in greatly reduced illumination of faraway reflecting surfaces because intervening attenuating objects (buildings, hills, etc.) are more likely to exist. Also, shorter port-to-portable distances decrease the attenuation of more direct and shorter reflection paths and increase the relative attenuation to faraway reflectors. These effects produce the significantly lower delay spread values observed in the portable radio environment as compared to the mobile radio environment.

In summary, the small-scale multipath time-delay characteristics that depend largely on wavelength and uniform angle-to-arrival distributions are similar for portable and mobile radio environments. These small-scale characteristics include the characteristics of the signal fluctuations at specific delays that are consistent with the GWSSUS channel description and were discussed in the previous section. In contrast, the large-scale multipath parameters that depend on the gross structure (locations and magnitudes) of reflecting surfaces are significantly different for portable and mobile radio environments. These large-scale characteristics include average power, delay spread and higher order central moments of the averaged power-delay profiles that represent different GWSSUS channels.

II. Narrowband Propagation Characteristics

The time-delay structure and delay spread described in the previous section limit the transmission rate and thus the bandwidth of signals transmitted over the multipath channels. Once the signal bandwidth is restricted to being much less than 1/(delay spread), i.e., pulse width >> delay spread, then narrowband signal descriptions and statistics become of greater interest. The signal bandwidth limitation essentially requires negligible change in the channel transfer function

with frequency throughout the bandwidth of the signal. That is, the multipath signal variation or fading becomes nearly flat over the signal bandwidth. The transfer function is, of course, the Fourier transform of the bandpass impulse response, $g(\tau)$, discussed in Section I.A. For the conditions that the width of $p(\tau)$ is much less than the delay spread, the measured $h(\tau) = g(\tau) * p(\tau) \approx g(\tau)$, and the transfer function is approximately the Fourier transform of $h(\tau)$.[6] [18]

The narrowband signal statistics appropriate to flat fading narrowband channels then can be determined from single-frequency transmission measurements.

A. Small-Scale Multipath Effects

Narrowband signals transmitted between portable sets and ports either inside or outside buildings experience large amplitude and phase variations as the portable sets move over small-scale distances on the order of a wavelength. These variations are a result of the random phase additions of the signals arriving over many paths. The paths include the resolved and unresolved paths illustrated and discussed in previous sections. The narrowband signal variations are caused by the same random phase mechanism as the variation at specific delays caused by unresolved paths.

An example of measurements of the envelope of single frequency small-scale variations is shown in Figure 6. The signal level recording was made at 900 MHz by moving a small antenna a distance of 4 feet within a building.[21] The transmitting and receiving antennas were copolarized, i.e., oriented with like polarization. A Rayleigh distribution is usually a good approximation for the statistics of the envelope of multipath signal variations.[1] [21] [22] [23] Figure 7 shows cumulative signal envelope distributions measured at 815 MHz for several small areas (4 feet square) within and outside a house.[22] Signal envelopes measured in small areas that have walls blocking the direct path between transmitter and receiver are approximately Rayleigh distributed. The envelope distribution from the outside area departs significantly from Rayleigh because of a strong direct path. The areas with stronger direct paths experience higher signal levels than those that have well-blocked direct paths. The low-signal areas dominated by multipath are those of most concern in determining portable radio system coverage and performance. Therefore, departures from Rayleigh for large-signal areas will not affect the accuracy of the Rayleigh model for most system analysis applications.

The multipath signals received in the low signal areas can be modeled[1] [24] as

$$y_c(z, t) = L(z)\, R(z, t) e^{j\omega t + j\phi(z,t)} \tag{5}$$

where $y_c(z, t)$ is the copolarized received signal, $\omega = 2\pi f$ with f the carrier frequency, t is time and the antenna is assumed to be moving in translation in the z direction. The amplitude function or envelope $R(z, t)$ is Rayleigh distributed with a stationary mean (or median) of unity within a small-scale area[1] [21] [22] [24] [23] where the power delay profile is stationary as discussed earlier. The Rayleigh probability density function, $p(r)$, is given[1] [25] by

$$p(r) = \frac{r}{N} e^{-r^2/2N} \tag{6}$$

where the median is $1.1774\sqrt{N}$ and the mean is $\sqrt{\frac{\pi N}{2}} \approx 1.25\sqrt{N}$. In (5), the phase, $\phi(z, t)$, is a resultant from a number of paths that are many wavelengths long, as in mobile radio. Therefore, it is reasonable to expect any value of $\phi(z, t)$ to be equally likely,[1] i.e., $\phi(z, t)$ is uniformly distributed from 0 to 2π. Often $\phi(z, t)$ experiences nearly π abrupt changes as the signal envelope goes through nulls. The t variation in ϕ and R result from motion of objects in the propagation paths, i.e., trees blowing in the wind, doors opening, people moving, and occurs with non-moving antennas. The z variation results from antenna motion and can be replaced in (5) by $z = vt$, where v is the antenna velocity. In most portable radio environments, the time variation resulting from motion of antennas is significantly greater than that resulting from motion of objects. Together, $R(z)\, e^{j\phi(z)}$ with $z = vt$ represents a complex Gaussian random process. That is,

$R(t)\, e^{j\phi(t)}\, e^{j\omega t} = x(t) \cos \omega t + jy(t) \sin \omega t$ and $x(t)$ and $y(t)$ are independent and Gaussian distributed. The variable $L(z)$ in (5) represents the large-scale signal level variation discussed earlier, i.e., the variation from room to room, house to house, inside to outside, over large-scale distances. Large-scale variations are discussed in a following section.

1. Spatial Correlation and Space Diversity

From Figure 6 it is evident that two antennas separated by a few inches, i.e., a fraction of a wavelength at 900 MHz, would not likely be in a deep signal null simultaneously. This lack of correlation of signal levels for spatially separated antennas is the basis of space diversity used to mitigate small-scale multipath signal variations.[1] [25]

Space diversity and diversity combining for the mobile radio environment and for other multipath environments for systems with fixed antenna orientations have been extensively studied.[1] [25] The diversity performance for fixed antenna orientations depends a) on the method used to combine the signals from two or more antennas, i.e., selection of the best signal or cophasing of signals from constant gain or variable gain receivers[1] [25] , and b) on the spatial correlation of the signal envelope variations for the different antennas. The spatial correlation $\rho(\Delta z)$, for the small scale Rayleigh distributed envelope variations is given by

$$\rho(\Delta z) = \overline{R(z, t)\, R(z+\Delta z, t)} \qquad (7)$$

where Δz is the antenna separation and the overbar indicates an average. For mobile radio environments with the angle of arrival of multipath signals uniformly distributed over 0 to 2π, the correlation is small for antenna separations on the order of $\lambda/4$ or greater.[1] [26] As discussed earlier, the angle-of-arrival distribution for multipath in the portable radio environment is expected to be similar to the distribution in the mobile radio environment. However, handheld portable radio equipment will not have a fixed antenna orientation. Therefore, portable radio diversity will be considered again with respect to both spatial signal variations and antenna angular variations in a later section.

2. Frequency Effects

The small-scale multipath effects result from phase addition of signals arriving over many paths distributed randomly in angle of arrival. The phases associated with the various paths are functions of carrier frequency, f, and path lengths.[1] Thus, the distance scale of the signal variation pattern in space represented by Figure 6 is a linear function of frequency. The null spacing is on the order of half wavelength, $\lambda/2$. The correlation function , $\rho(\cdot)$, in (7) is invariant when normalized to wavelength[1] over at least a 10 to 1 frequency range. That is, $\rho(\Delta z/\lambda)$ is invariant with frequency. The envelope variations remain Rayleigh distributed at any frequency as long as the physical environment produces severe multipath propagation that includes many propagation paths.

B. Large-Scale Variations

The mean or median of the small-scale Rayleigh-distributed multipath variations is approximately statistically stationary within small-scale areas.[22] That is, the multipath variations are stationary within areas where the overall multipath structure remains relatively constant and therefore the average power-delay profile is stationary. When the overall multipath structure is different, i.e., there are different reflection coefficients and/or different numbers of paths, the average power is different as represented by the average of the multipath variations. This narrowband average is the same as the area under the average power-delay profile (1). This is accounted for in (5) by normalizing to unity either the mean or median of the Rayleigh distributed variation, $R(\cdot)$ and representing the large-scale variation by $L(z)$.

1. Distance Dependence

Figure 8 is a scatter plot of median 815 MHz signal levels for many small scale areas [24] Each data point represents a value of $L(z)$ relative to its value for a free space path length of 24.2

feet. The vertical scale on the figure is distance, z, between port locations and small areas within which there is small-scale portable set motion. The data points are from several different port locations and several different small areas inside and around 8 houses in relatively flat terrain. The small areas were 4 feet square and include locations on first and second floors, in basements, and outside close to the houses. The port antenna height was 27 feet above ground. The dotted line represents equivalent free space propagation, $(1/z^2)$, between port and portable locations. The other straight lines are least-square regression lines through the data points indicating a strong dependence on distance in the highly scattered data. For all the data, the regression line slope is $z^{-4.5}$, indicating $L(z)$ proportional to $z^{-4.5}$.

Figure 9 is a scatter plot similar to Figure 8, but of median 815 MHz signal levels measured in a two-story office/laboratory building with a long straight corridor.[27] The circles and squares represent median signal levels measured between locations in corridors and offices or laboratories opening off the corridors. Unfilled circles and squares indicate measurements made with transmitter and receiver on the same floor. The least-square regression line slope for these measurements is $z^{-3.6}$. Filled circles and squares indicate measurements made with transmitter and receiver on adjacent floors. The least-square regression line slope for these measurements is $z^{-3.9}$. The similar slopes suggest a relatively constant isolation between floors. The value of this cross-floor isolation is 26 dB at 150 feet. Measurements in other buildings suggest that this relatively large value may be due to the presence of solid steel concrete pour forms in the floors.

The "X" symbols in Figure 9 indicate median signal levels measured with both transmitter and receiver on the main corridor, within optical line of sight. Except at the extreme ends of the corridor, only 2-4 dB of rapid signal variation was observed, suggesting the presence of a single dominant propagation path. The received signal level is greater than the free-space level over the entire distance span (by up to 11 dB in the 50- to 125-foot distance range), suggesting channeling of energy by the corridor.

An important inference from Figure 9 is that the received signal level can decrease abruptly by 25 dB or more at the transition from the corridor to an adjoining room is made (a distance of 20 feet or less).

Other measurements have been made in the 800 to 900 MHz range between locations (port and portable) entirely within large buildings.[23] [28] The results show similar scatter of measured values about a distance-dependent regression line. Distance dependences ranging from about z^{-2} to z^{-6} were observed for typical office and laboratory buildings with values of z^{-4} or z^{-5} appearing to be typical.

2. Statistics of Large-Scale Variation

After removal of the distance dependence from data representing $L(z)$, the remaini variation is approximately normally (Gaussian) distributed in dB, with a mean of 0. This is shown for the Figure 8 data in Figure 10.

These empirical observations suggest modeling $L(z)$ as a log-normally distributed random variable with a mean that varies with distance. That is, define a new random variable $U(z)$ as

$$U(z) = 10 \log_{10} L^2(z) . \tag{8}$$

Then $U(z)$ is Gaussian (normally) distributed with probability density

$$f_U(u) = \frac{1}{\sigma\sqrt{2\pi}} \exp\left[-(u-m)^2/2\sigma^2\right] \tag{9}$$

where the standard deviation, σ, is in dB and the mean, m, in dB varies with distance as

$$m = 10 \log_{10} (z^n) . \tag{10}$$

For example, the residential data from Figures 8 and 10 are represented by $n = -4.5$ and σ between 10 and 11 dB.

The excess rate of change of signal level over the free space rate of z^{-2} is partially accounted for by the reflection from the ground.[22] [24] [29] For propagation between two points separated a distance z and at heights h_r and h_t above flat ground, the power density, P_r at a receiver point relative to the transmitted power density, P_t, at the other point is given by[24] [30]

$$\frac{P_r}{P_t} = \frac{4}{z^2} \sin^2 \left[\frac{2\pi h_r h_t}{\lambda z} \right]. \qquad (11)$$

For large z, ($z >$ 1000 feet for typical port and portable heights), this approaches $P_r/P_t \propto z^{-4}$. Additional variation is probably due to additional attenuation resulting from reflection from and propagation through intervening houses and trees. The additional attenuation may be better represented by a dB/distance, i.e., an e^{-z} or 10^{-z}, variation rather than by a power-law variation, z^n, since the number of attenuating objects (houses, trees, etc.) increases more or less uniformly with distance, however, this has not been experimentally demonstrated. If this is true, the range of distances may be limited over which a given value of n and z^{-n} approximates the distance dependence of $L(z)$.

The description of $L(z)$ as a log-normally-distributed random variable with a distance-dependent mean as in (8-10) is qualitatively the same as the description for mobile radio environments.[1] [31] The magnitude of the distance-dependence exponent appears a little greater and the standard deviation somewhat larger for the measurements in the portable environment. The stronger distance dependence is probably a result of the lower port antenna heights with respect to ground and the deeper immersions of the port antennas within the buildings and trees. The larger standard deviation undoubtedly results from the variability of the additional attenuation through walls into the interiors of houses and buildings.

3. Effect of Antenna Height

The major overall effect of varying the height of either the port or portable antenna in a residential environment occurs because of the proximity of the ground.[29] The height effect is illustrated in equation (11). This remains true for small changes in height that do not result in a major change of the antenna in relation to its surrounding scattering environment; that is, as long as the height changes do not involve transitions through the height of treetops and houses. For typical port and portable heights and distances generally greater than 1000 feet, P_r/P_t in (11) becomes proportional to h^2. That is, P_r/P_t changes by 6 dB for a height change of either port or portable antenna by a factor of 2. Of course, this deterministic ground effect has random variation superimposed because of the effect of the multiple propagation paths.

The effect of antenna height above ground is illustrated in Figure 11. The open 0 and + data points indicate signal medians from measurements in and around 4 houses at 815 MHz.[29] The ordinate of a data point represents the median signal measured in a four-foot-square area for a port location using a 27 foot high port antenna, as in Figure 8. The abscissa of the point represents the median signal measured for the same four-foot-square area and the same port location, but using a 12.5 foot high port antenna. Port to portable distances, z, were greater than 1000 feet. The solid and dashed lines represent equation (11) assuming that the randomness of the signal variations is the same for both antenna heights. The solid data points and the * represent averages of all measurements outside, inside houses on the first floor, and in basements as indicated on the figure. The tight cluster of the data around the lines is consistent with the expectation from ground reflection.

4. Frequency Effects

The frequency dependence of the mean, m, in (10) is made up of several factors. One of the factors for residential areas is the $\sin^2[\frac{2\pi h_r h_t}{\lambda z}]$ term in the power density at a receiver location

caused by reflection from the ground (see 11). Another factor is the proportionality to λ^2 of the effective area, A_e, of a small (on order of $\frac{\lambda}{2}$ or less) dipole[32] or small loop antenna. Received signal power, equivalent to $[y_c(\ )]^2$ of (5), is the product of the power density, P_r, in (11) and A_e of the receiving antenna. For large separations, z, i.e., for $z > 1000$ feet, and for typical port and portable h_r and h_t, the $\sin^2$ term can be replaced by the square of its argument. Then $P_r A_e$ is independent of λ in this large z limit since the λ^2 in A_e cancels the $1/\lambda^2$ in P_r. For residential areas, this leaves only multipath propagation and attenuation through walls for frequency-dependent factors. The ground reflection situation is not clear, however, when both the port and portable antennas are located within a large building.

Available data related to frequency dependence of the mean (or equivalently the median for the Gaussian process) for the portable radio environment are very limited. For mobile radio environments with 600 foot base station antenna heights, Reference 1 indicates that the median large-scale attenuation in urban areas increases weakly with frequency between 100 MHz and 30 GHz. The increase is about 4 dB between 100 MHz and 10 GHz. An increase in average attenuation with frequency is, of course, a decrease in mean signal, m, with frequency. This mobile radio situation is somewhat indicative of the multipath effects outside buildings, at least in an urban environment.

Building penetration attenuation was measured at 860 MHz, 1550 MHz and 2570 MHz for 25 houses in 5 different cities.[33] These measurements suggest a decrease in mean signal, m, of about 2 dB between 860 MHz and 1550 MHz and of about 1 dB from 1550 to 2570 MHz because of the building walls. Of course, in addition to this building attenuation, the frequency-dependence factor for the multipath attenuation between port locations and houses needs to be determined. The mobile radio situation discussed in the previous paragraph is somewhat indicative of the frequency dependence of the multipath environment external to the buildings.

Measurements at 940 MHz and 60 GHz locations within buildings were reported.[34] They were not concurrent measurements and only qualitative comparisons can be made. However, the signal levels were markedly lower at 60 GHz and the authors made coverage estimates for 1 milliwatt transmitters. In a building with metal partition walls, estimated coverage at 940 MHz extended about 2 rooms from a port location in a room i.e., a distance of about 30 feet. For a similar environment, estimated coverage at 60 GHz was only within the same room and the immediately adjacent hallway. In frame buildings with plasterboard walls, estimated 940 MHz coverage was about 100 feet. For similar buildings, 60 GHz coverage extended only to adjacent rooms. These results include all transmission factors between port and portable locations within th buildings.

The cited portable radio measurements and the mobile radio estimates are not direc comparable; however, the available information suggests that the mean in (10) decreas significantly with frequency above 1 GHz for portable radio environments.

Measurements at 57 MHz, 177 MHz and 575 MHz were reported[35] for many locations on rooftops and within large buildings in New York City. Cumulative signal level distributions from these measurements can be used to infer relative average signal levels between areas outside and areas inside the large buildings. The relative levels were about 2 or 3 dB stronger at 575 MHz than at 177 MHz. The levels were about 2 dB stronger at 177 MHz than at 57 MHz.

Measurements at 460 MHz and 890 MHz were reported between outside locations and locations inside a building.[36] The parameter measured was excess attenuation, i.e., the attenuation caused by the building, ground, etc., in addition to the free space, $f^2 r^2$, attenuation. The results for this one building suggest an excess attenuation of 3 or 4 dB greater at 460 MHz than at 890 MHz. This suggests an average signal level of about 2 dB greater at 460 MHz than at 890 MHz when the 5.7 dB for the free space f^2 ratio is included. These measurements are not directly comparable with the building attenuation measurements since they include all path effects.

The frequency dependence of m below 1 GHz is less clear than above 1 GHz. Measurements suggest that m may increase from 1 GHz to 500 MHz but it may start to decrease

with frequency below 500 MHz. As with many of the propagation effects, the frequency dependence of m is probably also a function of the type and construction of buildings. Any overall effect, then, can only be obtained by averaging over many building types and constructions, which will result in a large standard deviation around the average.

5. Correlation and Macroscopic Space Diversity

Portable sets within a region of ports often could be served from more than one port, particularly when located at nearly maximum distance from the nearest ports.[37] The buildings and other obstructions along the paths from a portable set to the different nearest ports are likely to be different. These obstruction differences can be expected to cause different large-scale signal variations for the different paths,[38] that is, the large-scale variations can be expected to be partially uncorrelated. The selection of the port-to-portable path resulting in the best signal could provide diversity to mitigate the large-scale or macroscopic signal variations. The effectiveness of this macroscopic diversity depends on the correlation among the large-scale signal variations for the different ports.

The curves in Figure 12 from Reference 38 show cumulative signal level distributions for measurements of large-scale signal variations made within and around 8 houses.[24] The curves compare 2 branch and 3 branch selection macroscopic diversity with the signal distributions for a single port (i.e. 1 branch). The 2 branch diversity selects the best large-scale signal between pairs of ports; the 3 branch selects the best from sets of 3 ports. The signal levels accumulated are the median levels from four-foot-square areas as described for Figure 8. The subset of data accumulated for Figure 12 has nearly the same 10 dB standard deviation as the overall data set shown in Figures 8 and 10. The dashed theoretical macroscopic diversity curves in Figure 12 assume that the large-scale signal variations can be separated into two parts, l and p. One part of the variation, l, is correlated among the ports while the other part, p, is uncorrelated. For the dashed curves in the figure, the uncorrelated part of the signal variation was assumed to have a standard deviation, σ_p, of 8 dB contributing to the overall standard deviation of $\sigma_T = 10\ dB$. The theoretical model assumed that the l and p signal parts were independent so that the total standard deviation was related to the standard deviations of the parts as

$$\sigma_T^2 = \sigma_p^2 + \sigma_l^2 \qquad (12).$$

The separation of σ_p and σ_l with $\sigma_p = 8$ dB for the dashed curves in Figure 12 provides a reasonable fit to the data in the portion of the distributions near 1%. Other subsets of the available data having differing values of σ_T are also fit well with this model using $\sigma_p = 8$ dB.[38]

C. Crosspolarization Coupling

The reflecting and scattering of radio signals in the multipath propagation environment also couple power from the transmitted polarization into the crossed (orthogonal) polarization. At any receiving point, the power in the crossed polarization also arrives over paths with different time delays and different angles of arrival. The multipath signal received on a crosspolarized antenna, $y_x(z,t)$, can be modeled similarly to the copolarized signal in (5) as

$$y_x(z,t) = X(z)L(z)R_x(z,t)e^{j\omega t + j\phi_x(z,t)} \qquad (13)$$

where the corresponding variables have the same properties as the copolarized signal variables in (5). The subscript x indicates the variable is associated with the crosspolarized signal. $R_x(\ )$ and $\phi_x(\ )$ have the same statistical distributions and normalizations as $R(\ )$ and $\phi(\ )$, but they may have different instantaneous values. The variable $X(z)$ is a slowly varying crosspolarization coupling coefficient[22] [39] with variation on the scale of $L(z)$. That is, $X(z)$ represents the large-scale crosspolarization coupling averaged over the small-scale variations.

Figure 13 is a scatter plot of crosspolarization coupling $X(z)$ as a function of $L(z)$ measured in and around 8 houses.[39] The $L(z)$ scale is the same as that on Figure 8. Each data

point represents $X(z)$ for a 4-foot-square small area. In the region of low signal levels, the crosspolarization couplings are all greater than -6 dB and range up to slightly over 0 dB. Some of the scatter in the data is due to measurement error and statistical uncertainty. Similar measurements in large buildings[39] show even larger values of crosspolarization coupling. Measurements in Tokyo on sidewalks also yielded values in the -5 to -7 dB range.[40]

1. Random Orientation and Antenna Diversity

Changes in the orientation of portable radio antennas could superimpose additional signal variations on the multipath variations.[41] [42] This could occur because of polarization misalignment, if there were little crosspolarization coupling. A well-disciplined user who has great need for portable communications, e.g., a policeman or fireman, might be expected to hold a handset antenna in a fixed orientation; however, such an orientation restriction is not likely to be accepted by a casual general user. A person using a portable communications set can readily change its orientation through any vertical or horizontal angle. Such a wide range of angular variation will result in essentially random orientation of the antenna or antennas. The effects of the random orientation on the signal are mitigated by the crosspolarization coupling in the multipath propagation medium. Antenna diversity can further reduce the orientation effects as well as mitigating the small-scale multipath signal variations.

Cumulative distributions of relative signal-to-noise ratio (S/N) in Figure 14 illustra signal improvements from crosspolarization coupling and diversity. These distributions were obtained by computer simulation[41] [42] assuming that multipath propagation signals arrive at a portable set location in the horizontal plane but uniformly distributed in azimuth angle around the location. The Rayleigh distribution would result from moving a fixed-oriented vertically polarized antenna through a region excited by a vertically polarized fixed antenna (e.g., at a port). The distribution labeled "2 Br Mobile Select" would result from the use of selection diversity, i.e., always selecting the antenna with the strongest signal, between two such fixed oriented antennas separated by $\lambda/4$ and moving in the same multipath region. The diversity improvement results because of the low spatial correlation of the multipath signal variation discussed earlier. The solid, dashed, and dotted distributions would result from the following radio link condition: a) the use of selection diversity between a vertically polarized and a horizontally polarized antenna at a port, b) a single antenna on a randomly oriented portable set and c) cross polarization coupling $X(z)$ in the multipath with the values labeled on the curves. The two distributions to the left of the Rayleigh distribution and labeled 1D or 1L and v or h are for one antenna (a dipole or a loop) on a randomly oriented portable set and either a vertically polarized or a horizontally polarized antenna on a port. Crosspolarization coupling is either -6 dB or 0 dB as labeled. The curves illustrate th following: a) a decrease in the percentage of time spent at low signal levels (large negative S/N values) resulting from selection diversity and from increased crosspolarization coupling and b) an increase in percentage of time spent at low signal levels because of the random orientation.

2. Polarization Diversity

References 41 and 42 and Section C.1 above discuss the improvement in link reliability obtainable from polarization diversity. Reference 39 indicates that crosspolarization coupling is near 0 dB over paths with no line-of-sight component. Later measurements[43] show that signals received on orthogonal polarizations have low instantaneous correlations and may be used as inputs to any form of diversity combiner.[1] [25] Figure 15 is an example of signals received simultaneously at 815 MHz over a non-line-of-sight path within an office building on two orthogonal polarizations. A dual-polarized microstrip patch receiving antenna was used, with identical patterns on both polarizations. The linearly-polarized transmitter was scanned over a 4-foot square to make the measurement. The low correlation and nearly-equal power levels on the two polarizations are evident.

An example of similar measurements over line-of-sight paths down a corridor is shown in Figure 16. Measurements over such paths show less fluctuation and much lower crosspolarization coupling.

Figure 17 is a histogram of the correlation coefficient between polarizations observed in a large number of measurements such as those of Figures 15 and 16. The measurements presented are for paths within office buildings; however, identical results were observed for residential inside-outside paths. Over non-line-of-sight paths, the correlation coefficients observed were always low enough for polarization diversity to provide nearly ideal diversity gain.[1] [25] For paths with a strong line-of-sight component, polarization diversity would provide protection against random handset orientation.[41]

REFERENCES

1. W. C. Jakes, ed., "Microwave Mobile Communications," New York, John Wiley, 1974.
2. D. C. Cox, "910 MHz Urban Mobile Radio Propagation: Multipath Characteristics in New York City," IEEE Trans. on Comm., COM-21, November 1973, pp. 1188-1194.
3. D. C. Cox, "Delay-Doppler Characteristics of Multipath Propagation at 910 MHz in a Suburban Mobile Radio Environment," IEEE Trans. on Ant. and Prop., AP-20, September 1972, pp. 625-635.
4. W. R. Young, Jr., and L. Y. Lacy, "Echoes in Transmission at 450 Megacycles from Land-to-Car Radio Units," Proc. IRE, Vol. 38, March 1950, pp. 225-258.
5. G. L. Turin, F. D. Clapp, T. L. Johnson, S. B. Fine, and D. Lavy, "A Statistical Model of Urban Multipath Propagation," IEEE Trans. Veh. Tech., VT-21, February 1972, pp. 1-9.
6. D. C. Cox, "Time and Frequency Domain Characterizations of Multipath Propagation at 910 MHz in a Suburban Mobile Radio Environment,' Radio Science, Vol. 7, No. 12, December 1972, pp. 1069-1077.
7. D. C. Cox, "A Measured Delay-Doppler Scattering Function for Multipath Propagation at 91[illegible] MHz in an Urban Mobile Radio Environment,' Proceedings of the IEEE, Vol. 61, April 1973, pp. 479-480.
8. D. C. Cox, R. P. Leck, "Distributions of Multipath Delay Spread and Average Excess Delay for 910 MHz Urban Mobile Radio Paths," IEEE Trans. on Ant. and Prop., AP-23, March 1975, pp. 206-213.
9. D. C. Cox, "Multipath Delay Spread and Path Loss Correlation for 910 MHz Urban Mobile Radio Propagation,' IEEE Trans. on Veh. Tech., Special Issue on Propagation, VT-26, November 1977, pp. 340-344.
10. D. M. J. Devasirvatham, "Time Delay Spread Measurements of Wideband Radio Signals Within a Building," Electronics Letters, Vol. 20, November 8, 1984, pp. 950-951.
11. D. M. J. Devasirvatham, "Time Delay Spread and Signal Level Measurements of 850 MHz Radio Waves in Building Environments," IEEE Trans Ant. and Prop., vol. AP-34, November 1986, pp. 1300-1305.
12. D. M. J. Devasirvatham, "A Comparison of Time Delay Spread and Signal Level Measurement Within Two Dissimilar Office Buildings,' IEEE Trans. Ant. and Prop., to be published 1987.
13. P. A. Bello, "Characterization of Randomly Time-Variant Linear Channels,' IEEE Tran Commun. Syst., CS-11, December 1963, pp. 360-393.
14. P. A. Bello and B. D. Nelin, "The Effect of Frequency Selective Fading on the Binary Error Probabilities of Incoherent and Differentially Coherent Matched Filter Receivers," IEEE Trans. Commun. Systems, CS-11, June 1963, pp. 170-186.
15. P. A. Bello and B. D. Nelin, "The Effect of Frequency Selective Fading on Intermodulation Distortion and Subcarrier Phase Stability in Frequency Modulation Systems," IEEE Trans. Commun Systems, March 1964, pp. 87-101.
16. A. Papoulis, "Probability, Random Variables and Stochastic Processes," McGraw Hill, New York, 1965.
17. C. C. Bailey and J. C. Lindenlaub, "Further Results Concerning the Effect of Frequency Selective Fading on Differentially Coherent Matched Filter Receivers," IEEE Trans. Comm. Tech., COM-16, October 1968, pp. 749-751.

18. D. C. Cox and R. P. Leck, "Correlation Bandwidth and Delay Spread Multipath Propagation Statistics for 910 MHz Urban Mobile Radio Channels," IEEE Trans. on Comm., COM-23, November 1975, pp. 1271-1280.

19. J. C-I. Chuang, "Modeling and Analysis of a Digital Portable Communications Channel with Time Delay Spread," IEEE Vehicular Technology Conference, Dallas, Texas, May 20-22, 1986, proceedings.

20. J. C-I. Chuang, "Simulation of Digital Modulation on Portable Radio Communications Channels with Frequency-Selective Fading," IEEE Globecom '86, December 1-4, 1986, Houston, Texas, pp. 1120-1126.

21. H. H. Hoffman and D. C. Cox, "Attenuation of 900 MHz Radio Waves Propagating into a Metal Building," IEEE Trans. on Ant. and Prop., AP-30, July 1982, pp. 808-811.

22. D. C. Cox, R. R. Murray and A. W. Norris, "Measurements of 800 MHz Radio Transmission into Buildings with Metallic Walls," BSTJ, Vol. 62, November 1983, pp. 2695-2717.

23. S. E. Alexander, "Characterizing Buildings for Propagation at 900 MHz," Electronics Letters, Vol. 19, September 29, 1983, p. 860.

24. D. C. Cox, R. R. Murray and A. W. Norris, "800 MHz Attenuation Measured In and Around Suburban Houses," BLTJ, July-August 1984, pp. 921-954.

25. M. Schwartz, W. R. Bennett and S. Stein, "Communication Systems and Techniques," New York, McGraw Hill, 1966.

26. R. H. Clarke, "A Statistical Theory of Mobile Radio Reception," BSTJ, July-August 1968, pp. 957-1000.

27. R. R. Murray, H. W. Arnold and D. C. Cox, "815 MHz Radio Attenuation Measured Within a Commecial Building," IEEE Antennas and Propagation Symposium, June 9-13, 1986, Philadelphia, Penna.

28. S. E. Alexander, "Radio Propagation Within Buildings at 900 MHz," Electronics Letters, Vol. 18, October 14, 1982, pp. 913-914.

29. D. C. Cox, R. R. Murray and A. W. Norris, "Antenna Height Dependence of 800 MHz Attenuation Measured in Houses," IEEE Trans. on Veh. Tech., VT-34, May 1985, pp. 108-115.

30. P. A. Mathews, "Radio Wave Propagation, VHF and Above," London: Chapman and Hall, Ltd., 1985, Chapter 2.

31. G. P. Ott and A. Plitkins, "Urban Path-Loss Characteristics at 820 MHz," IEEE Trans on Veh. Tech., VT-27, Nov. 1978, pp. 189-197.

32. Ramo, Whinnery, and Van Duzer, "Fields and Waves in Communications Electronics," John Wiley & Sons, New York, 1965, Chapter 12.

33. P. I. Wells and P. V. Tryon, "The Attenuation of UHF Radio Signals by Houses," US Dept. of Commerce Report, OT Report 76-98, August 1976 and IEEE Trans on Veh. Tech., VT-26, November 1977. pp. 358-362.

34. S. E. Alexander and G. Pugliese, "Cordless Communication Within Buildings: Results of Measurements at 900 MHz and 60 GHz," British Telecom Technology Journal, July 1983, pp. 99-105.

35. G. V. Waldo, "Report on the Analysis of Measurements and Observations, New York City UHF-New York City UHF-TV Project," IEEE Trans. on Broadcasting, Vol. 9, 1963, pp. 7-36.

36. J. Shefer, "Propagation Statistics of 900 MHz and 450 MHz Signals Inside Buildings," Microwave Mobile Radio Symposium, March 7-9 1973, Boulder, Colorado.

37. D. C. Cox, Co-Channel Interference Considerations in Frequency Reuse Small-Coverage Area Radio Systems," IEEE Trans. on Commun., COM-30, January 1982, pp. 135-142.

38. H. W. Arnold, R. R. Murray and D. C. Cox, "Macroscopic Diversity in the Portable Radiocommunication Environment," 1985 North American Radio Science Meeting (URSI), Vancouver, Canada, June 17-21, 1985.

39. D. C. Cox, R. R. Murray, H. W. Arnold, A. W. Norris and M. F. Wazowicz, "Crosspolarization Coupling Measured for 800 MHz Radio Transmission In and Around Houses and Large Buildings," IEEE Trans. on Anr. and Prop., AP-34, January 1986, pp. 83-87.

40. A. Akeyamo, T. Tsuruhara and Y. Tanaka, "920 MHz Mobile Propagation Test for Portable Telephone," Trans. of IECE of Japan, Vol. E65, September 1982, pp. 542-543.

41. D. C. Cox, "Antenna Diversity Performance in Mitigating the Effects of Portable Radiotelephone Orientation and Multipath Propagation," IEEE Trans. on Commun., COM-31, May 1983, pp. 620-628.

42. D. C. Cox, "Time Diversity Adaptive Retransmission for Reducing Signal Impairments in Portable Radiotelephones," IEEE Trans. on Veh. Tech., VT-32, August 1983, pp. 230-238.

43. S. A. Bergman and H. W. Arnold, "Polarization Diversity in Portable Communications Environment," Electronics Letters, Vol. 22, No. 11, May 22, 1986, pp. 609-610.

Figure Captions

Figure 1a Average Relative Power Received as a Function of Time Delay for a Probing Transmitter and Receiver Located in Different Places in a Large Building. The Transmitter and Receiver Locations Were Obscured from Each Other by Walls.

Figure 1b Average Relative Power Received as a Function of Time Delay Similar to Figure 1a. For Figure 1b, the Transmitter and Receiver Were Located in Different Places in the Building than They Were for Figure 1a.

Figure 2 Individual Profiles of Relative Power Received as a Function of Time Delay Used to Make Up the Average Profile of Figure 1a. The Power Scale Has Been Greatly Compressed From the Scale Used in Figure 1a.

Figure 3 Cumulative Distributions of Time Delay Spread for Propagation Paths Within a Large and a Small Office Building. The Solid Curve is the Delay Distribution for the Larger Building. The Dotted Curve is the Delay Distribution for the Smaller Building, Which Had Linear Dimensions Less Than One-Third Those of the Larger Building.

Figure 4 Cumulative Distributions of Time Delay Spread for Propagation Paths from Several Port Locations to Rooms Inside a Small Office Building and a House. The Solid Curve is for Measurements in the Office Building. The Dotted Curve is for Measurements in the House.

Figure 5 Cumulative Distributions of Time Delay Spread for Propagation Paths Within a Large Office Building. The Solid Curve is for Measurements Between a Corridor and Rooms Opening Off the Corridor. The Dotted Curve is for Measurements Between a Corridor and Offices Opening Off That Corridor and Adjacent Corridors.

Figure 6 Small Scale Variations of a Narrowband Signal at 900 MHz as an Antenna is Moved at Different Heights in the Multipath Environment within a Building.

Figure 7 Cumulative Signal Envelope Distributions for Four Small Areas Inside and Outside a House. The Measurements Were Made at 815 MHz.

Figure 8 Scatter Plot of Median 815 MHz Signal Levels for Many Small Areas Within and Outside 8 Houses. Measurements Were Made from Different Port Locations at Different Distances from the Houses.

Figure 9 Scatter Plot of Median 815 MHz Signal Levels Along a Corridor of a Small Office Building. Measurements Were Made Along the Corridor and Between the Corridor and Adjoining Offices on the Same and on Adjacent Floors.

Figure 10 Cumulative Distributions of Large Scale Signal Variations (Scatter) in Figure 8 after Removal of the Overall Regression Line Distance Dependence.

Figure 11 Comparison of Median Signal Levels from Small Areas for Port Antenna Heights of 27 Feet and 12.5 Feet. Measurements Were Made at 815 MHz in Small Areas Within and Around 4 Houses.

Figure 12 Cumulative Distributions of Median Signal Levels from Small Areas for Port Antennas Located at Different Angular Locations Around 8 Houses. The Curves Labeled 2 Branch and 3 Branch Indicate the Selection of the Best Signal in a Small Area from Either 2 or 3 Different Port Locations, Respectively. The 2 and 3 Branch Distributions Indicate the Effectiveness of Selection Macroscopic Diversity as Discussed in the Text.

Figure 13 Scatter Plot of Crosspolarization Coupling as a Function of Median Copolarized Signal Level. Measurements Were Made at 815 MHz Within and Around 8 Houses.

Figure 14 Computer-Simulated Cumulative Distributions of Relative Signal-to-Noise Ratio for Different Antenna and Crosspolarization Conditions Discussed in the Text. The Distributions Indicate the Effects of Random Antenna Orientation, Crosspolarization Coupling and Microscopic Selection Diversity.

Figure 15 Small Scale Variations of a Narrowband Signal Transmitted at 815 MHz on One Linear Polarization and Received Simultaneously on Two Linear Orthogonal Polarizations. The Transmitter and Receiver Locations Were Obscured from Each Other by Walls. The Two Signals Have Nearly Equal Average Powers and are Nearly Uncorrelated.

Figure 16 Small Scale Signal Variations Received Simultaneously on Two Linear Orthogonal Polarizations as in Figure 15. The Transmitter and Receiver Locations were Within Line of Sight Along a Corridor. The Copolarized Signal Has Little Fluctuation and is Much Stronger than the Crosspolarized Signal.

Figure 17 Histogram of Correlation of Small Scale Signal Variations Received Simultaneously on Two Linear Orthogonal Polarizations, as in Figures 15 and 16. Little Correlation is Seen for Paths Obscured by Walls. Higher Correlation is Seen for Paths Where the Transmitter and Receiver were Within Line of Sight.

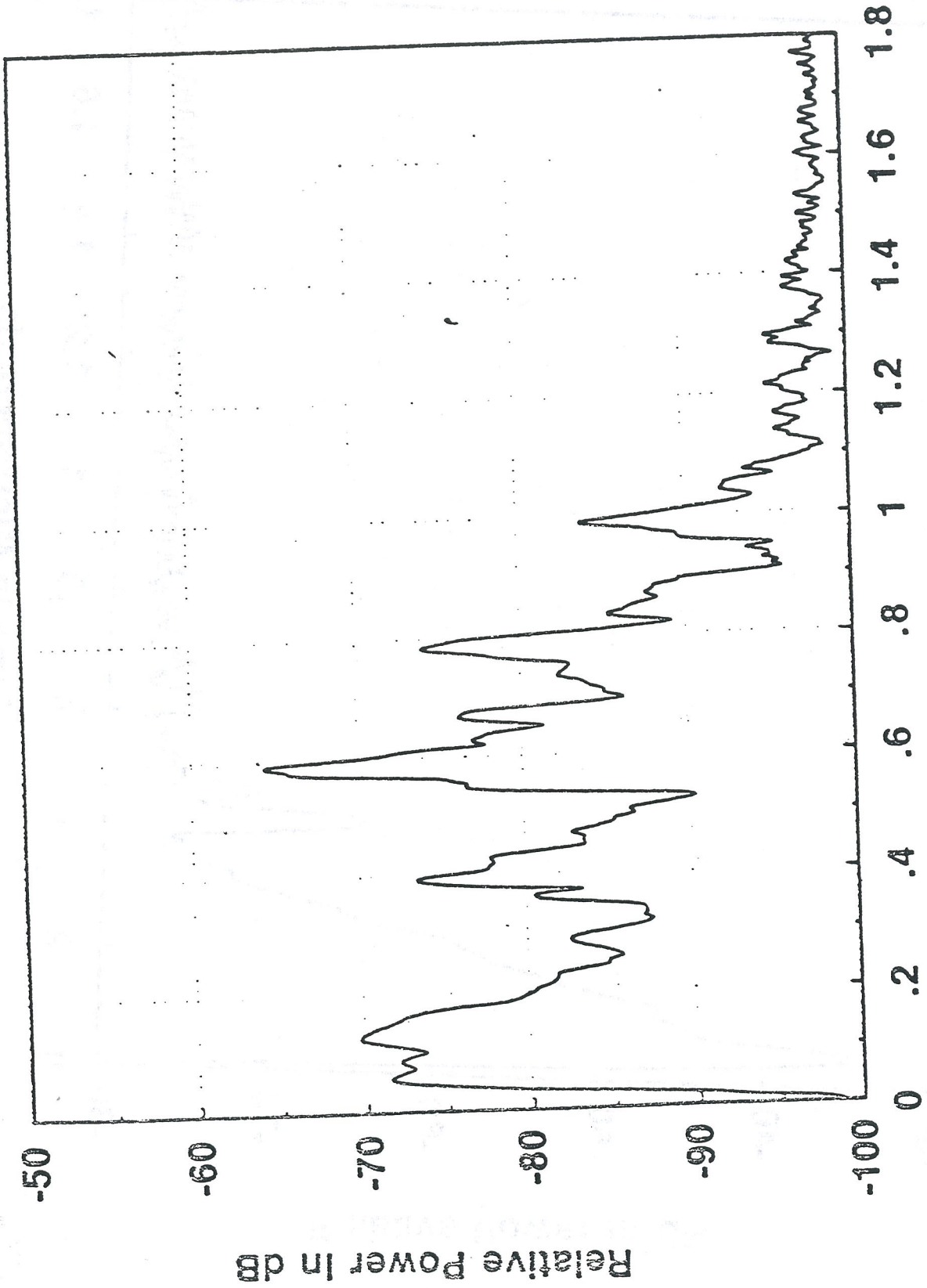
Relative Power in dB
-50
-60
-70
-80
-90
-100
0
.2
.4
.6
.8
1
1.2
1.4
1.6
1.8
Time In Microseconds

FIGURE 1a

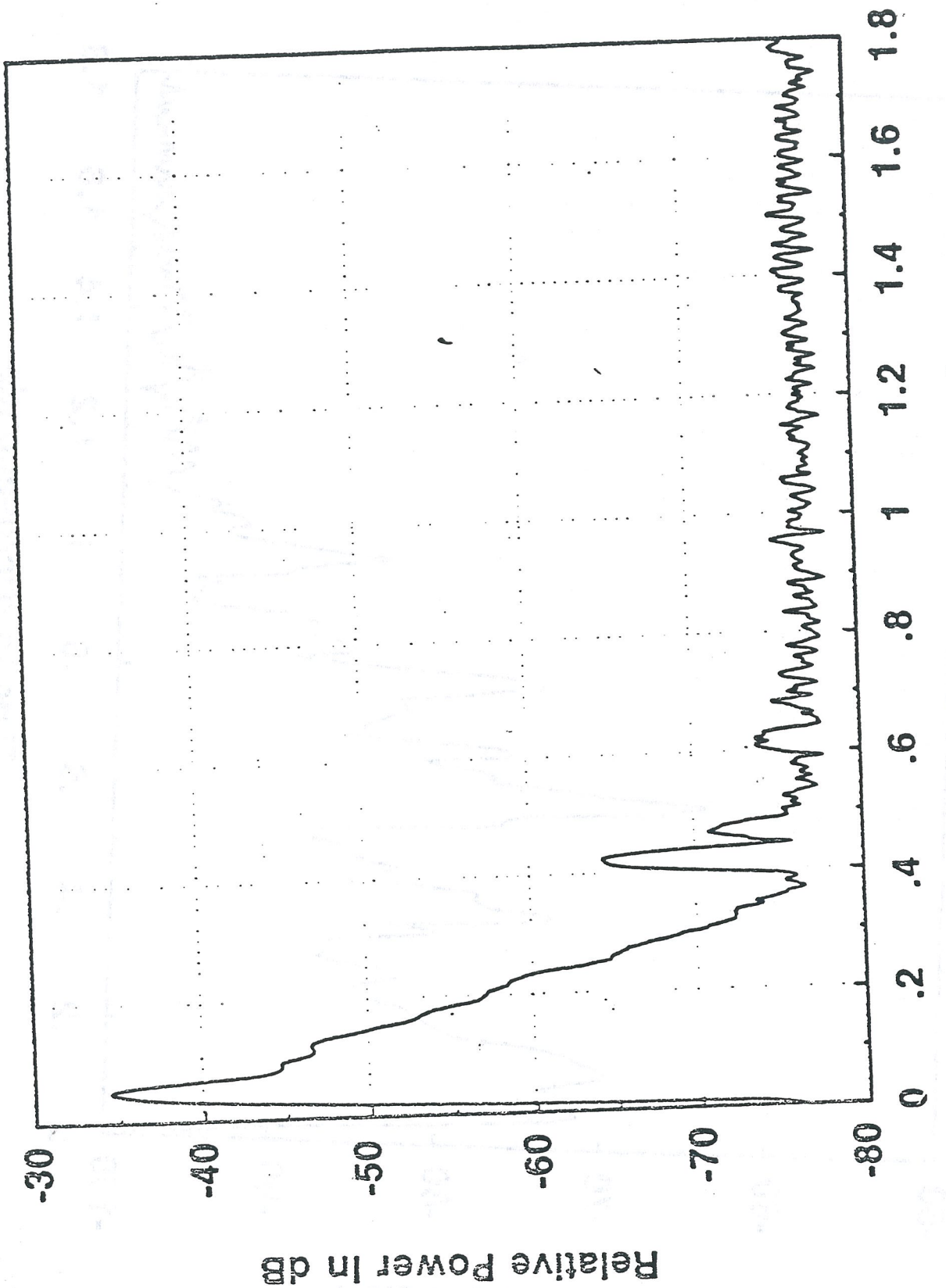
Relative Power In dB
-30
-40
-50
-60
-70
-80
0
.2
.4
.6
.8
1
1.2
1.4
1.6
1.8
Time In Microseconds

FIGURE 1b

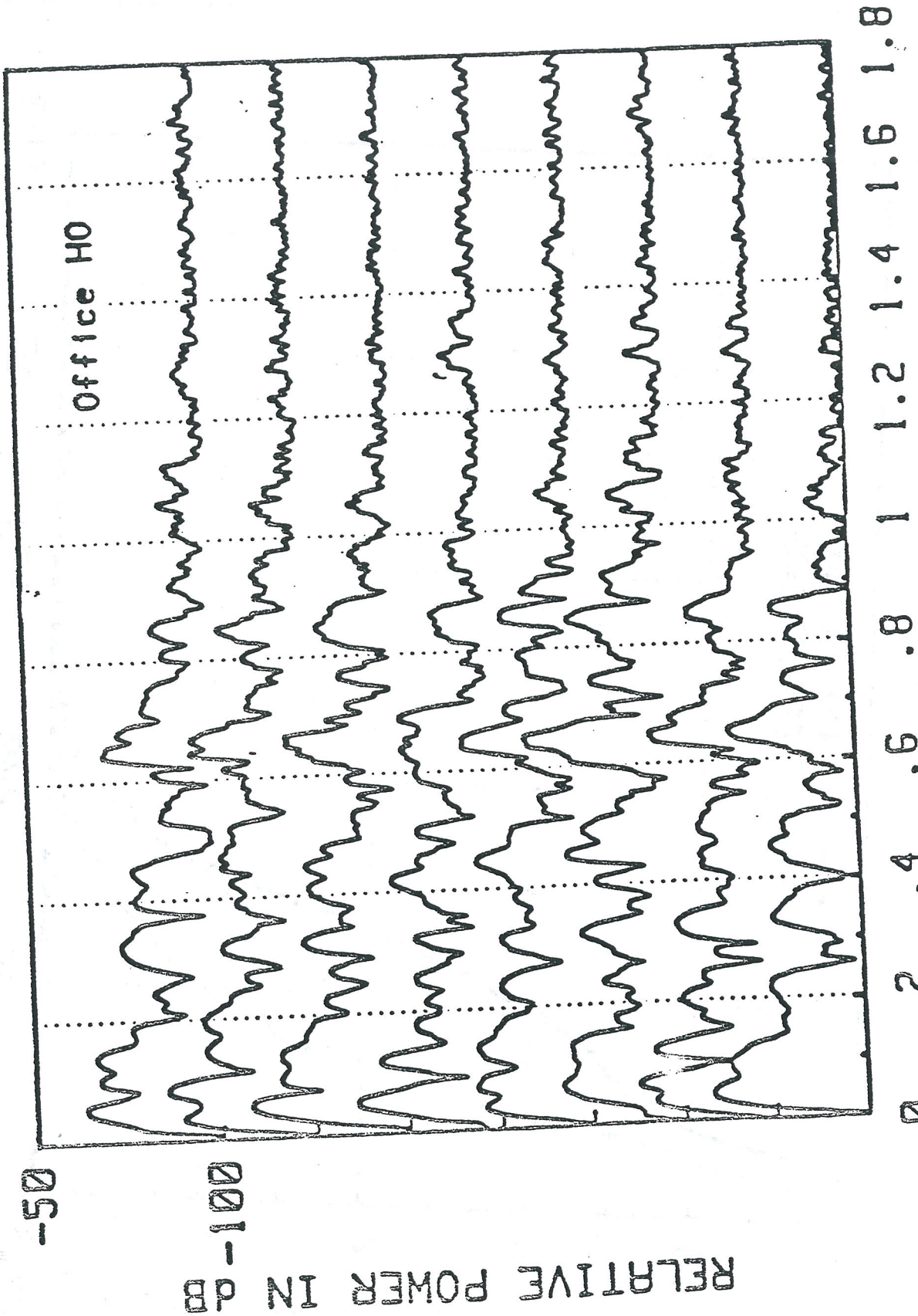
Office HO
-50
-100
RELATIVE POWER IN dB
0
.2
.4
.6
.8
1
1.2
1.4
1.6
1.8
TIME IN MICROSECONDS

FIGURE 2

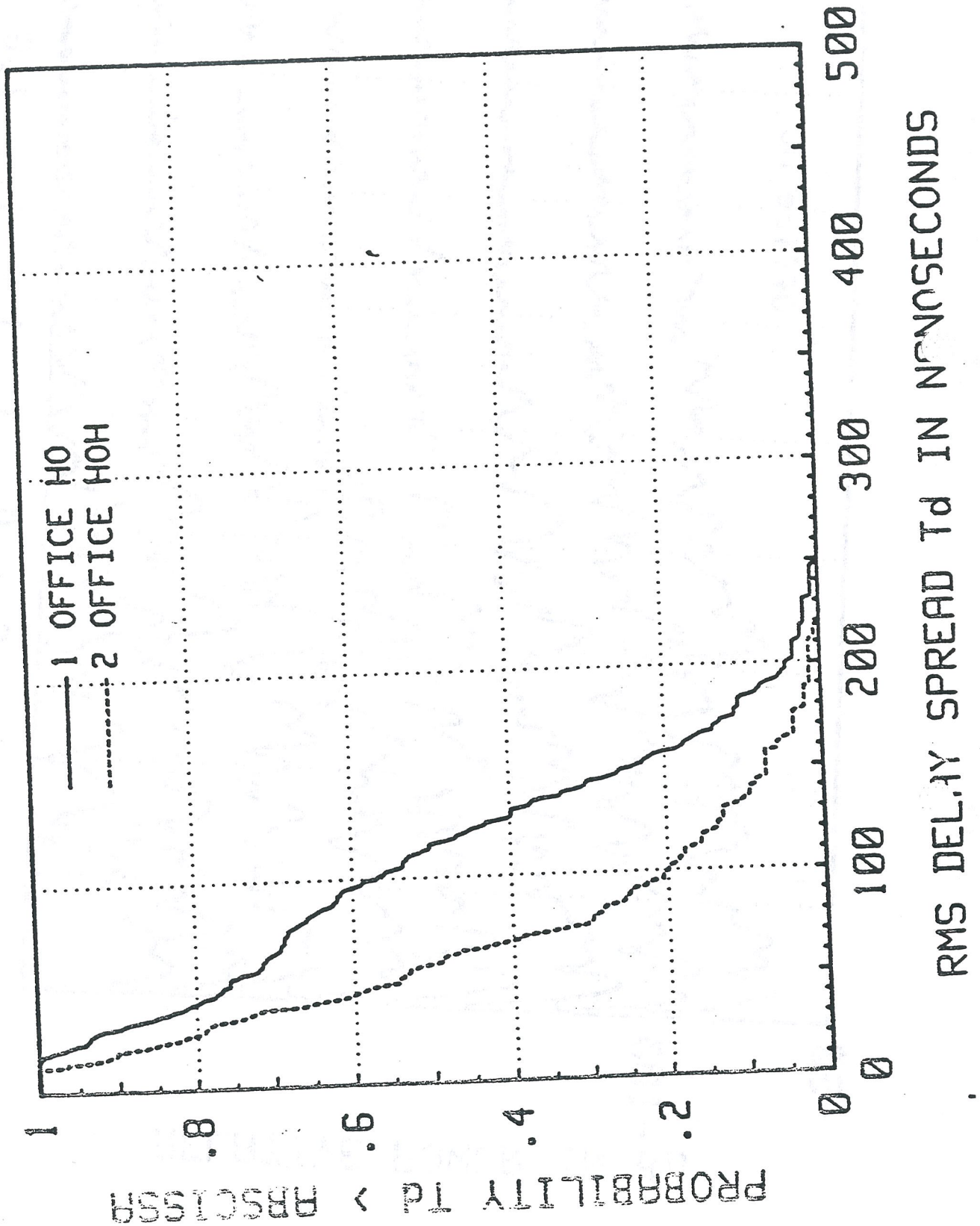
1 OFFICE HO
2 OFFICE HOH
PROBABILITY Td > ABSCISSA
1
.8
.6
.4
.2
0
0
100
200
300
400
500
RMS DELAY SPREAD Td IN NANOSECONDS

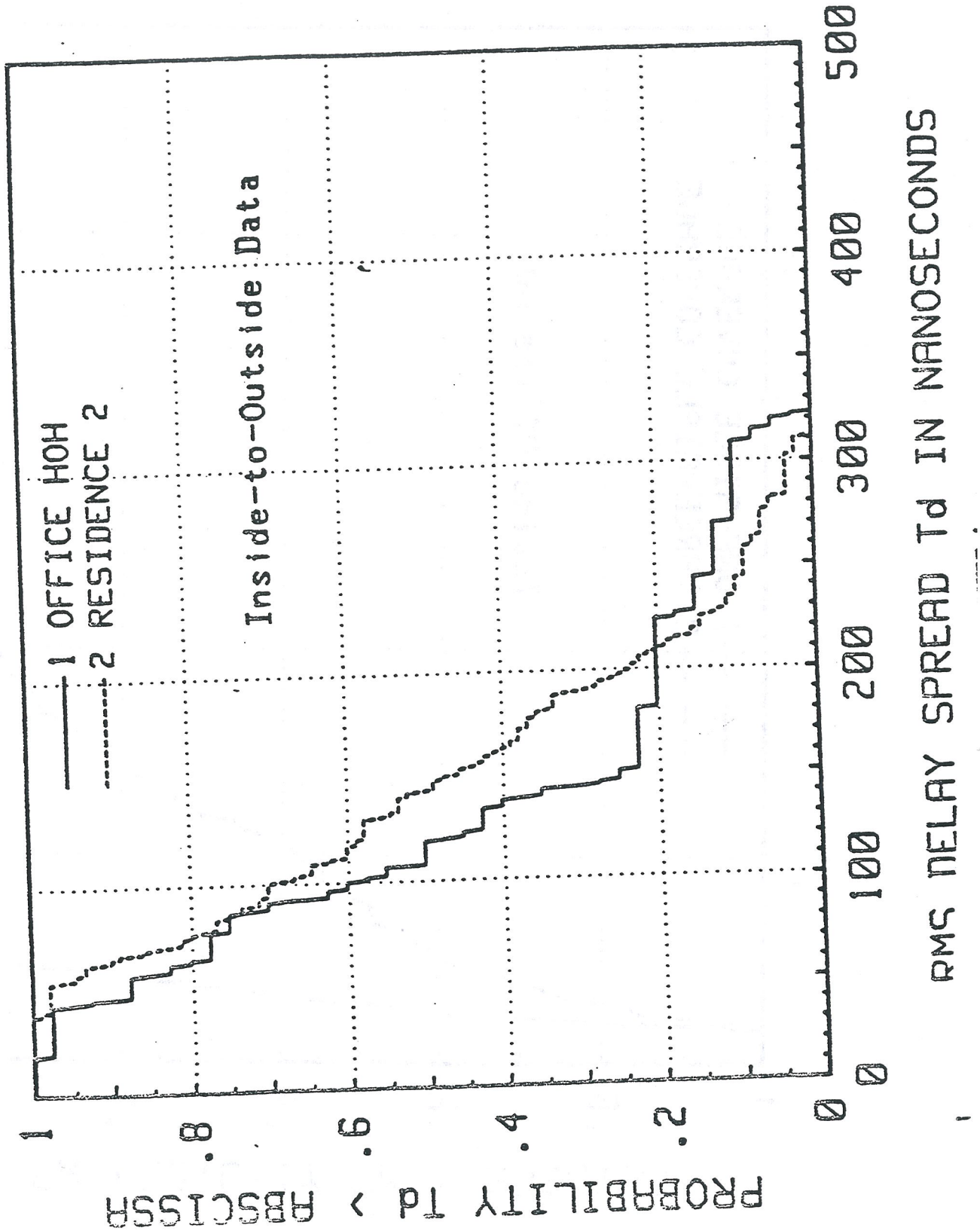
1 OFFICE HOH
2 RESIDENCE 2
Inside-to-Outside Data
PROBABILITY Td > ABSCISSA
1
.8
.6
.4
.2
0
0
100
200
300
400
500
RMS DELAY SPREAD Td IN NANOSECONDS

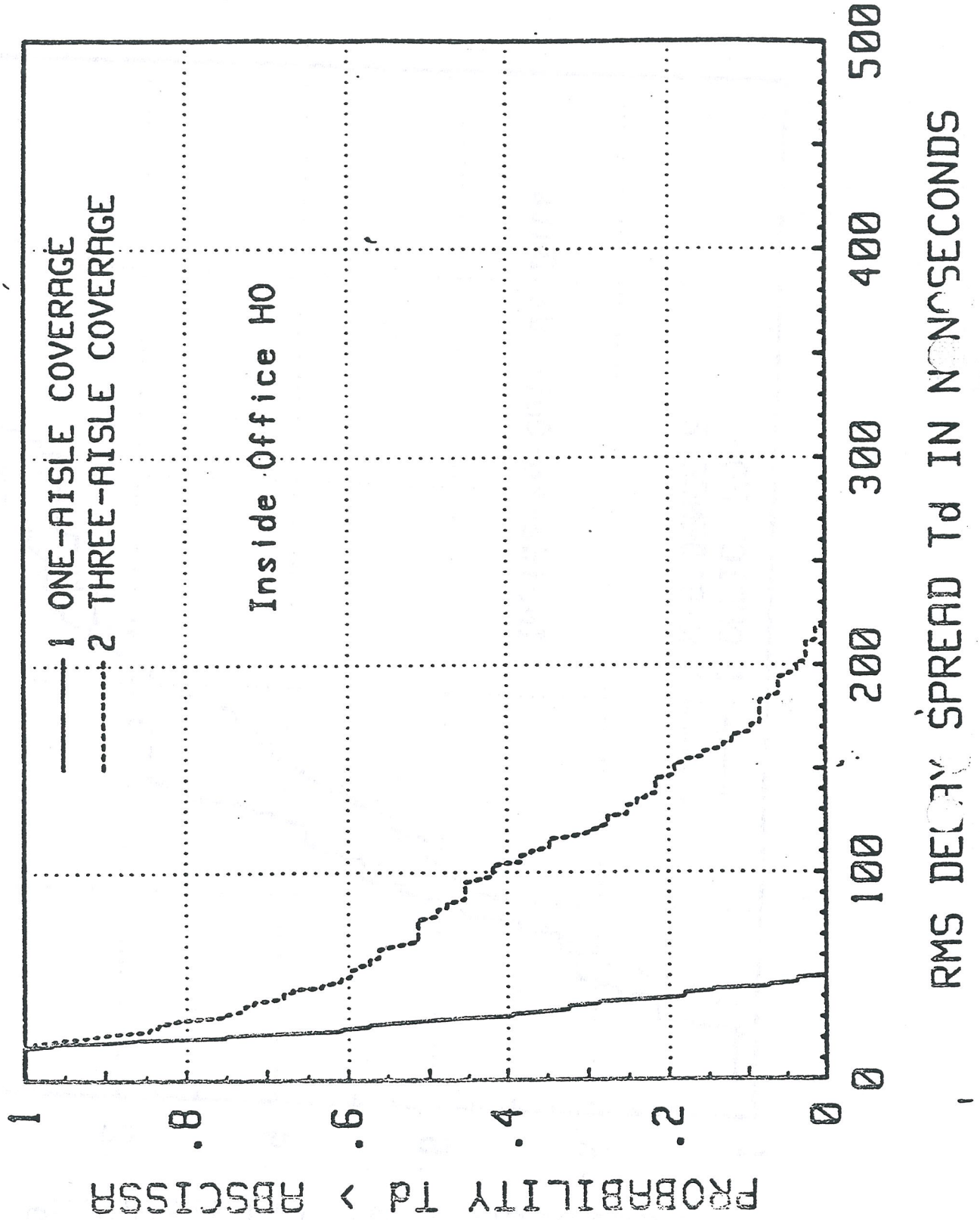
1 ONE-AISLE COVERAGE
2 THREE-AISLE COVERAGE
Inside Office HO
PROBABILITY Td > ABSCISSA
1
.8
.6
.4
.2
0
0
100
200
300
400
500
RMS DELAY SPREAD Td IN NANOSECONDS

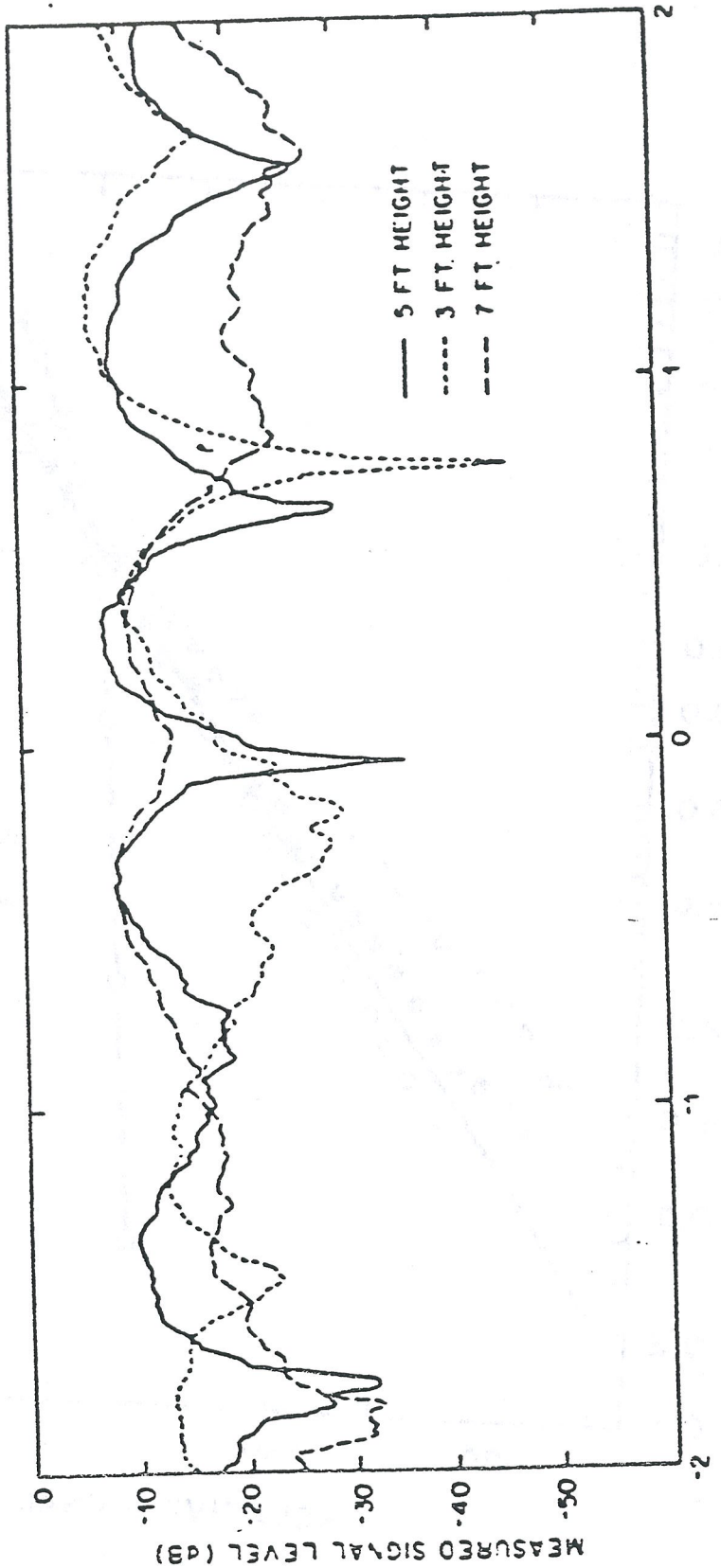
5 FT HEIGHT
3 FT. HEIGHT
7 FT. HEIGHT
MEASURED SIGNAL LEVEL (dB)
0
-10
-20
-30
-40
-50
2
1
0
-1
-2
DISTANCE (FEET)

FIGURE 6

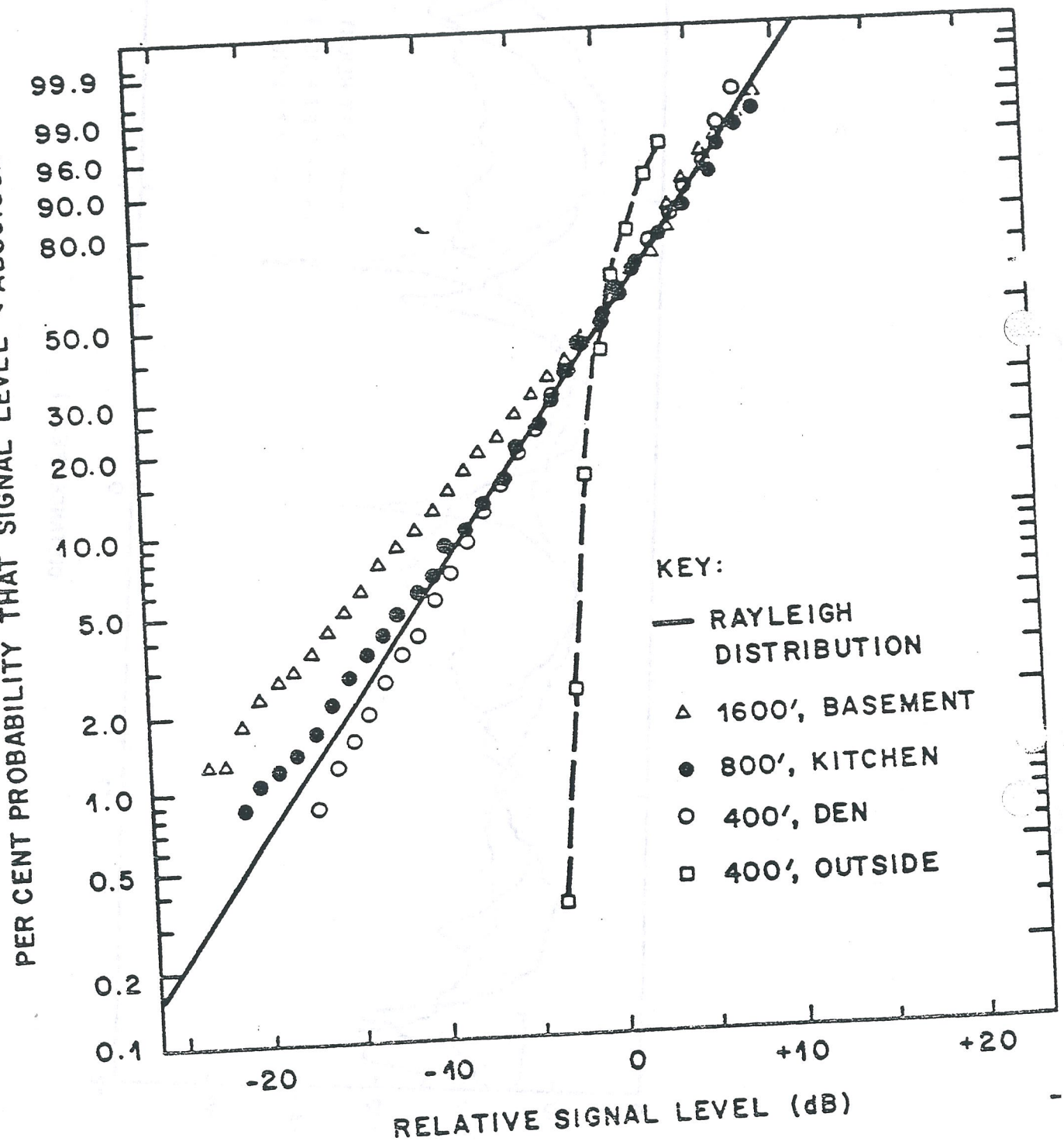
PER CENT PROBABILITY THAT SIGNAL LEVEL < ABSCISSA
99.9
99.0
96.0
90.0
80.0
50.0
30.0
20.0
10.0
5.0
2.0
1.0
0.5
0.2
0.1
-20
-10
0
+10
+20
RELATIVE SIGNAL LEVEL (dB)
KEY:
RAYLEIGH DISTRIBUTION
1600', BASEMENT
800', KITCHEN
400', DEN
400', OUTSIDE

FIGURE 7

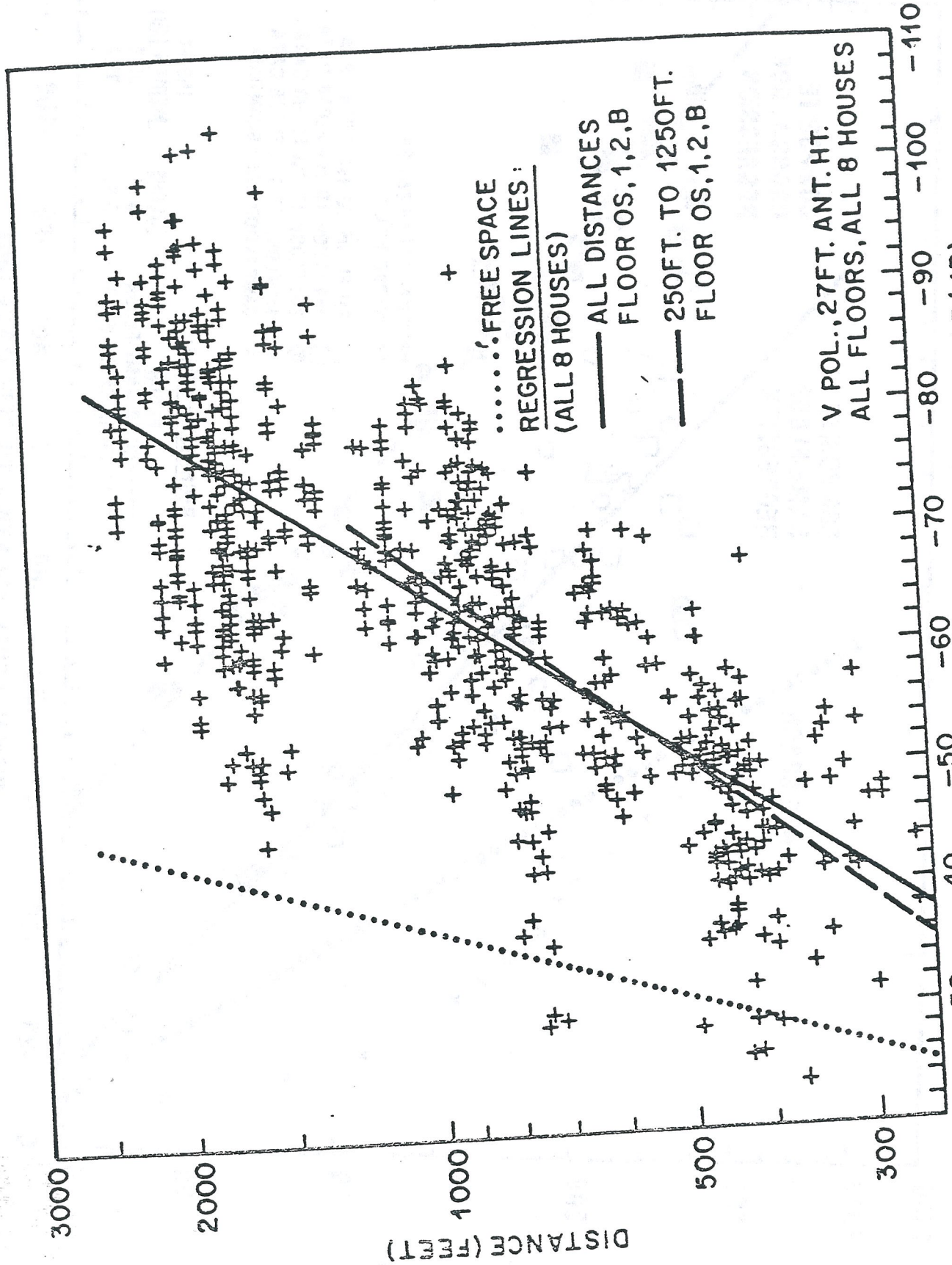
V POL.,27FT. ANT.HT.
ALL FLOORS, ALL 8 HOUSES
SIGNAL LEVEL RELATIVE TO REFERENCE (dB)
-20
-30
-40
-50
-60
-70
-80
-90
-100
-110
DISTANCE (FEET)
300
500
1000
2000
3000
ALL DISTANCES
FLOOR OS, 1,2,B
250FT. TO 1250FT.
FLOOR OS, 1,2,B
FREE SPACE
REGRESSION LINES:
(ALL 8 HOUSES)

FIGURE 8

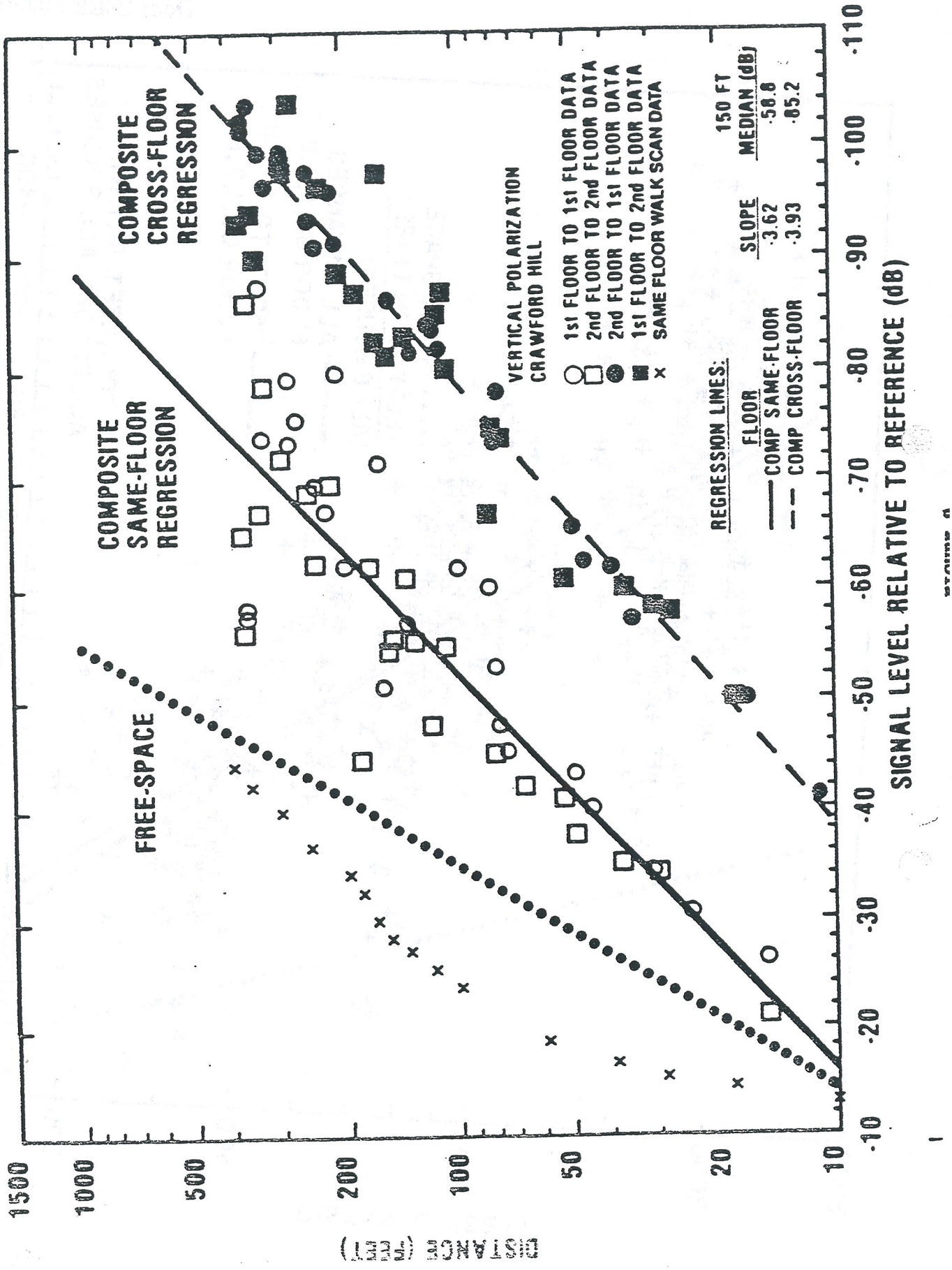
COMPOSITE
CROSS-FLOOR
REGRESSION
COMPOSITE
SAME-FLOOR
REGRESSION
FREE-SPACE
VERTICAL POLARIZATION
CRAWFORD HILL
1st FLOOR TO 1st FLOOR DATA
2nd FLOOR TO 2nd FLOOR DATA
2nd FLOOR TO 1st FLOOR DATA
1st FLOOR TO 2nd FLOOR DATA
SAME FLOOR WALK SCAN DATA
REGRESSION LINES:
FLOOR
SLOPE
150 FT MEDIAN (dB)
COMP SAME-FLOOR
-3.62
-58.8
COMP CROSS-FLOOR
-3.93
-85.2
SIGNAL LEVEL RELATIVE TO REFERENCE (dB)
-10
-20
-30
-40
-50
-60
-70
-80
-90
-100
-110
DISTANCE (FEET)
10
20
50
100
200
500
1000
1500

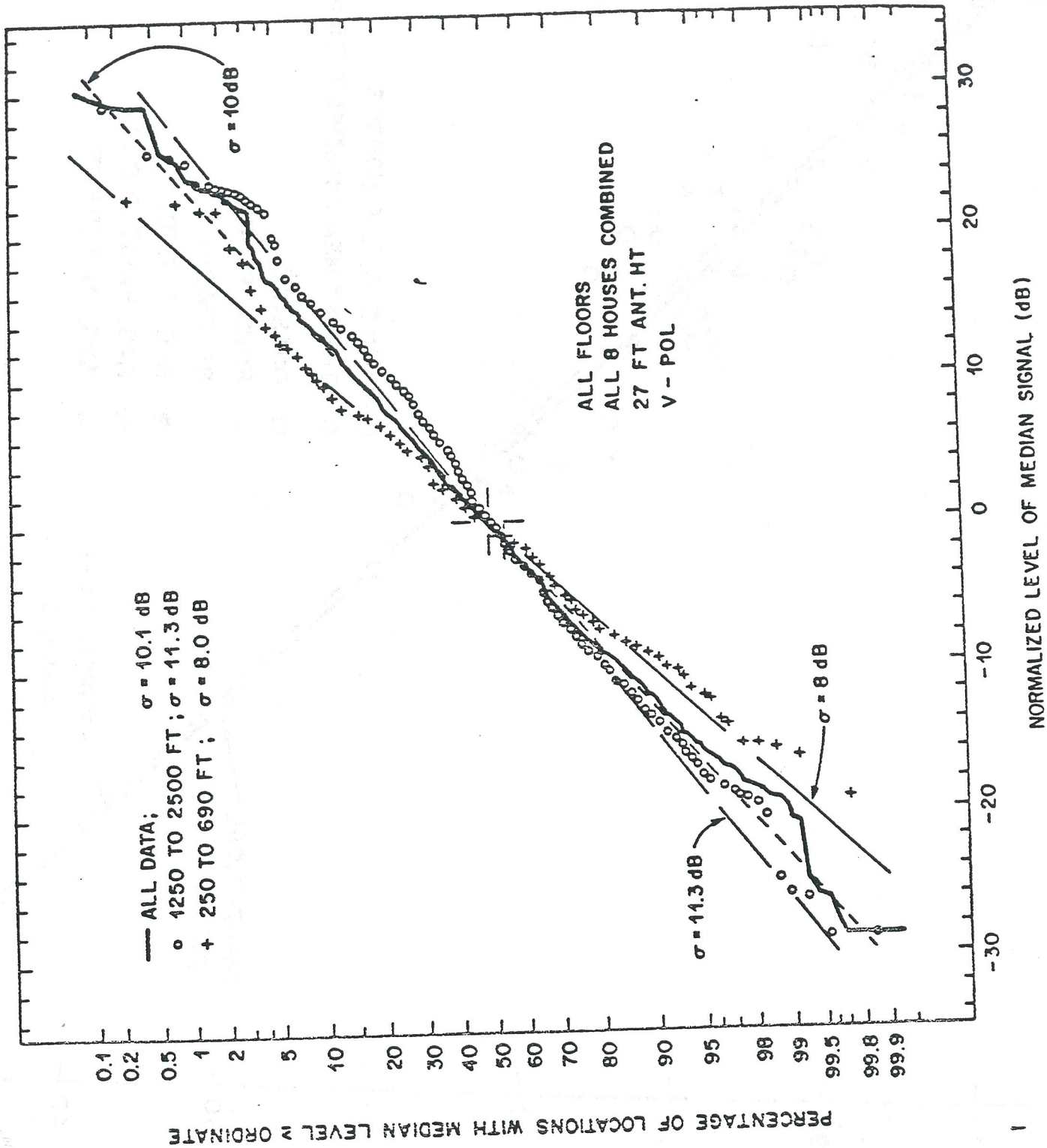
ALL DATA; σ = 10.1 dB
o 1250 TO 2500 FT ; σ = 11.3 dB
+ 250 TO 690 FT ; σ = 8.0 dB
ALL FLOORS
ALL 8 HOUSES COMBINED
27 FT ANT. HT
V - POL
σ = 10dB
σ = 11.3 dB
σ = 8 dB
PERCENTAGE OF LOCATIONS WITH MEDIAN LEVEL > ORDINATE
0.1
0.2
0.5
1
2
5
10
20
30
40
50
60
70
80
90
95
98
99
99.5
99.8
99.9
30
20
10
0
-10
-20
-30
NORMALIZED LEVEL OF MEDIAN SIGNAL (dB)

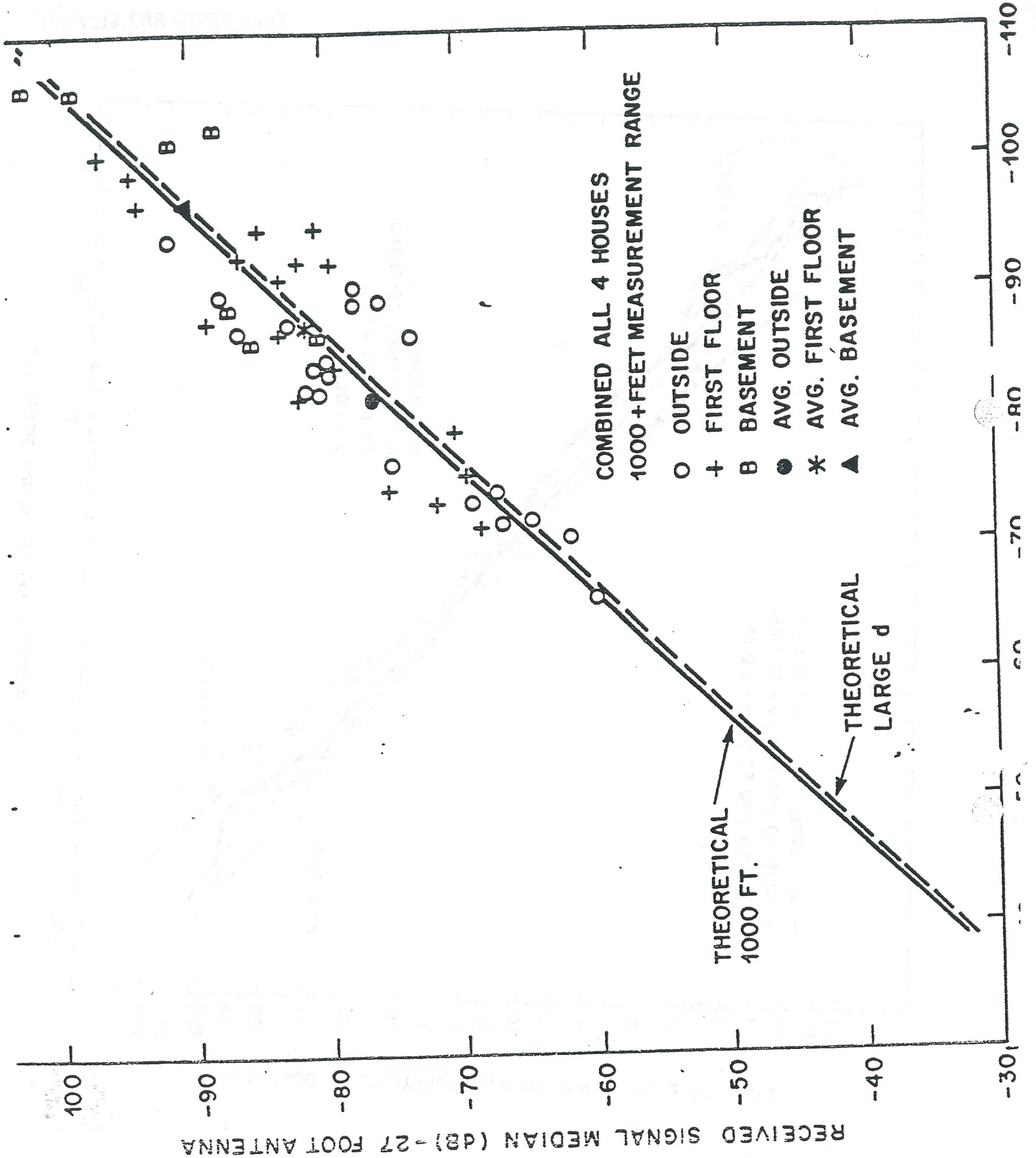
COMBINED ALL 4 HOUSES
1000+FEET MEASUREMENT RANGE
O OUTSIDE
+ FIRST FLOOR
B BASEMENT
● AVG. OUTSIDE
* AVG. FIRST FLOOR
▲ AVG. BASEMENT
THEORETICAL
1000 FT.
THEORETICAL
LARGE d
RECEIVED SIGNAL MEDIAN (dB) -27 FOOT ANTENNA
100
-90
-80
-70
-60
-50
-40
-110
-100
-90
-80
-70

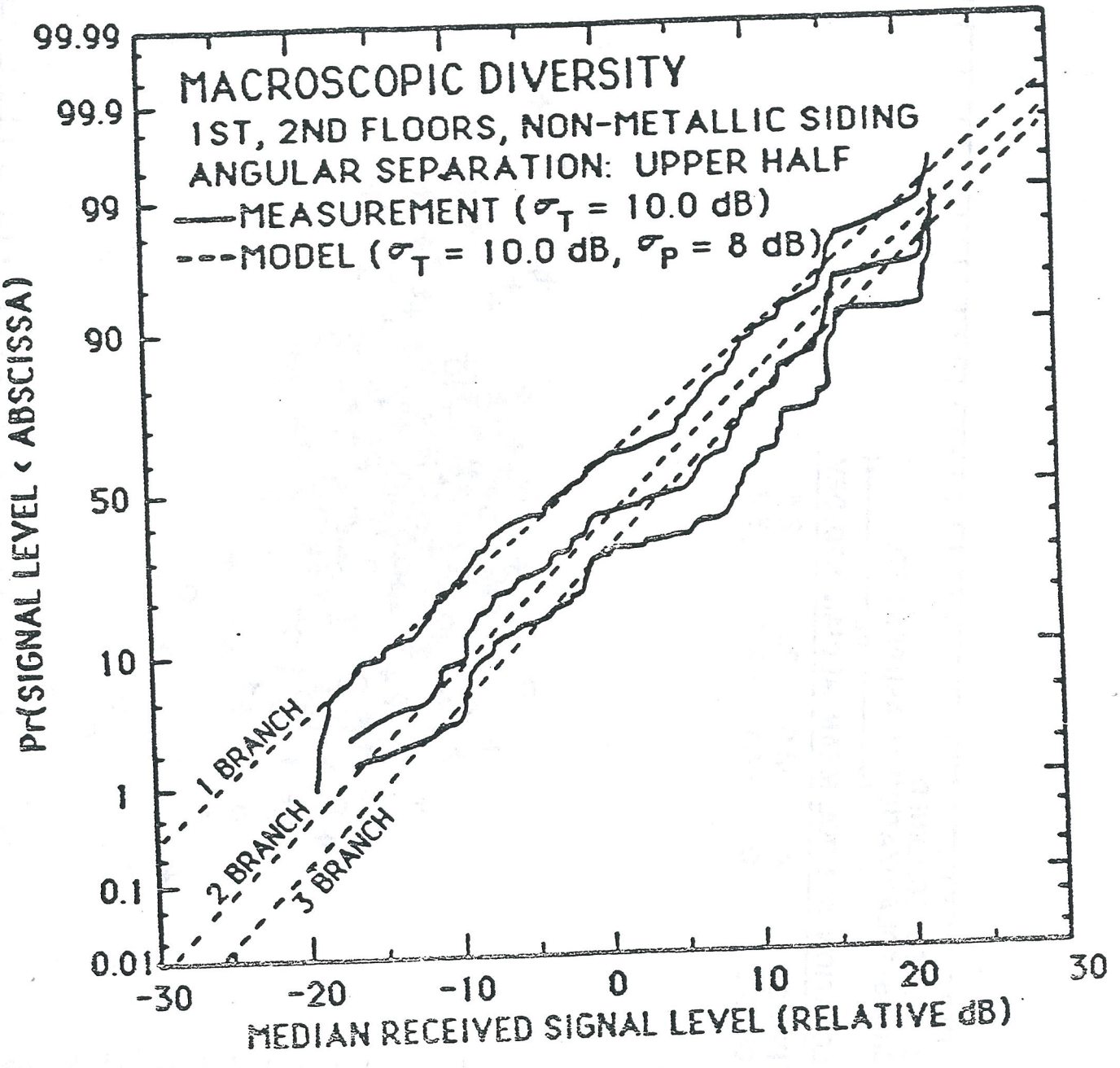
MACROSCOPIC DIVERSITY
1ST, 2ND FLOORS, NON-METALLIC SIDING
ANGULAR SEPARATION: UPPER HALF
—MEASUREMENT (σ_T = 10.0 dB)
---MODEL (σ_T = 10.0 dB, σ_P = 8 dB)
Pr(SIGNAL LEVEL < ABSCISSA)
99.99
99.9
99
90
50
10
1
0.1
0.01
1 BRANCH
2 BRANCH
3 BRANCH
-30
-20
-10
0
10
20
30
MEDIAN RECEIVED SIGNAL LEVEL (RELATIVE dB)

FIGURE 12

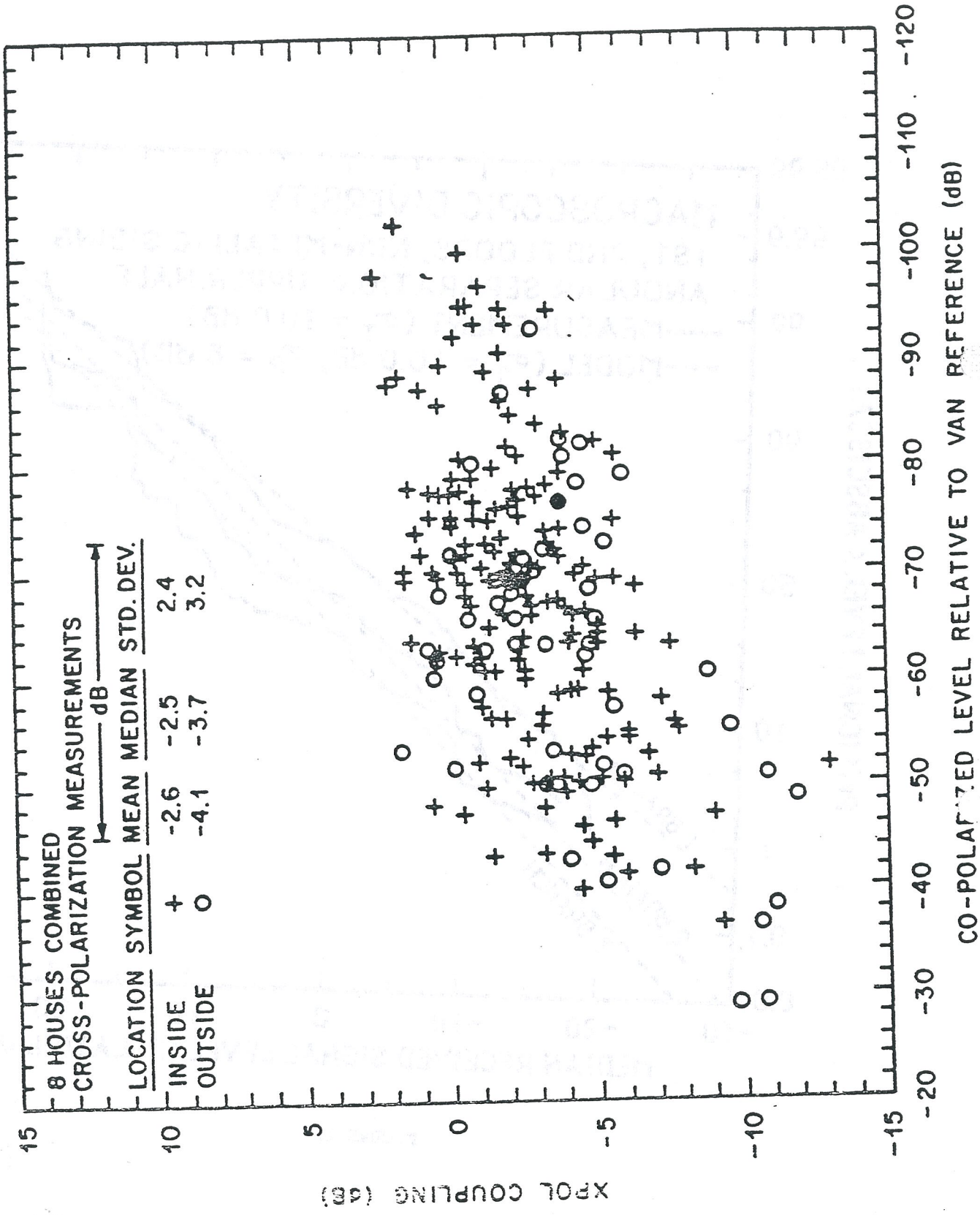
8 HOUSES COMBINED
CROSS-POLARIZATION MEASUREMENTS
dB
LOCATION SYMBOL MEAN MEDIAN STD. DEV.
INSIDE + -2.6 -2.5 2.4
OUTSIDE O -4.1 -3.7 3.2
XPOL COUPLING (dB)
15
10
5
0
-5
-10
-15
-20
-30
-40
-50
-60
-70
-80
-90
-100
-110
-120
CO-POLARIZED LEVEL RELATIVE TO VAN REFERENCE (dB)

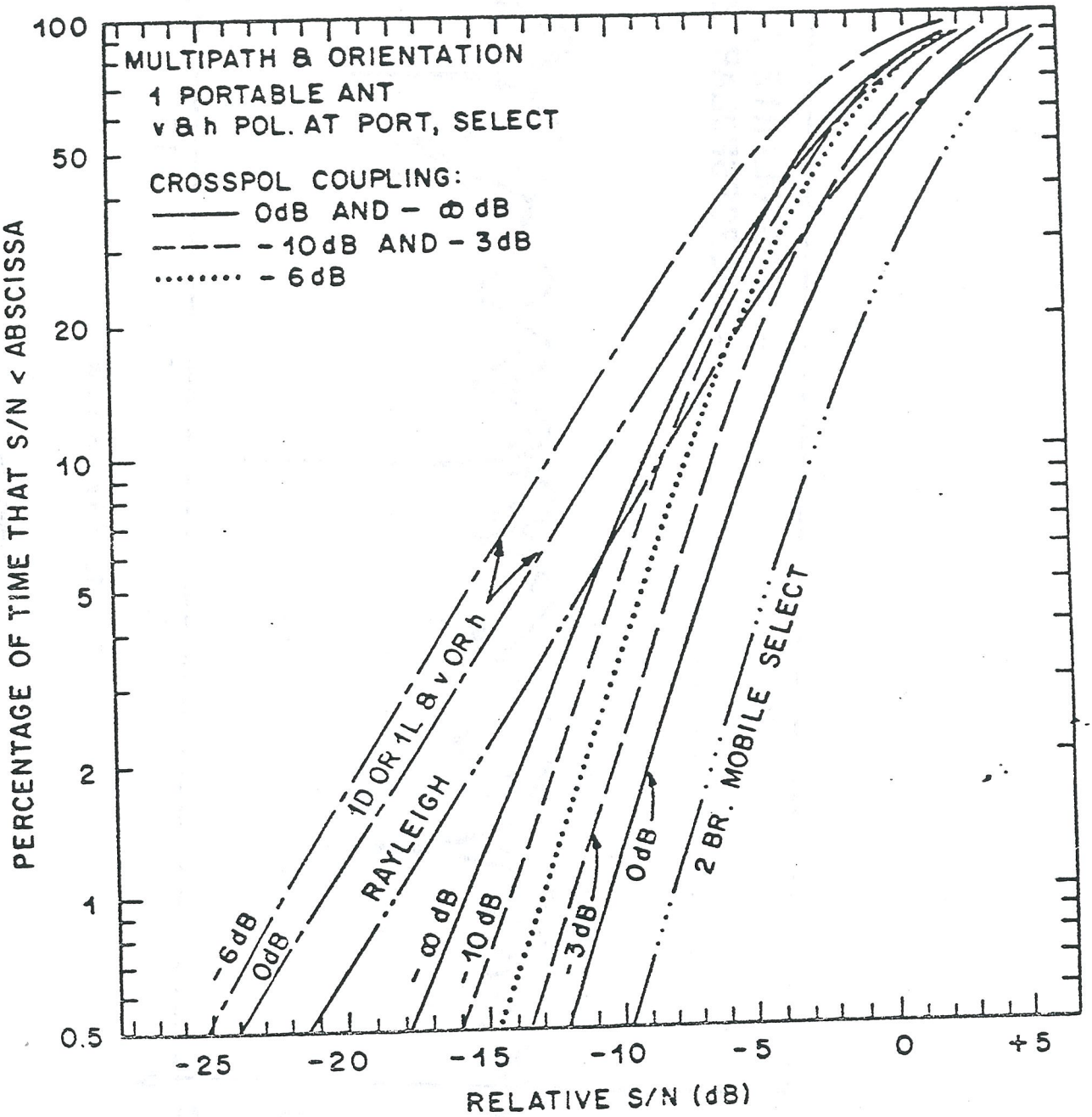
MULTIPATH & ORIENTATION
1 PORTABLE ANT
v & h POL. AT PORT, SELECT
CROSSPOL COUPLING:
0dB AND - ∞ dB
-10dB AND -3dB
-6dB
PERCENTAGE OF TIME THAT S/N < ABSCISSA
100
50
20
10
5
2
1
0.5
-25
-20
-15
-10
-5
0
+5
RELATIVE S/N (dB)
1D OR 1L & v OR h
RAYLEIGH
2 BR. MOBILE SELECT
-6dB
0dB
-∞ dB
-10dB
-3dB
0dB

FIGURE 14

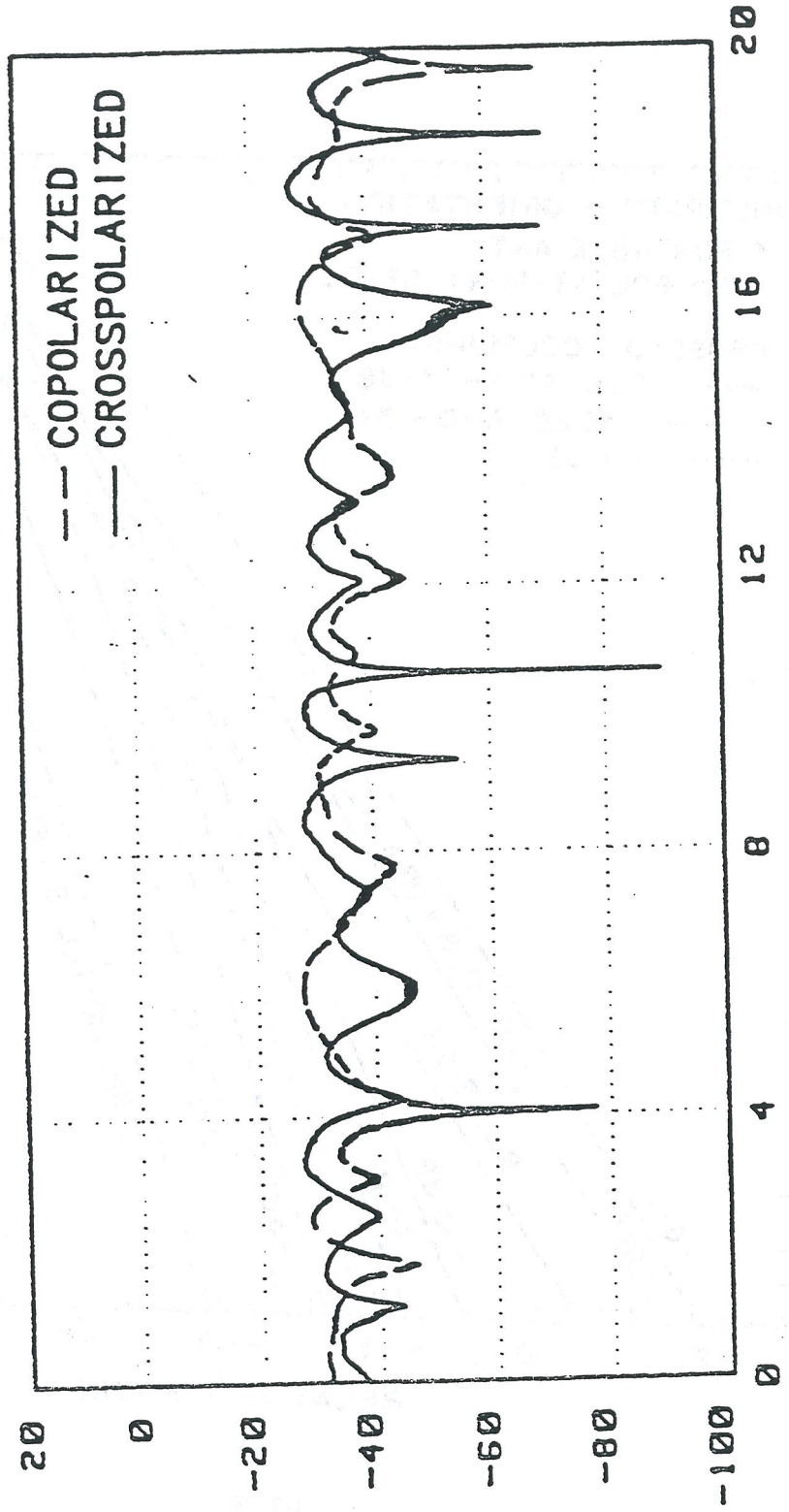
COPOLARIZED
CROSSPOLARIZED
20
0
-20
-40
-60
-80
-100
0
4
8
12
16
20
TIME (in secs)
POWER (in dBm)

FIGURE 15

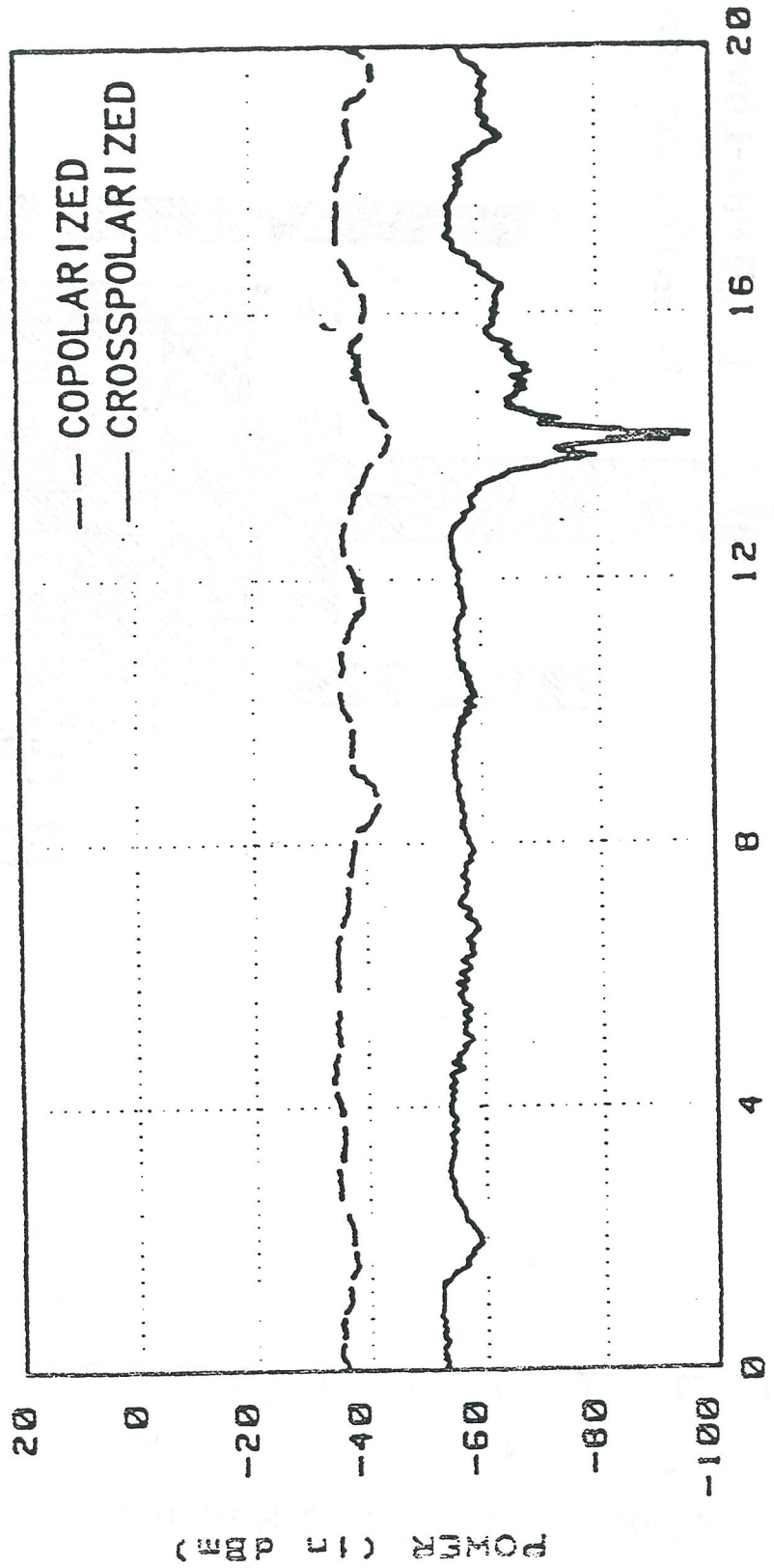
COPOLARIZED
CROSSPOLARIZED
20
0
-20
-40
-60
-80
-100
POWER (in dBm)
0
4
8
12
16
20
TIME (in secs)

FIGURE 16

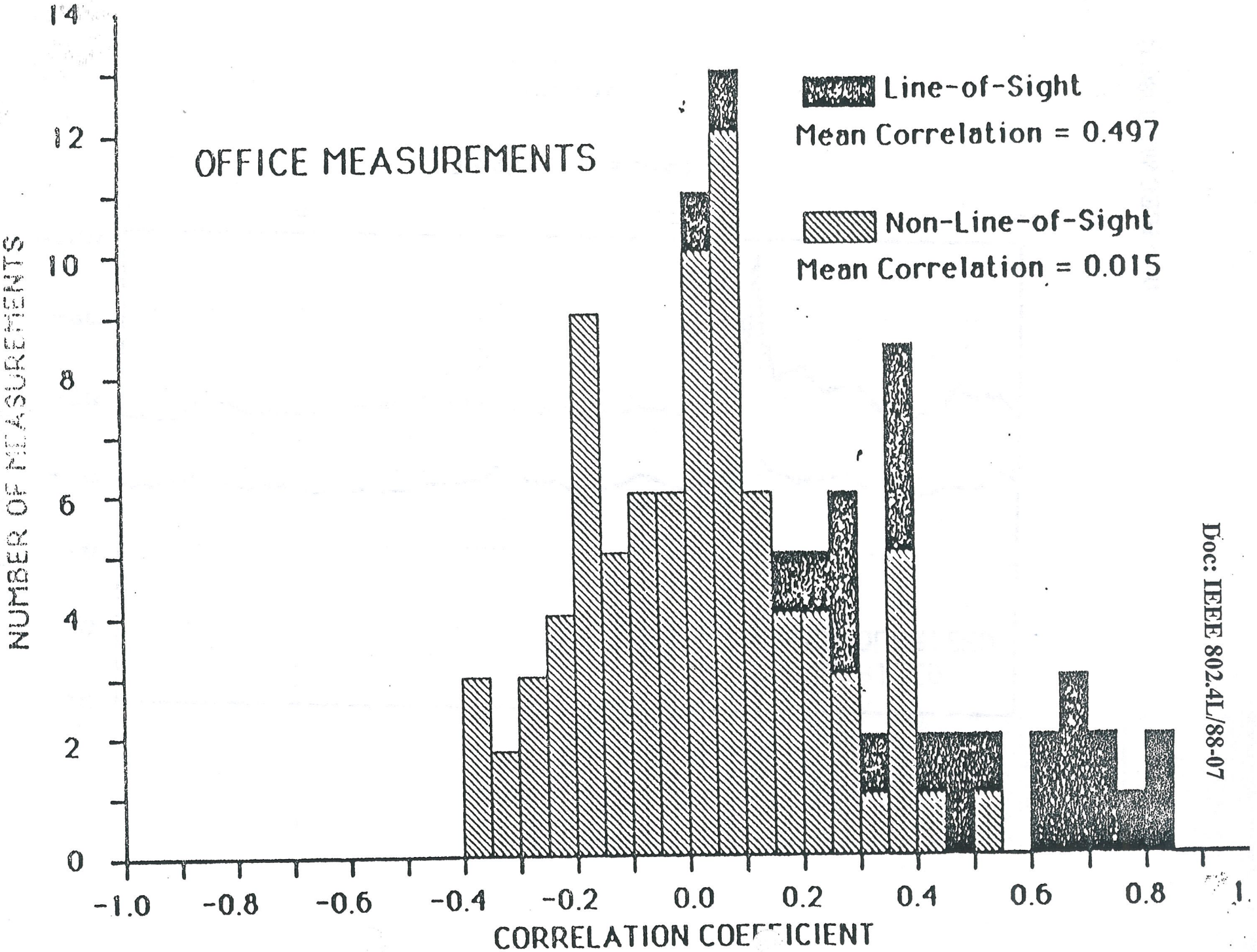

Doc: IEEE 802.4L/88-07

Doc: IEEE 802.4L/88-07

C. A. Rypinski
130 Stewart Drive
Tiburon, CA 94920

Documents
CCIR Study Groups
Period 1986-1990

Document US 8/13-3 Rev. 1
27 January 1987
Original: English

Subject: Input to Document IWP 8/13-27, Rev. 3, Draft Report

United States of America

THE PORTABLE RADIO PROPAGATION ENVIRONMENT

PHIL PORTER, BELLCORE

In Section 3.6 of Draft Report IWP 8/13 Rev. 2, contributions were solicited from administrations on propagation information relevant to future land mobile telecommunications systems. This document summarizes recently available propagation measurements made in and around houses and buildings and proposes models for several characteristics of such radio channels. Future low-power portable radio communications systems may operate in this environment. Further information is needed concerning propagation in this environment, particularly related to delay-spread characterization--experimental data, analysis, and simulation.

Fundamental limitations on portable radio system parameters and on the application of radio link techniques result from the effects of radio propagation within and around houses and buildings. This is a very complex and difficult radio propagation environment because the shortest direct path between any pair of fixed and portable set locations is usually blocked by walls, ceilings or other objects. Often many attenuated propagation paths exist between any pair of locations. The different propagation paths are produced by reflections from walls, ceilings and objects. Each path may have a different time delay and a different attenuation. The overall result is a complex and widely varying multipath transmission channel between fixed radio terminals (henceforth called ports) and portable sets. Because of the complexity and variability, analytical determination of many of the multiple-path propagation parameters is not feasible. It is usually necessary to resort to measurements and to empirically determine statistical distributions of many of the parameters for different locations of ports and portable sets.

Radio transmission over a port-to-portable radio link is reciprocal. That is, the locations of signal transmission and of signal reception can be interchanged without changing the received signal characteristics. This location interchange does not include the interchange of the antennas and requires some specific conditions on antenna, receiver and transmitter impedances. It is sufficient (but not necessary) that these impedances all be real and of the same magnitude. Because of reciprocity, the discussion can proceed on the basis of transmission in either direction without loss of generality.

The portable radio environment is qualitatively similar to the mobile (vehicular) radio environment.[1] [2] [3] [4] [5] [6] [7] [8] [9] That is, propagation is dominated by the effects of shadowing and reflections from walls, objects and the ground. Therefore, some of the small-scale multipath propagation characteristics are the same in both environments. However, in the portable environment, antenna heights will be lower, or antennas will be located within buildings, and distances between transmitters and receivers will be shorter than in the mobile environment. These physical differences cause quantitative differences between some of the large-scale portable and mobile propagation parameters discussed in the following sections. Since there have been more mobile radio propagation measurements made, these will be used to extend the portable radio propagation picture where appropriate.

Most portable and mobile radio measurements have been made at frequencies near 1 GHz. These results can be extrapolated with some confidence over a frequency range of at least 2:1; therefore they are applicable to some of the identified ranges of potential portable and mobile radio frequencies.

I. Multipath Time Delay Structure

The multipath time delay structure, i.e., the "echo pattern," of portable radio transmission channels can be measured by transmitting wide-band pulse-like signals between potential port and portable locations. Figure 1 illustrates measurements made at 850 MHz with a 0.025 μ sec. time resolution. The measurements were made between locations within a large building.[10] [11] [12] The graphs show the relative average power received as a function of propagation time delay. A measure of the widths of such averaged power delay profiles or power impulse responses is needed in order to determine limits on the digital transmission rates possible over such radio channels.[1] [2] The zero references for the decibel power level and the time delay scales on the figures are arbitrary.

A. Small Scale Signal Variations

The power level at a particular delay in Figure 1a represents the average of the power level received at that delay for eight different receiver locations within a 4 foot square area.[10] The power values that were averaged were in power units (watts), not in dB. The transmitter location was fixed. The power level at a particular delay fluctuates from receiver location to receiver location within a small area and with motion of people in the aisles of the building. An example of these fluctuating power levels is seen in Figure 2. The figure shows the eight individual measurements of power level versus delay used to perform the averaging operation described above to produce the results of Figure 1a. These fluctuating power levels are indicative of the existence of propagation paths with time delays that differ by less than the resolution of the measurement.[2] [3] For example, the measurement resolution of .025 μ seconds corresponds to a path distance resolution of 25 feet. Many of the walls of rooms and aisles in the building are separated by 5 to 10 feet, much less than the 25 foot resolution. The signals received over unresolved paths have phases that vary many degrees with receiver location changes on the order of an inch, since the wavelength is only 14 inches. These phase changes cause the unresolved multipath signals to add in phase at some locations and out of phase at others, producing the observed fluctuations. The unresolved-path signal fluctuations are similar to the fluctuations of a single-frequency signal illustrated in a later section.

Similar wideband multipath measurements have been made in mobile radio environments.[2] [3] [4] [5] [6] [7] [8] [9] Unresolved-path signal fluctuations are shown in references 2 and 3. The multiplicity of unresolved paths at specific delays was illustrated by simultaneously resolving the paths in delay and in Doppler frequency shift caused by vehicle motion. The Doppler frequency shift of each path is related to its angle of arrival at the receiver location.[2] [3] [7] Reflections from room and hallway walls within buildings are expected to produce wide angle-of-arrival distributions similar to the wide distributions observed from reflections from building walls along streets.

The unresolved paths within a resolved profile peak in Figure 1a probably result from reflections from walls and other objects near the transmitter or the receiver. Angles to these nearby reflectors are distributed throughout 360°. The individual peaks probably result from the attenuated direct path and from walls defining large open areas or located at the ends of hallways. Signals arriving over the longer delayed paths all experience close-in reflections similar to those arriving over the shorter paths. For example, if the receiver is within a room, the unresolved paths probably result from reflections from the room walls and from objects within the room. Signals entering the room after being reflected from a faraway wall (i.e., delayed several tenths of a μ sec.) are still subjected to close-in reflections within the room.

Averaging out the signal fluctuations caused by the phase changes of the unresolved shorter paths yields a picture of the magnitudes of the reflections at various delays. Nearly the same power average results from any set of measurements taken within the same small area. This occurs because the magnitudes of the dominant reflections at the longer delays do not change signifi antly for small changes in receiver (or transmitter) location of a few wavelengths, that is, for motion over small-scale distances.

The average received power within a small area is the integral of a power delay profile with proper calibration of the power density scale. That is, average power received, $\overline{P_a}$, is

$$\overline{P_a} = K \int_0^\infty P(\tau) d\tau \qquad (1)$$

where $P(\tau)$ is the power delay profile scaled in power units (watts), τ is time delay and K is the overall power scaling factor for the profile.

The time-varying multipath transmission channel represented by a power delay profile (power impulse response) has been called a G[illegible] Channel or GWSSUS channel.[14] [15] [2] [3] [4] [5] [6] The word "Gaussian" (G) refers to a Gaussian random process[1] for describing the fluctuations of the unresolved path signals at each delay. A Gaussian process has an envelope that is Rayleigh distributed. It was shown for mobile radio multipath propagation that the envelope fluctuations at a particular delay can usually be approximated well by a Rayleigh distribution.[2] [3] The sum of a large number of signals with random amplitudes and uniformly distributed random phases approximates a Gaussian process. By the central limit theorem,[16] the approximation continues to improve as the number of signals increases. The portable radio multipath channel is similar to the mobile radio channel since both have a large number of unresolved paths resulting in a large number of random signals at each delay. Therefore, the fluctuations at each delay for portable radio channels are also expected to be well approximated by Gaussian random processes.

The term "wide sense stationary" (WSS) refers to the average or means being the same, i.e., statistically stationary, for different collections of samples taken from the same area. The random phase addition process for motions over small-scale distances results in an approximately stationary power average at each delay. Again, in the similar mobile radio environment, it was shown that the power averages were approximately wide sense stationary[2] [3] over small-scale distances.

The term "uncorrelated scattering" (US) refers to the correlation between signal fluctuations at different delays. The uncorrelated property results if the Doppler spectrum is different for different delays, i.e., if the angle-of-arrival spectrum is different. Different Doppler spectra at different delays were also shown for mobile radio channels[2] [3] [7] and again can be expected for the portable radio environment.

The averaged power delay profiles, $P(\tau)$, are then the quantities needed to describe the GWSSUS channels for conditions that are appropriate to digital portable radio multipath channels.[13] [14] [15] [17] These conditions are that 1) the width of the signaling pulses transmitted over the channel is much greater than the delay spread defined later, and 2) the pulse transmission rate (i.e., the baud rate) is much greater than the variation rate of the small scale signal fluctuations (i.e., the Doppler spectrum width). If these conditions are not satisfied, low error rate transmission is not generally possible over the channel. When the conditions are met, the power delay profile is then

$$P(\tau) = \langle |h(\tau)|^2 \rangle = \langle |p(\tau) * g(\tau)| \rangle \qquad (2)$$

where the brackets $\langle\ \rangle$ indicate averaging over an ensemble of small-scale locations, the $*$ indicates convolution, the $h(\tau)$ are samples of complex bandlimited bandpass impulse responses of the random multipath medium, the $g(\tau)$ are samples of the complex bandpass impulse responses of the medium without bandlimiting, and $p(\tau)$ is a function representing the bandlimiting by the equivalent pulse of the wideband signal used to probe the propagation medium.[6] [18] If the width of $p(\tau)$ is much less than the spread of $P(\tau)$, as in Figure 1, the bandlimiting effect of $p(\tau)$ is insignificant.

The error rates for digital transmission through multipath channels, and particularly GWSSUS channels, are most strongly dependent on the delay spread or width of the power delay profile defined as the square root of the second central moment.[13] [14] [15] [17] That is

$$\text{delay spread} = \left[\frac{\int_0^\infty (\tau - D)^2 P(\tau)\, d\tau}{\int_0^\infty P(\tau)\, d\tau} \right]^{\frac{1}{2}} \tag{3}$$

where the average delay D is

$$D = \frac{\int_0^\infty (\tau)\, P(\tau)\, d\tau}{\int_0^\infty P(\tau)\, d\tau} . \tag{4}$$

The delay spread for Figure 1a is about 0.25 μ second.[10] As an example, a non-equalized channel transmitting binary biphase modulation with raised cosine pulses and differential detection (i.e., DPSK) would have an irreducible bit error rate[1] of 10^{-3} for a bit rate of about 300 kilobits/second and the 0.25 μ second delay spread of Figure 1a. The irreducible error rate is the error rate that occurs at high signal-to-noise ratios for which the noise contribution to errors is negligible. The error rate depends somewhat on the shape of the power-delay profile; however, the effect of profile shape is much less than the statistical uncertainty of the knowledge of the delay spread statistics that exists because of the limited number of measurements that are available. Also, different types of digital modulation and different pulse shapings have different susceptibilities to delay spread. Further analysis, computer simulation and laboratory experiments are needed to assess the susceptibilities of the different modulations that are appropriate candidates for portable radio systems.[19] [20]

B. Large-Scale Signal Variations

Moving the receiver (or transmitter) to a different room (or a different street or building) results in different dominant reflecting surfaces at longer delays and in different attenuations of shorter, nearly direct, paths. Therefore, averaged power-delay profiles from different rooms, etc., are qualitatively and quantitatively quite different. Since the reflection magnitudes and the number of reflectors are different, the total average received power is different in different locations also.

The averaged power delay profile in Figure 1b was measured in a different location from the one in Figure 1a. Comparison of the two figures graphically illustrates the gross differences between profiles measured for different transmitter-receiver locations. The relative power scales (the power levels representing 0 dB) are also different by many dB for Figures 1a and b.

The large differences between power-delay profiles show that the multipath propagation process is only approximately statistically stationary (quasi-stationary) over small areas and is highly non-stationary over large distances, from room to room, from building to building, etc.

Since the single parameter, delay spread, dominates irreducible radio link error rate, two-step modeling of the multipath channels is appropriate.[2] [8] Small areas can be modeled as GWSSUS channels and their power-delay profiles and delay spreads determined. Then distributions of delay spread can be used to determine the highest bit rate providing the desired error performance over a specified fraction of the overall portable radio environment.

Examples of such distributions of delay spread measured at 850 MHz are shown in Figures 3 through 5. Figure 3 shows the cumulative distributions of time delay spread measured in

two office buildings differing in linear dimensions by more than a factor of three.[12] The solid curve (1) shows the delay distribution measured within the larger building, while the dotted curve (2) shows the distribution measured within the smaller building. The distributions are similar, and the worst-case time delays observed for the larger (250 nanoseconds) and smaller (220 nanoseconds) are nearly identical. This could be caused by reflections from a hill immediately behind the smaller building.

Figure 4 shows the cumulative distribution of delay spread (solid curve 1) measured at the smaller office building over paths from locations within the building to simulated port locations within a few hundred feet outside the building.[11] The dotted curve (2) shows the corresponding distribution measured for similar inside-to-outside paths at a two-story residence on a one-acre flat lot. The distributions are similar, with worst-case delay spreads around 320 nanoseconds.

The presence of a strong direct path between the transmitter and receiver can significantly reduce the time delay spread observed. Figure 5 shows cumulative distributions of delay spread in the large office building of Figure 3, when the receiver was in an aisle and the transmitter was in the same aisle or one of its rooms (one aisle coverage), and in the adjacent aisles and rooms as well (three aisle coverage).[12] The maximum delay spread observed drops to under 100 nanoseconds in the former case. This result has been seen consistently in all similar measurements.

The measurements above and all others from references 10,11, and 12, other similar measurements in houses and other buildings, and the mobile radio measurements in residential areas[3] suggest that bit rates of a few hundred kilobits/second should be usable for ports inside buildings and for outside ports having antenna heights less than 30 feet and ranges to portable sets on the order of 1000 feet.

It should be noted that delay spreads are often several microseconds in mobile radio environments with base station antenna heights of a hundred feet or more and distances between base-stations and mobiles of over a mile. The high base station antennas strongly illuminate reflecting surfaces (walls, hills, etc.) several miles away. Buildings between base stations and mobiles sometimes attenuate shorter, more direct, paths more than paths to the farther-away reflectors. Thus, the far-out paths cause propagation delays of many microseconds and can be significant in overall received power delay profiles for such mobile radio channels. The lower antenna heights for ports result in greatly reduced illumination of faraway reflecting surfaces because intervening attenuating objects (buildings, hills, etc.) are more likely to exist. Also, shorter port-to-portable distances decrease the attenuation of more direct and shorter reflection paths and increase the relative attenuation to faraway reflectors. These effects produce the significantly lower delay spread values observed in the portable radio environment as compared to the mobile radio environment.

In summary, the small-scale multipath time-delay characteristics that depend largely on wavelength and uniform angle-to-arrival distributions are similar for portable and mobile radio environments. These small-scale characteristics include the characteristics of the signal fluctuations at specific delays that are consistent with the GWSSUS channel description and were discussed in the previous section. In contrast, the large-scale multipath parameters that depend on the gross structure (locations and magnitudes) of reflecting surfaces are significantly different for portable and mobile radio environments. These large-scale characteristics include average power, delay spread and higher order central moments of the averaged power-delay profiles that represent different GWSSUS channels.

II. Narrowband Propagation Characteristics

The time-delay structure and delay spread described in the previous section limit the transmission rate and thus the bandwidth of signals transmitted over the multipath channels. Once the signal bandwidth is restricted to being much less than 1/(delay spread), i.e., pulse width >> delay spread, then narrowband signal descriptions and statistics become of greater interest. The signal bandwidth limitation essentially requires negligible change in the channel transfer function

with frequency throughout the bandwidth of the signal. That is, the multipath signal variation or fading becomes nearly flat over the signal bandwidth. The transfer function is, of course, the Fourier transform of the bandpass impulse response, $g(\tau)$, discussed in Section I.A. For the conditions that the width of $p(\tau)$ is much less than the delay spread, the measured $h(\tau) = g(\tau) * p(\tau) \approx g(\tau)$, and the transfer function is approximately the Fourier transform of $h(\tau)$.[6] [18]

The narrowband signal statistics appropriate to flat fading narrowband channels then can be determined from single-frequency transmission measurements.

A. Small-Scale Multipath Effects

Narrowband signals transmitted between portable sets and ports either inside or outside buildings experience large amplitude and phase variations as the portable sets move over small-scale distances on the order of a wavelength. These variations are a result of the random phase additions of the signals arriving over many paths. The paths include the resolved and unresolved paths illustrated and discussed in previous sections. The narrowband signal variations are caused by the same random phase mechanism as the variation at specific delays caused by unresolved paths.

An example of measurements of the envelope of single frequency small-scale variations shown in Figure 6. The signal level recording was made at 900 MHz by moving a small antenna a distance of 4 feet within a building.[21] The transmitting and receiving antennas were copolarized, i.e., oriented with like polarization. A Rayleigh distribution is usually a good approximation for the statistics of the envelope of multipath signal variations.[1] [21] [22] [23] Figure 7 shows cumulative signal envelope distributions measured at 815 MHz for several small areas (4 feet square) within and outside a house.[22] Signal envelopes measured in small areas that have walls blocking the direct path between transmitter and receiver are approximately Rayleigh distributed. The envelope distribution from the outside area departs significantly from Rayleigh because of a strong direct path. The areas with stronger direct paths experience higher signal levels than those that have well-blocked direct paths. The low-signal areas dominated by multipath are those of most concern in determining portable radio system coverage and performance. Therefore, departures from Rayleigh for large-signal areas will not affect the accuracy of the Rayleigh model for most system analysis applications.

The multipath signals received in the low signal areas can be modeled[1] [24] as

$$y_c(z, t) = L(z)\, R(z, t) e^{j\omega t + j\phi(z,t)} \tag{5}$$

where $y_c(z, t)$ is the copolarized received signal, $\omega = 2\pi f$ with f the carrier frequency, t is tim and the antenna is assumed to be moving in translation in the z direction. The amplitude funct or envelope $R(z, t)$ is Rayleigh distributed with a stationary mean (or median) of unity within a small-scale area[1] [21] [22] [24] [23] where the power delay profile is stationary as discussed earlier. The Rayleigh probability density function, $p(r)$, is given[1] [25] by

$$p(r) = \frac{r}{N} e^{-r^2/2N} \tag{6}$$

where the median is $1.1774\sqrt{N}$ and the mean is $\sqrt{\frac{\pi N}{2}} \approx 1.25\sqrt{N}$. In (5), the phase, $\phi(z, t)$, is a resultant from a number of paths that are many wavelengths long, as in mobile radio. Therefore, it is reasonable to expect any value of $\phi(z, t)$ to be equally likely,[1] i.e., $\phi(z, t)$ is uniformly distributed from 0 to 2π. Often $\phi(z, t)$ experiences nearly π abrupt changes as the signal envelope goes through nulls. The t variation in ϕ and R result from motion of objects in the propagation paths, i.e., trees blowing in the wind, doors opening, people moving, and occurs with non-moving antennas. The z variation results from antenna motion and can be replaced in (5) by $z = vt$, where v is the antenna velocity. In most portable radio environments, the time variation resulting from motion of antennas is significantly greater than that resulting from motion of objects. Together, $R(t)\, e^{j\phi(t)}$ with $z = vt$ represents a complex Gaussian random process. That is,

$R(t)\, e^{j\phi(t)}\, e^{j\omega t} = x(t) \cos \omega t + jy(t) \sin \omega t$ and $x(t)$ and $y(t)$ are independent and Gaussian distributed. The variable $L(z)$ in (5) represents the large-scale signal level variation discussed earlier, i.e., the variation from room to room, house to house, inside to outside, over large-scale distances. Large-scale variations are discussed in a following section.

1. Spatial Correlation and Space Diversity

From Figure 6 it is evident that two antennas separated by a few inches, i.e., a fraction of a wavelength at 900 MHz, would not likely be in a deep signal null simultaneously. This lack of correlation of signal levels for spatially separated antennas is the basis of space diversity used to mitigate small-scale multipath signal variations.[1] [25]

Space diversity and diversity combining for the mobile radio environment and for other multipath environments for systems with fixed antenna orientations have been extensively studied.[1] [25] The diversity performance for fixed antenna orientations depends a) on the method used to combine the signals from two or more antennas, i.e., selection of the best signal or cophasing of signals from constant gain or variable gain receivers[1] [25] , and b) on the spatial correlation of the signal envelope variations for the different antennas. The spatial correlation $\rho(\Delta z)$, for the small scale Rayleigh distributed envelope variations is given by

$$\rho(\Delta z) = \overline{R(z, t)\, R(z+\Delta z, t)} \qquad (7)$$

where Δz is the antenna separation and the overbar indicates an average. For mobile radio environments with the angle of arrival of multipath signals uniformly distributed over 0 to 2π, the correlation is small for antenna separations on the order of $\lambda/4$ or greater.[1] [26] As discussed earlier, the angle-of-arrival distribution for multipath in the portable radio environment is expected to be similar to the distribution in the mobile radio environment. However, handheld portable radio equipment will not have a fixed antenna orientation. Therefore, portable radio diversity will be considered again with respect to both spatial signal variations and antenna angular variations in a later section.

2. Frequency Effects

The small-scale multipath effects result from phase addition of signals arriving over many paths distributed randomly in angle of arrival. The phases associated with the various paths are functions of carrier frequency, f, and path lengths.[1] Thus, the distance scale of the signal variation pattern in space represented by Figure 6 is a linear function of frequency. The null spacing is on the order of half wavelength, $\lambda/2$. The correlation function , $\rho(\cdot)$, in (7) is invariant when normalized to wavelength[1] over at least a 10 to 1 frequency range. That is, $\rho(\Delta z/\lambda)$ is invariant with frequency. The envelope variations remain Rayleigh distributed at any frequency as long as the physical environment produces severe multipath propagation that includes many propagation paths.

B. Large-Scale Variations

The mean or median of the small-scale Rayleigh-distributed multipath variations is approximately statistically stationary within small-scale areas.[22] That is, the multipath variations are stationary within areas where the overall multipath structure remains relatively constant and therefore the average power-delay profile is stationary. When the overall multipath structure is different, i.e., there are different reflection coefficients and/or different numbers of paths, the average power is different as represented by the average of the multipath variations. This narrowband average is the same as the area under the average power-delay profile (1). This is accounted for in (5) by normalizing to unity either the mean or median of the Rayleigh distributed variation, $R(\cdot)$ and representing the large-scale variation by $L(z)$.

1. Distance Dependence

Figure 7 is a scatter plot of median 815 MHz signal levels for many small scale areas [27]. Each data point represents a value of $L(z)$ relative to its value for a free space path length [illegible]

feet. The vertical scale on the figure is distance, z, between port locations and small areas within which there is small-scale portable set motion. The data points are from several different port locations and several different small areas inside and around 8 houses in relatively flat terrain. The small areas were 4 feet square and include locations on first and second floors, in basements, and outside close to the houses. The port antenna height was 27 feet above ground. The dotted line represents equivalent free space propagation, $(1/z^2)$, between port and portable locations. The other straight lines are least-square regression lines through the data points indicating a strong dependence on distance in the highly scattered data. For all the data, the regression line slope is $z^{-4.5}$, indicating $L(z)$ proportional to $z^{-4.5}$.

Figure 9 is a scatter plot similar to Figure 8, but of median 815 MHz signal levels measured in a two-story office/laboratory building with a long straight corridor.[27] The circles and squares represent median signal levels measured between locations in corridors and offices or laboratories opening off the corridors. Unfilled circles and squares indicate measurements made with transmitter and receiver on the same floor. The least-square regression line slope for these measurements is $z^{-3.6}$. Filled circles and squares indicate measurements made with transmitter and receiver on adjacent floors. The least-square regression line slope for these measurements is $z^{-3.9}$. The similar slopes suggest a relatively constant isolation between floors. The value of this cross-floor isolation is 26 dB at 150 feet. Measurements in other buildings suggest that this relatively large value may be due to the presence of solid steel concrete pour forms in the floors.

The "X" symbols in Figure 9 indicate median signal levels measured with both transmitter and receiver on the main corridor, within optical line of sight. Except at the extreme ends of the corridor, only 2-4 dB of rapid signal variation was observed, suggesting the presence of a single dominant propagation path. The received signal level is greater than the free-space level over the entire distance span (by up to 11 dB in the 50- to 125-foot distance range), suggesting channeling of energy by the corridor.

An important inference from Figure 9 is that the received signal level can decrease abruptly by 25 dB or more at the transition from the corridor to an adjoining room is made (a distance of 20 feet or less).

Other measurements have been made in the 800 to 900 MHz range between locations (port and portable) entirely within large buildings.[23] [28] The results show similar scatter of measured values about a distance-dependent regression line. Distance dependences ranging from about z^{-2} to z^{-6} were observed for typical office and laboratory buildings with values of z^{-4} or z^{-5} appearing to be typical.

2. Statistics of Large-Scale Variation

After removal of the distance dependence from data representing $L(z)$, the remaining variation is approximately normally (Gaussian) distributed in dB, with a mean of 0. This is shown for the Figure 8 data in Figure 10.

These empirical observations suggest modeling $L(z)$ as a log-normally distributed random variable with a mean that varies with distance. That is, define a new random variable $U(z)$ as

$$U(z) = 10 \log_{10} L^2(z) . \tag{8}$$

Then $U(z)$ is Gaussian (normally) distributed with probability density

$$f_U(u) = \frac{1}{\sigma\sqrt{2\pi}} \exp\left[-(u-m)^2/2\sigma^2\right] \tag{9}$$

where the standard deviation, σ, is in dB and the mean, m, in dB varies with distance as

$$m \propto 10 \log_{10} (z^n) . \tag{10}$$

For example, the residential data from Figures 8 and 10 are represented by $n = -4.5$ and σ between 10 and 11 dB.

The excess rate of change of signal level over the free space rate of z^{-2} is partially accounted for by the reflection from the ground.[22] [24] [29] For propagation between two points separated a distance z and at heights h_r and h_t above flat ground, the power density, P_r, at a receiver point relative to the transmitted power density, P_t, at the other point is given by:[24] [30]

$$\frac{P_r}{P_t} = \frac{4}{z^2} \sin^2 \left[\frac{2\pi h_r h_t}{\lambda z} \right]. \qquad (11)$$

For large z, ($z >$ 1000 feet for typical port and portable heights), this approaches $P_r/P_t \propto z^{-4}$. Additional variation is probably due to additional attenuation resulting from reflection from and propagation through intervening houses and trees. The additional attenuation may be better represented by a dB/distance, i.e., an e^{-z} or 10^{-z}, variation rather than by a power-law variation, z^n, since the number of attenuating objects (houses, trees, etc.) increases more or less uniformly with distance, however, this has not been experimentally demonstrated. If this is true, the range of distances may be limited over which a given value of n and z^{-n} approximates the distance dependence of $L(z)$.

The description of $L(z)$ as a log-normally-distributed random variable with a distance-dependent mean as in (8-10) is qualitatively the same as the description for mobile radio environments.[1] [31] The magnitude of the distance-dependence exponent appears a little greater and the standard deviation somewhat larger for the measurements in the portable environment. The stronger distance dependence is probably a result of the lower port antenna heights with respect to ground and the deeper immersions of the port antennas within the buildings and trees. The larger standard deviation undoubtedly results from the variability of the additional attenuation through walls into the interiors of houses and buildings.

3. Effect of Antenna Height

The major overall effect of varying the height of either the port or portable antenna in a residential environment occurs because of the proximity of the ground.[29] The height effect is illustrated in equation (11). This remains true for small changes in height that do not result in a major change of the antenna in relation to its surrounding scattering environment; that is, as long as the height changes do not involve transitions through the height of treetops and houses. For typical port and portable heights and distances generally greater than 1000 feet, P_r/P_t in (11) becomes proportional to h^2. That is, P_r/P_t changes by 6 dB for a height change of either port or portable antenna by a factor of 2. Of course, this deterministic ground effect has random variation superimposed because of the effect of the multiple propagation paths.

The effect of antenna height above ground is illustrated in Figure 11. The open 0 and + data points indicate signal medians from measurements in and around 4 houses at 815 MHz.[29] The ordinate of a data point represents the median signal measured in a four-foot-square area for a port location using a 27 foot high port antenna, as in Figure 8. The abscissa of the point represents the median signal measured for the same four-foot-square area and the same port location, but using a 12.5 foot high port antenna. Port to portable distances, z, were greater than 1000 feet. The solid and dashed lines represent equation (11) assuming that the randomness of the signal variations is the same for both antenna heights. The solid data points and the • represent averages of all measurements outside, inside houses on the first floor, and in basements as indicated on the figure. The tight cluster of the data around the lines is consistent with the expectation from ground reflection.

4. Frequency Effects

The frequency dependence of the mean, m, in (10) is made up of several factors. One of the factors for residential areas is the $\sin^2[\frac{2\pi h_r h_t}{\lambda z}]$ term in the power density at a receiver location

caused by reflection from the ground (see 11). Another factor is the proportionality to λ^2 of the effective area, A_e, of a small (on order of $\frac{\lambda}{2}$ or less) dipole[32] or small loop antenna. Received signal power, equivalent to $[y_c(\ )]^2$ of (5), is the product of the power density, P_r, in (11) and A_e of the receiving antenna. For large separations, z, i.e., for $z > 1000$ feet, and for typical port and portable h_r and h_t, the $\sin^2$ term can be replaced by the square of its argument. Then $P_r A_e$ is independent of λ in this large z limit since the λ^2 in A_e cancels the $1/\lambda^2$ in P_r. For residential areas, this leaves only multipath propagation and attenuation through walls for frequency-dependent factors. The ground reflection situation is not clear, however, when both the port and portable antennas are located within a large building.

Available data related to frequency dependence of the mean (or equivalently the median for the Gaussian process) for the portable radio environment are very limited. For mobile radio environments with 600 foot base station antenna heights, Reference 1 indicates that the median large-scale attenuation in urban areas increases weakly with frequency between 100 MHz and 30 GHz. The increase is about 4 dB between 100 MHz and 10 GHz. An increase in average attenuation with frequency is, of course, a decrease in mean signal, m, with frequency. This mobile radio situation is somewhat indicative of the multipath effects outside buildings, at least in an urban environment.

Building penetration attenuation was measured at 860 MHz, 1550 MHz and 2570 MHz for 25 houses in 5 different cities.[33] These measurements suggest a decrease in mean signal, m, of about 2 dB between 860 MHz and 1550 MHz and of about 1 dB from 1550 to 2570 MHz because of the building walls. Of course, in addition to this building attenuation, the frequency-dependence factor for the multipath attenuation between port locations and houses needs to be determined. The mobile radio situation discussed in the previous paragraph is somewhat indicative of the frequency dependence of the multipath environment external to the buildings.

Measurements at 940 MHz and 60 GHz locations within buildings were reported.[34] They were not concurrent measurements and only qualitative comparisons can be made. However, the signal levels were markedly lower at 60 GHz and the authors made coverage estimates for 1 milliwatt transmitters. In a building with metal partition walls, estimated coverage at 940 MHz extended about 2 rooms from a port location in a room i.e., a distance of about 30 feet. For a similar environment, estimated coverage at 60 GHz was only within the same room and the immediately adjacent hallway. In frame buildings with plasterboard walls, estimated 940 MHz coverage was about 100 feet. For similar buildings, 60 GHz coverage extended only to adjacent rooms. These results include all transmission factors between port and portable locations within th buildings.

The cited portable radio measurements and the mobile radio estimates are not directly comparable; however, the available information suggests that the mean in (10) decreases significantly with frequency above 1 GHz for portable radio environments.

Measurements at 57 MHz, 177 MHz and 575 MHz were reported[35] for many locations on rooftops and within large buildings in New York City. Cumulative signal level distributions from these measurements can be used to infer relative average signal levels between areas outside and areas inside the large buildings. The relative levels were about 2 or 3 dB stronger at 575 MHz than at 177 MHz. The levels were about 2 dB stronger at 177 MHz than at 57 MHz.

Measurements at 460 MHz and 890 MHz were reported between outside locations and locations inside a building.[36] The parameter measured was excess attenuation, i.e., the attenuation caused by the building, ground, etc., in addition to the free space, $f^2 r^2$, attenuation. The results for this one building suggest an excess attenuation of 3 or 4 dB greater at 460 MHz than at 890 MHz. This suggests an average signal level of about 2 dB greater at 460 MHz than at 890 MHz when the 5.7 dB for the free space f^2 ratio is included. These measurements are not directly comparable with the building attenuation measurements since they include all path effects.

The frequency dependence [illegible] below 1 GHz is less clear than above 1 GHz. Measurements suggest that [illegible] from 1 GHz to 500 MHz but it may start to decrease

with frequency below 500 MHz. As with many of the propagation effects, the frequency dependence of m is probably also a function of the type and construction of buildings. Any overall effect, then, can only be obtained by averaging over many building types and constructions, which will result in a large standard deviation around the average.

5. Correlation and Macroscopic Space Diversity

Portable sets within a region of ports often could be served from more than one port, particularly when located at nearly maximum distance from the nearest ports.[37] The buildings and other obstructions along the paths from a portable set to the different nearest ports are likely to be different. These obstruction differences can be expected to cause different large-scale signal variations for the different paths,[38] that is, the large-scale variations can be expected to be partially uncorrelated. The selection of the port-to-portable path resulting in the best signal could provide diversity to mitigate the large-scale or macroscopic signal variations. The effectiveness of this macroscopic diversity depends on the correlation among the large-scale signal variations for the different ports.

The curves in Figure 12 from Reference 38 show cumulative signal level distributions for measurements of large-scale signal variations made within and around 8 houses.[24] The curves compare 2 branch and 3 branch selection macroscopic diversity with the signal distributions for a single port (i.e. 1 branch). The 2 branch diversity selects the best large-scale signal between pairs of ports; the 3 branch selects the best from sets of 3 ports. The signal levels accumulated are the median levels from four-foot-square areas as described for Figure 8. The subset of data accumulated for Figure 12 has nearly the same 10 dB standard deviation as the overall data set shown in Figures 8 and 10. The dashed theoretical macroscopic diversity curves in Figure 12 assume that the large-scale signal variations can be separated into two parts, l and p. One part of the variation, l, is correlated among the ports while the other part, p, is uncorrelated. For the dashed curves in the figure, the uncorrelated part of the signal variation was assumed to have a standard deviation, σ_p, of 8 dB contributing to the overall standard deviation of $\sigma_T = 10\ dB$. The theoretical model assumed that the l and p signal parts were independent so that the total standard deviation was related to the standard deviations of the parts as

$$\sigma_T^2 = \sigma_p^2 + \sigma_l^2 \qquad (12).$$

The separation of σ_p and σ_l with $\sigma_p = 8$ dB for the dashed curves in Figure 12 provides a reasonable fit to the data in the portion of the distributions near 1%. Other subsets of the available data having differing values of σ_T are also fit well with this model using $\sigma_p = 8$ dB.[38]

C. Crosspolarization Coupling

The reflecting and scattering of radio signals in the multipath propagation environment also couple power from the transmitted polarization into the crossed (orthogonal) polarization. At any receiving point, the power in the crossed polarization also arrives over paths with different time delays and different angles of arrival. The multipath signal received on a crosspolarized antenna, $y_x(z,t)$, can be modeled similarly to the copolarized signal in (5) as

$$y_x(z,t) = X(z)L(z)R_x(z,t)e^{j\omega t + j\phi_x(z,t)} \qquad (13)$$

where the corresponding variables have the same properties as the copolarized signal variables in (5). The subscript x indicates the variable is associated with the crosspolarized signal. $R_x(\,)$ and $\phi_x(\,)$ have the same statistical distributions and normalizations as $R(\,)$ and $\phi(\,)$, but they may have different instantaneous values. The variable $X(z)$ is a slowly varying crosspolarization coupling coefficient[22] [39] with variation on the scale of $L(z)$. That is, $X(z)$ represents the large-scale crosspolarization coupling averaged over the small-scale variations.

Figure 13 is a scatter plot of crosspolarization coupling $X(z)$ as a function of $L(z)$ measured in and around 8 houses.[39] The $L(z)$ scale is the same as that on Figure 8. Each data

point represents $X(z)$ for a 4-foot-square small area. In the region of low signal levels, the crosspolarization couplings are all greater than -6 dB and range up to slightly over 0 dB. Some of the scatter in the data is due to measurement error and statistical uncertainty. Similar measurements in large buildings[39] show even larger values of crosspolarization coupling. Measurements in Tokyo on sidewalks also yielded values in the -5 to -7 dB range.[40]

1. Random Orientation and Antenna Diversity

Changes in the orientation of portable radio antennas could superimpose additional signal variations on the multipath variations.[41] [42] This could occur because of polarization misalignment, if there were little crosspolarization coupling. A well-disciplined user who has great need for portable communications, e.g., a policeman or fireman, might be expected to hold a handset antenna in a fixed orientation; however, such an orientation restriction is not likely to be accepted by a casual general user. A person using a portable communications set can readily change its orientation through any vertical or horizontal angle. Such a wide range of angular variation will result in essentially random orientation of the antenna or antennas. The effects of the random orientation on the signal are mitigated by the crosspolarization coupling in the multipath propagation medium. Antenna diversity can further reduce the orientation effects as well mitigating the small-scale multipath signal variations.

Cumulative distributions of relative signal-to-noise ratio (S/N) in Figure 14 illustrate signal improvements from crosspolarization coupling and diversity. These distributions were obtained by computer simulation[41] [42] assuming that multipath propagation signals arrive at a portable set location in the horizontal plane but uniformly distributed in azimuth angle around the location. The Rayleigh distribution would result from moving a fixed-oriented vertically polarized antenna through a region excited by a vertically polarized fixed antenna (e.g., at a port). The distribution labeled "2 Br Mobile Select" would result from the use of selection diversity, i.e., always selecting the antenna with the strongest signal, between two such fixed oriented antennas separated by $\lambda/4$ and moving in the same multipath region. The diversity improvement results because of the low spatial correlation of the multipath signal variation discussed earlier. The solid, dashed, and dotted distributions would result from the following radio link condition: a) the use of selection diversity between a vertically polarized and a horizontally polarized antenna at a port, b) a single antenna on a randomly oriented portable set and c) cross polarization coupling $X(z)$ in the multipath with the values labeled on the curves. The two distributions to the left of the Rayleigh distribution and labeled 1D or 1L and *v* or *h* are for one antenna (a dipole or a loop) on a randomly oriented portable set and either a vertically polarized or a horizontally polarized antenna on a port. Crosspolarization coupling is either -6 dB or 0 dB as labeled. The curves illustrate the following: a) a decrease in the percentage of time spent at low signal levels (large negative S/N values) resulting from selection diversity and from increased crosspolarization coupling and b) an increase in percentage of time spent at low signal levels because of the random orientation.

2. Polarization Diversity

References 41 and 42 and Section C.1 above discuss the improvement in link reliability obtainable from polarization diversity. Reference 39 indicates that crosspolarization coupling is near 0 dB over paths with no line-of-sight component. Later measurements[43] show that signals received on orthogonal polarizations have low instantaneous correlations and may be used as inputs to any form of diversity combiner.[1] [25] Figure 15 is an example of signals received simultaneously at 815 MHz over a non-line-of-sight path within an office building on two orthogonal polarizations. A dual-polarized microstrip patch receiving antenna was used, with identical patterns on both polarizations. The linearly-polarized transmitter was scanned over a 4-foot square to make the measurement. The low correlation and nearly-equal power levels on the two polarizations are evident.

An example of similar measurements over line-of-sight paths down a corridor is shown in Figure 16. Measurements over such paths show less fluctuation and much lower crosspolarization coupling.

Figure 17 is a histogram of the correlation coefficient between polarizations observed in a large number of measurements such as those of Figures 15 and 16. The measurements presented are for paths within office buildings; however, identical results were observed for residential inside-outside paths. Over non-line-of-sight paths, the correlation coefficients observed were always low enough for polarization diversity to provide nearly ideal diversity gain.[1] [25] For paths with a strong line-of-sight component, polarization diversity would provide protection against random handset orientation.[41]

REFERENCES

1. W. C. Jakes, ed., "Microwave Mobile Communications," New York, John Wiley, 1974.
2. D. C. Cox, "910 MHz Urban Mobile Radio Propagation: Multipath Characteristics in New York City," IEEE Trans. on Comm., COM-21, November 1973, pp. 1188-1194.
3. D. C. Cox, "Delay-Doppler Characteristics of Multipath Propagation at 910 MHz in a Suburban Mobile Radio Environment," IEEE Trans. on Ant. and Prop., AP-20, September 1972, pp. 625-635.
4. W. R. Young, Jr., and L. Y. Lacy, "Echoes in Transmission at 450 Megacycles from Land-to-Car Radio Units," Proc. IRE, Vol. 38, March 1950, pp. 225-258.
5. G. L. Turin, F. D. Clapp, T. L. Johnson, S. B. Fine, and D. Lavy, "A Statistical Model of Urban Multipath Propagation," IEEE Trans. Veh. Tech., VT-21, February 1972, pp. 1-9.
6. D. C. Cox, "Time and Frequency Domain Characterizations of Multipath Propagation at 910 MHz in a Suburban Mobile Radio Environment,' Radio Science, Vol. 7, No. 12, December 1972, pp. 1069-1077.
7. D. C. Cox, "A Measured Delay-Doppler Scattering Function for Multipath Propagation at 910 MHz in an Urban Mobile Radio Environment,' Proceedings of the IEEE, Vol. 61, April 1973, pp. 479-480.
8. D. C. Cox, R. P. Leck, "Distributions of Multipath Delay Spread and Average Excess Delay for 910 MHz Urban Mobile Radio Paths," IEEE Trans. on Ant. and Prop., AP-23, March 1975, pp. 206-213.
9. D. C. Cox, "Multipath Delay Spread and Path Loss Correlation for 910 MHz Urban Mobile Radio Propagation,' IEEE Trans. on Veh. Tech., Special Issue on Propagation, VT-26, November 1977, pp. 340-344.
10. D. M. J. Devasirvatham, "Time Delay Spread Measurements of Wideband Radio Signals Within a Building," Electronics Letters, Vol. 20, November 8, 1984, pp. 950-951.
11. D. M. J. Devasirvatham, "Time Delay Spread and Signal Level Measurements of 850 MHz Radio Waves in Building Environments," IEEE Trans Ant. and Prop., vol. AP-34, November 1986, pp. 1300-1305.
12. D. M. J. Devasirvatham, "A Comparison of Time Delay Spread and Signal Level Measurement Within Two Dissimilar Office Buildings,' IEEE Trans. Ant. and Prop., to be published 1987.
13. P. A. Bello, "Characterization of Randomly Time-Variant Linear Channels,' IEEE Trans. Commun. Syst., CS-11, December 1963, pp. 360-393.
14. P. A. Bello and B. D. Nelin, "The Effect of Frequency Selective Fading on the Binary Error Probabilities of Incoherent and Differentially Coherent Matched Filter Receivers," IEEE Trans. Commun. Systems, CS-11, June 1963, pp. 170-186.
15. P. A. Bello and B. D. Nelin, "The Effect of Frequency Selective Fading on Intermodulation Distortion and Subcarrier Phase Stability in Frequency Modulation Systems," IEEE Trans. Commun Systems, March 1964, pp. 87-101.
16. A. Papoulis, "Probability, Random Variables and Stochastic Processes," McGraw Hill, New York, 1965.
17. C. C. Bailey and J. C. Lindenlaub, "Further Results Concerning the Effect of Frequency-Selective Fading on Differentially Coherent Matched Filter Receivers," IEEE Trans. Comm. Tech., COM-16, October 1968, pp. 749-751.

18. D. C. Cox and R. P. Leck, "Correlation Bandwidth and Delay Spread Multipath Propagation Statistics for 910 MHz Urban Mobile Radio Channels," IEEE Trans. on Comm., COM-23, November 1975, pp. 1271-1280.

19. J. C-I. Chuang, "Modeling and Analysis of a Digital Portable Communications Channel with Time Delay Spread," IEEE Vehicular Technology Conference, Dallas, Texas, May 20-22, 1986, proceedings.

20. J. C-I. Chuang, "Simulation of Digital Modulation on Portable Radio Communications Channels with Frequency-Selective Fading," IEEE Globecom '86, December 1-4, 1986, Houston, Texas, pp. 1120-1126.

21. H. H. Hoffman and D. C. Cox, "Attenuation of 900 MHz Radio Waves Propagating into a Metal Building," IEEE Trans. on Ant. and Prop., AP-30, July 1982, pp. 808-811.

22. D. C. Cox, R. R. Murray and A. W. Norris, "Measurements of 800 MHz Radio Transmission into Buildings with Metallic Walls," BSTJ, Vol. 62, November 1983, pp. 2695-2717.

23. S. E. Alexander, "Characterizing Buildings for Propagation at 900 MHz," Electronics Letters, Vol. 19, September 29, 1983, p. 860.

24. D. C. Cox, R. R. Murray and A. W. Norris, "800 MHz Attenuation Measured In and Around Suburban Houses," BLTJ, July-August 1984, pp. 921-954.

25. M. Schwartz, W. R. Bennett and S. Stein, "Communication Systems and Techniques," New York, McGraw Hill, 1966.

26. R. H. Clarke, "A Statistical Theory of Mobile Radio Reception," BSTJ, July-August 1968, pp. 957-1000.

27. R. R. Murray, H. W. Arnold and D. C. Cox, "815 MHz Radio Attenuation Measured Within a Commecial Building," IEEE Antennas and Propagation Symposium, June 9-13, 1986, Philadelphia, Penna.

28. S. E. Alexander, "Radio Propagation Within Buildings at 900 MHz," Electronics Letters, Vol. 18, October 14, 1982, pp. 913-914.

29. D. C. Cox, R. R. Murray and A. W. Norris, "Antenna Height Dependence of 800 MHz Attenuation Measured in Houses," IEEE Trans. on Veh. Tech., VT-34, May 1985, pp. 108-115.

30. P. A. Mathews, "Radio Wave Propagation, VHF and Above," London: Chapman and Hall, Ltd., 1985, Chapter 2.

31. G. P. Ott and A. Plitkins, "Urban Path-Loss Characteristics at 820 MHz," IEEE Trans on Veh. Tech., VT-27, Nov. 1978, pp. 189-197.

32. Ramo, Whinnery, and Van Duzer, "Fields and Waves in Communications Electronics," John Wiley & Sons, New York, 1965, Chapter 12.

33. P. I. Wells and P. V. Tryon, "The Attenuation of UHF Radio Signals by Houses," US Dept. of Commerce Report, OT Report 76-98, August 1976 and IEEE Trans on Veh. Tech., VT-26, November 1977. pp. 358-362.

34. S. E. Alexander and G. Pugliese, "Cordless Communication Within Buildings: Results of Measurements at 900 MHz and 60 GHz," British Telecom Technology Journal, July 1983, pp. 99-105.

35. G. V. Waldo, "Report on the Analysis of Measurements and Observations, New York City UHF-New York City UHF-TV Project," IEEE Trans. on Broadcasting, Vol. 9, 1963, pp. 7-36.

36. J. Shefer, "Propagation Statistics of 900 MHz and 450 MHz Signals Inside Buildings," Microwave Mobile Radio Symposium, March 7-9 1973, Boulder, Colorado.

37. D. C. Cox, Co-Channel Interference Considerations in Frequency Reuse Small-Coverage Area Radio Systems," IEEE Trans. on Commun., COM-30, January 1982, pp. 135-142.

38. H. W. Arnold, R. R. Murray and D. C. Cox, "Macroscopic Diversity in the Portable Radiocommunication Environment," 1985 North American Radio Science Meeting (URSI), Vancouver, Canada, June 17-21, 1985.

39. D. C. Cox, R. R. Murray, H. W. Arnold, A. W. Norris and M. F. Wazowicz, "Crosspolarization Coupling Measured for 800 MHz Radio Transmission In and Around Houses and Large Buildings," IEEE Trans. on Anr. and Prop., AP-34, January 1986, pp. 83-87.

40. A. Akeyamo, T. Tsuruhara and Y. Tanaka, "920 MHz Mobile Propagation Test for Portable Telephone," Trans. of IECE of Japan, Vol. E65, September 1982, pp. 542-543.

41. D. C. Cox, "Antenna Diversity Performance in Mitigating the Effects of Portable Radiotelephone Orientation and Multipath Propagation," IEEE Trans. on Commun., COM-31, May 1983, pp. 620-628.

42. D. C. Cox, "Time Diversity Adaptive Retransmission for Reducing Signal Impairments in Portable Radiotelephones," IEEE Trans. on Veh. Tech., VT-32, August 1983, pp. 230-238.

43. S. A. Bergman and H. W. Arnold, "Polarization Diversity in Portable Communications Environment," Electronics Letters, Vol. 22, No. 11, May 22, 1986, pp. 609-610.

Figure Captions

Figure 1a Average Relative Power Received as a Function of Time Delay for a Probing Transmitter and Receiver Located in Different Places in a Large Building. The Transmitter and Receiver Locations Were Obscured from Each Other by Walls.

Figure 1b Average Relative Power Received as a Function of Time Delay Similar to Figure 1a. For Figure 1b, the Transmitter and Receiver Were Located in Different Places in the Building than They Were for Figure 1a.

Figure 2 Individual Profiles of Relative Power Received as a Function of Time Delay Used to Make Up the Average Profile of Figure 1a. The Power Scale Has Been Greatly Compressed From the Scale Used in Figure 1a.

Figure 3 Cumulative Distributions of Time Delay Spread for Propagation Paths Within a Large and a Small Office Building. The Solid Curve is the Delay Distribution for the Larger Building. The Dotted Curve is the Delay Distribution for the Smaller Building, Which Had Linear Dimensions Less Than One-Third Those of the Larger Building.

Figure 4 Cumulative Distributions of Time Delay Spread for Propagation Paths from Several Port Locations to Rooms Inside a Small Office Building and a House. The Solid Curve is for Measurements in the Office Building. The Dotted Curve is for Measurements in the House.

Figure 5 Cumulative Distributions of Time Delay Spread for Propagation Paths Within a Large Office Building. The Solid Curve is for Measurements Between a Corridor and Rooms Opening Off the Corridor. The Dotted Curve is for Measurements Between a Corridor and Offices Opening Off That Corridor and Adjacent Corridors.

Figure 6 Small Scale Variations of a Narrowband Signal at 900 MHz as an Antenna is Moved at Different Heights in the Multipath Environment within a Building.

Figure 7 Cumulative Signal Envelope Distributions for Four Small Areas Inside and Outside a House. The Measurements Were Made at 815 MHz.

Figure 8 Scatter Plot of Median 815 MHz Signal Levels for Many Small Areas Within and Outside 8 Houses. Measurements Were Made from Different Port Locations at Different Distances from the Houses.

Figure 9 Scatter Plot of Median 815 MHz Signal Levels Along a Corridor of a Small Office Building. Measurements Were Made Along the Corridor and Between the Corridor and Adjoining Offices on the Same and on Adjacent Floors.

Figure 10 Cumulative Distributions of Large Scale Signal Variations (Scatter) in Figure 8 after Removal of the Overall Regression Line Distance Dependence.

Figure 11 Comparison of Median Signal Levels from Small Areas for Port Antenna Heights of 27 Feet and 12.5 Feet. Measurements Were Made at 815 MHz in Small Areas Within and Around 4 Houses.

Figure 12 Cumulative Distributions of Median Signal Levels from Small Areas for Port Antennas Located at Different Angular Locations Around 8 Houses. The Curves Labeled 2 Branch and 3 Branch Indicate the Selection of the Best Signal in a Small Area from Either 2 or 3 Different Port Locations, Respectively. The 2 and 3 Branch Distributions Indicate the Effectiveness of Selection Macroscopic Diversity as Discussed in the Text.

Figure 13 Scatter Plot of Crosspolarization Coupling as a Function of Median Copolarized Signal Level. Measurements Were Made at 815 MHz Within and Around 8 Houses.

Figure 14 Computer-Simulated Cumulative Distributions of Relative Signal-to-Noise Ratio for Different Antenna and Crosspolarization Conditions Discussed in the Text. The Distributions Indicate the Effects of Random Antenna Orientation, Crosspolarization Coupling and Microscopic Selection Diversity.

Figure 15 Small Scale Variations of a Narrowband Signal Transmitted at 815 MHz on One Linear Polarization and Received Simultaneously on Two Linear Orthogonal Polarizations. The Transmitter and Receiver Locations Were Obscured from Each Other by Walls. The Two Signals Have Nearly Equal Average Powers and are Nearly Uncorrelated.

Figure 16 Small Scale Signal Variations Received Simultaneously on Two Linear Orthogonal Polarizations as in Figure 15. The Transmitter and Receiver Locations were Within Line of Sight Along a Corridor. The Copolarized Signal Has Little Fluctuation and is Much Stronger than the Crosspolarized Signal.

Figure 17 Histogram of Correlation of Small Scale Signal Variations Received Simultaneously on Two Linear Orthogonal Polarizations, as in Figures 15 and 16. Little Correlation is Seen for Paths Obscured by Walls. Higher Correlation is Seen for Paths Where the Transmitter and Receiver were Within Line of Sight.

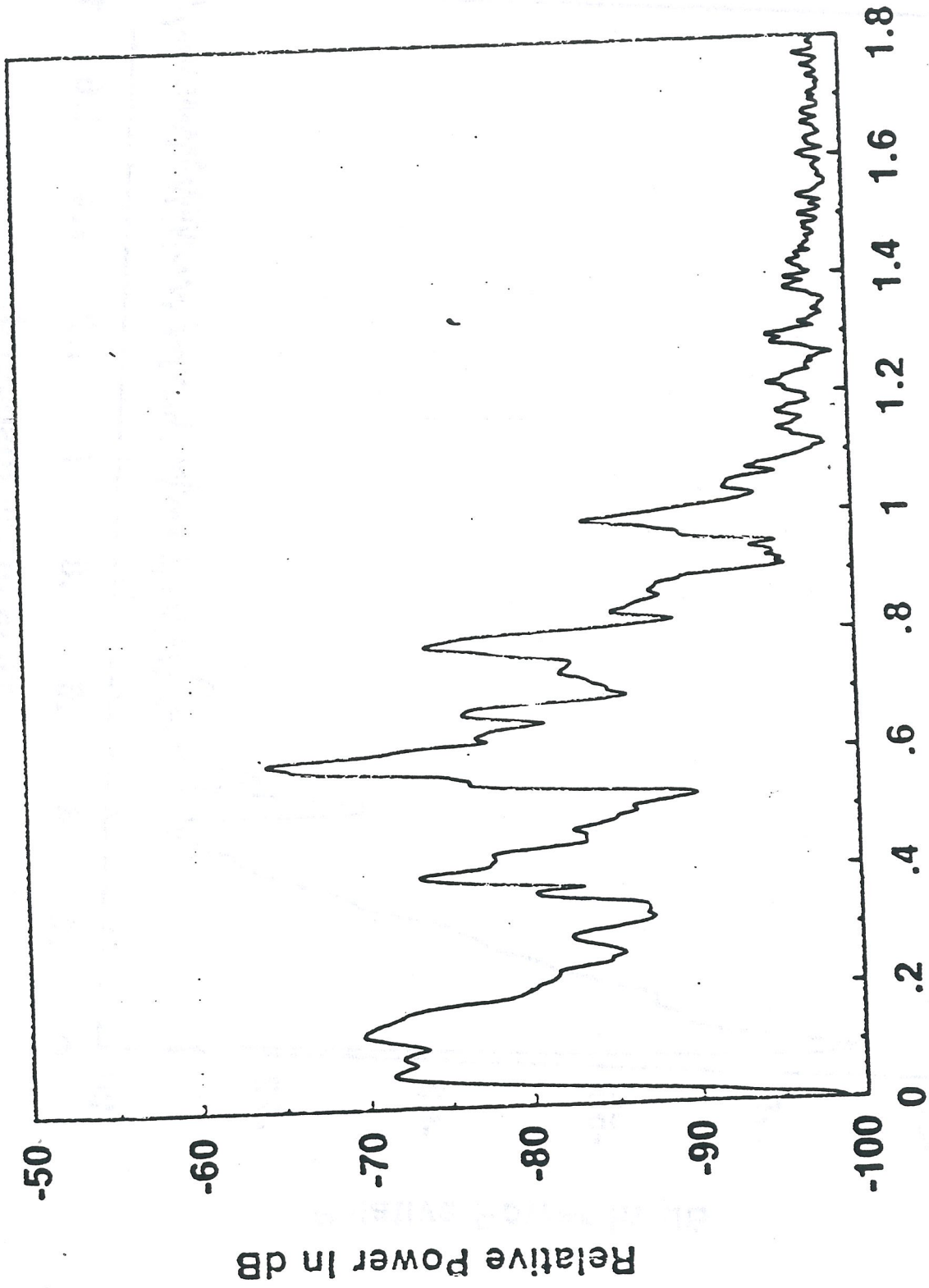
Relative Power in dB
-50
-60
-70
-80
-90
-100
0
.2
.4
.6
.8
1
1.2
1.4
1.6
1.8
Time in Microseconds

FIGURE 1a

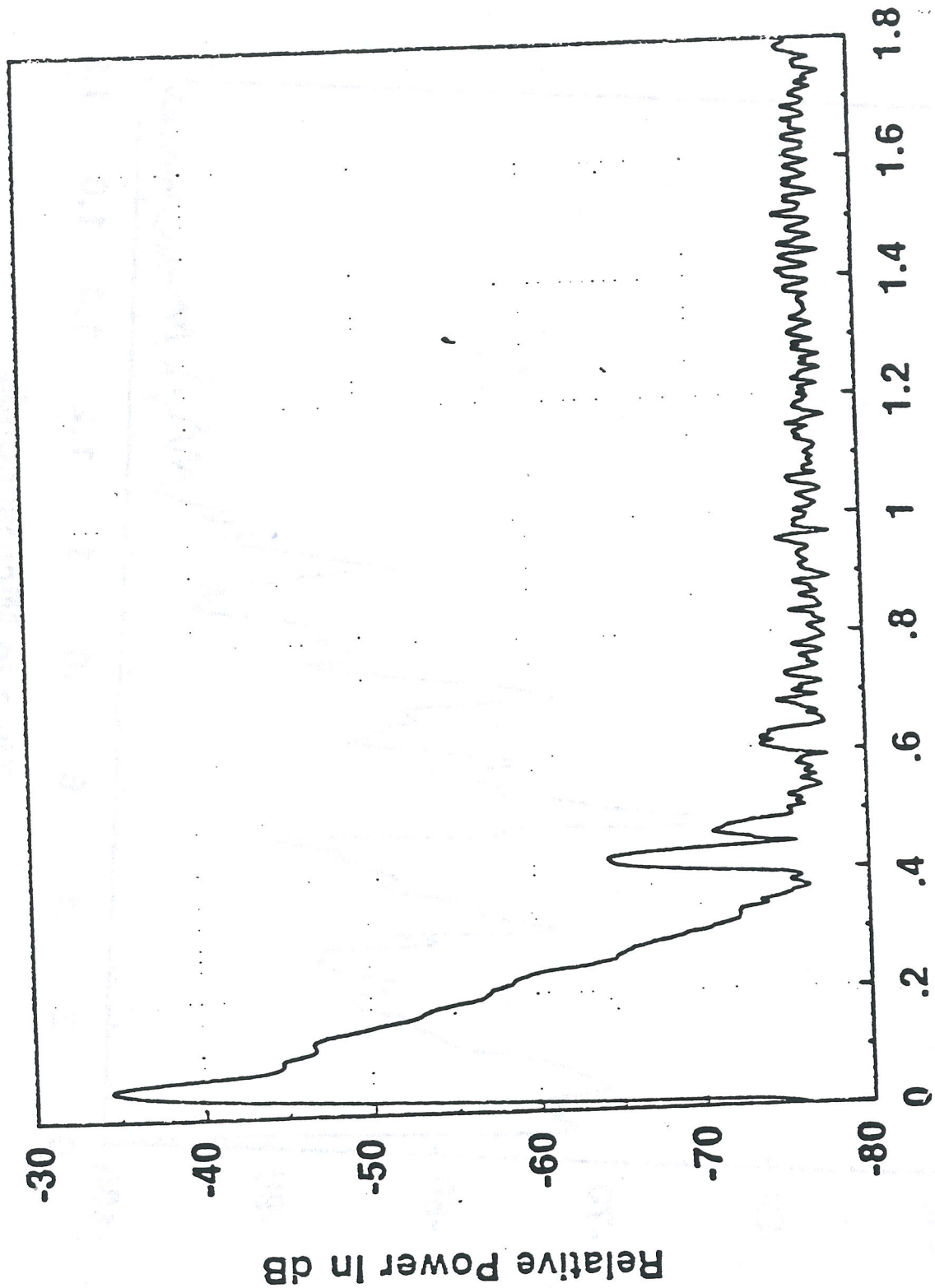
Relative Power In dB
-30
-40
-50
-60
-70
-80
0
.2
.4
.6
.8
1
1.2
1.4
1.6
1.8
Time In Microseconds

FIGURE 1b

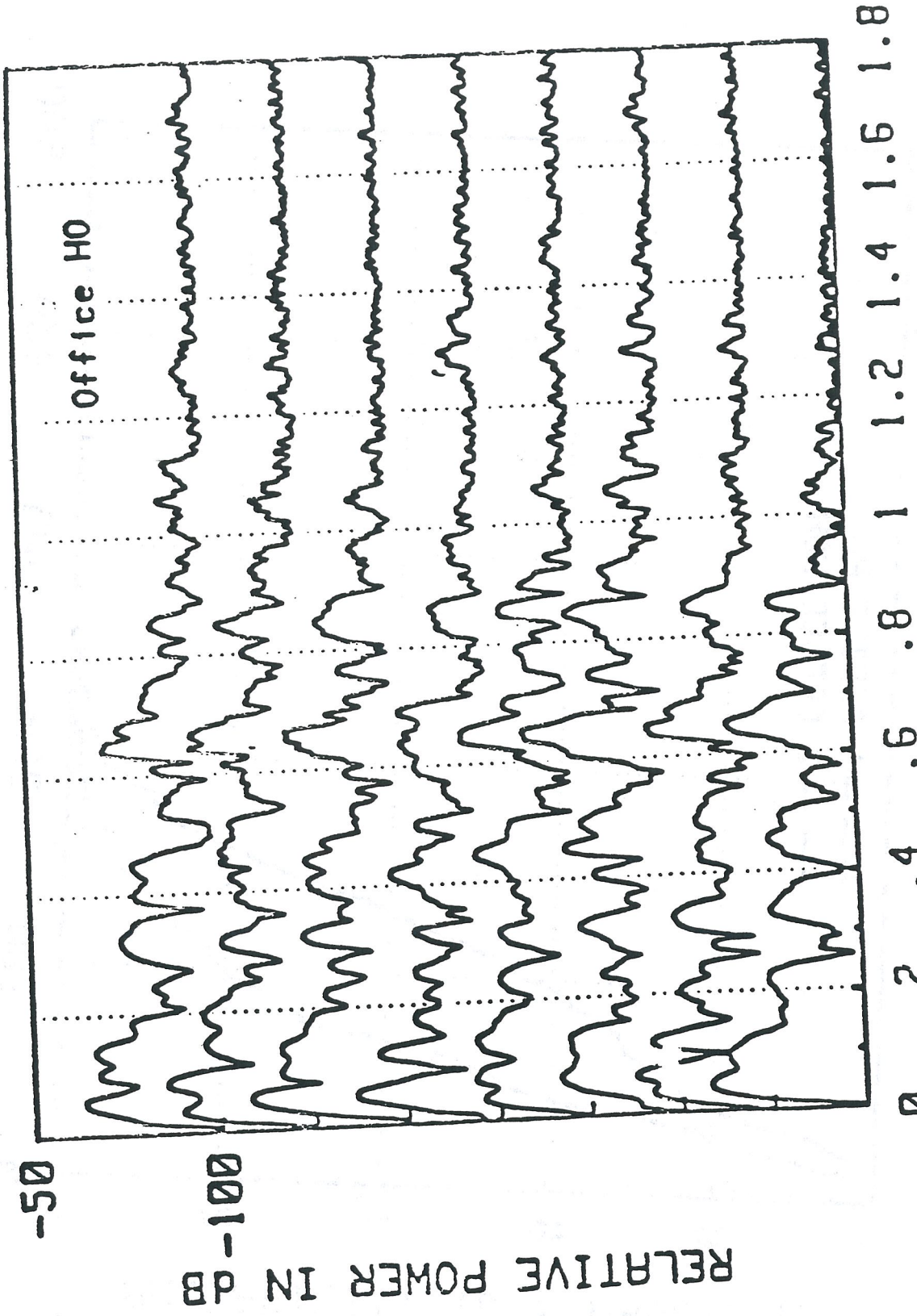
Office HO
-50
-100
RELATIVE POWER IN dB
0
.2
.4
.6
.8
1
1.2
1.4
1.6
1.8
TIME IN MICROSECONDS

FIGURE 2

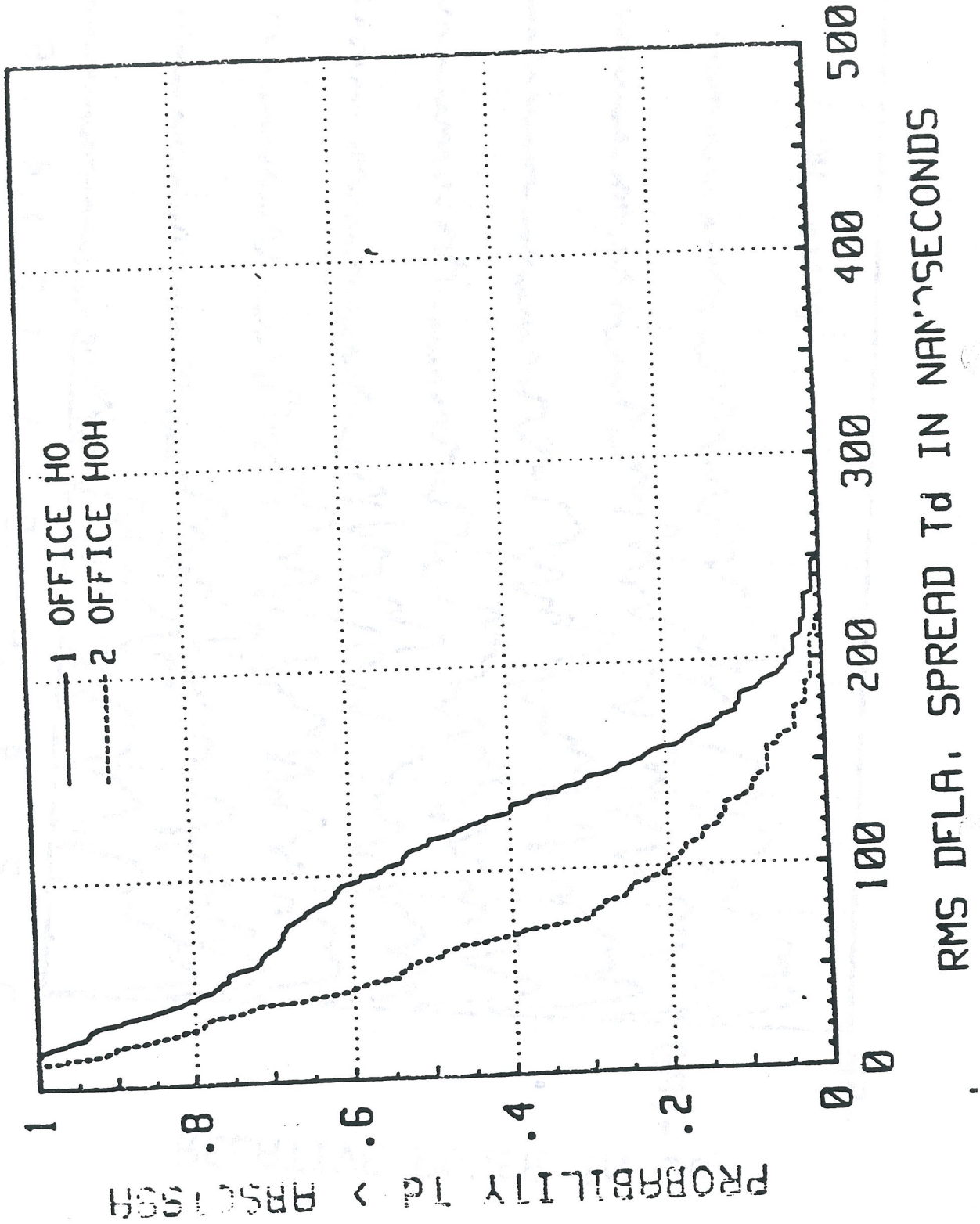
1 OFFICE HO
2 OFFICE HOH
PROBABILITY Td > ABSCISSA
1
.8
.6
.4
.2
0
0
100
200
300
400
500
RMS DFLA, SPREAD Td IN NANOSECONDS

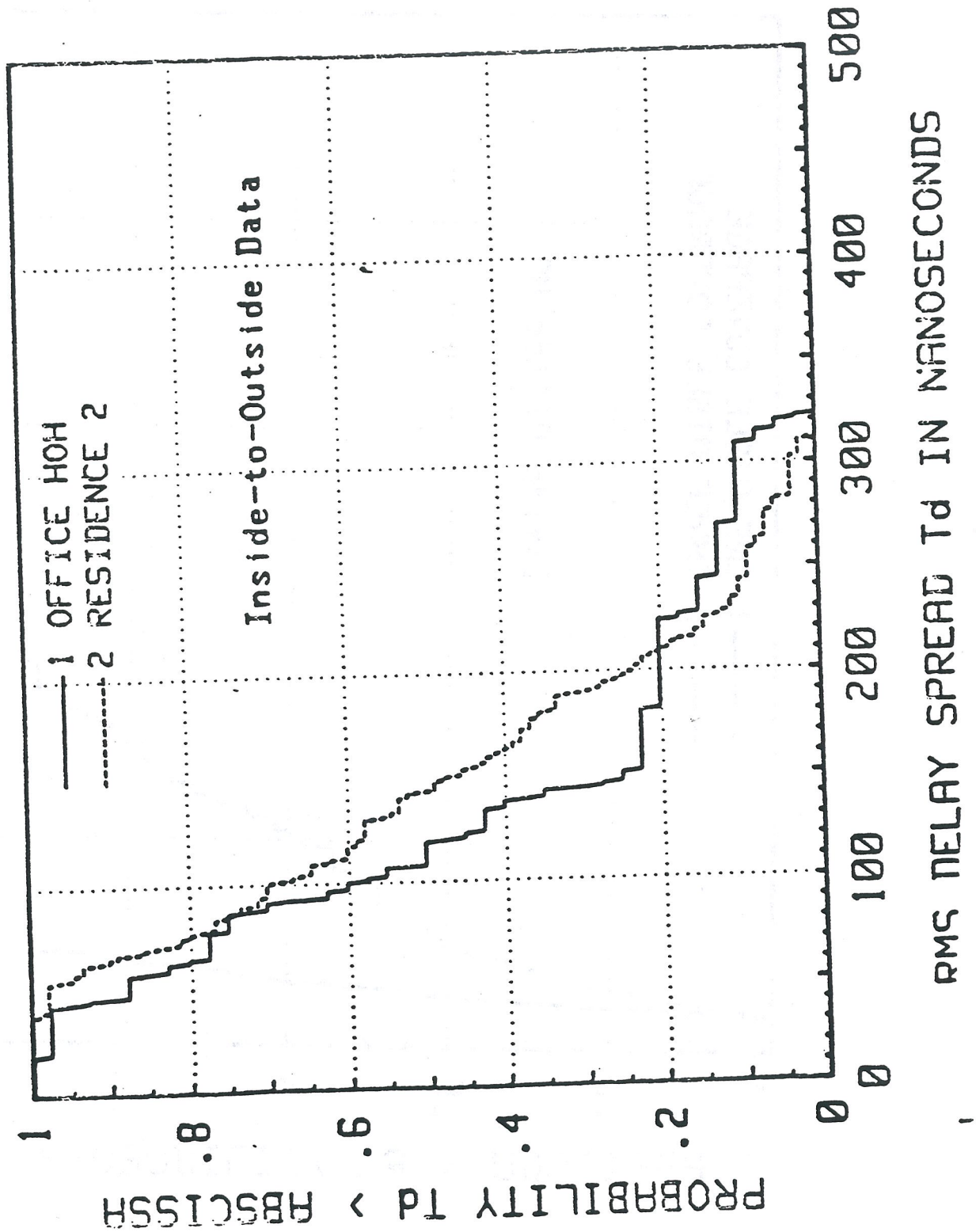
1 OFFICE HOH
2 RESIDENCE 2
Inside-to-Outside Data
PROBABILITY Td > ABSCISSA
1
.8
.6
.4
.2
0
0
100
200
300
400
500
RMS DELAY SPREAD Td IN NANOSECONDS

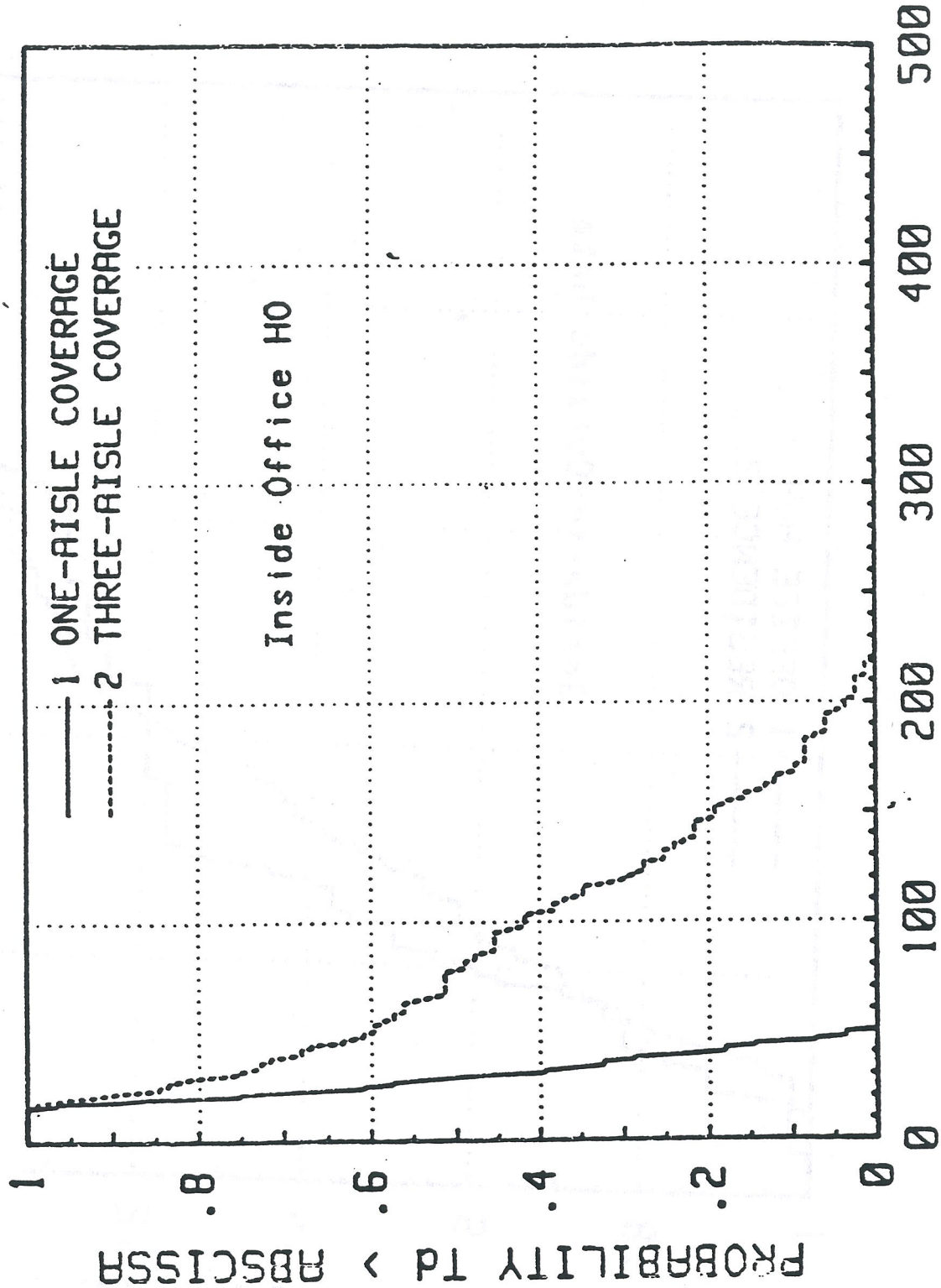
1 ONE-AISLE COVERAGE
2 THREE-AISLE COVERAGE
Inside Office HO
PROBABILITY Td > ABSCISSA
1
.8
.6
.4
.2
0
0
100
200
300
400
500
RMS DELAY SPREAD Td IN NANOSECONDS

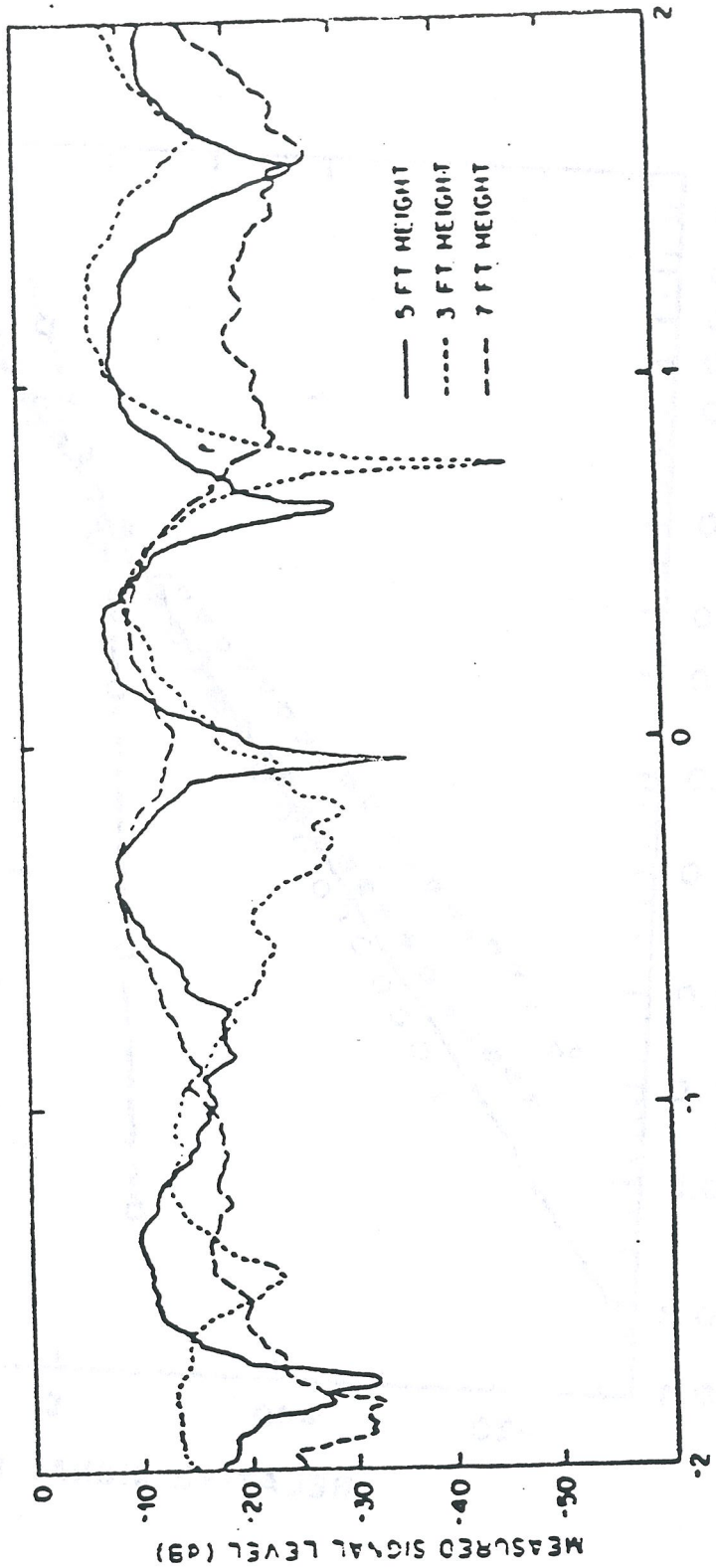
5 FT HEIGHT
3 FT HEIGHT
7 FT HEIGHT
MEASURED SIGNAL LEVEL (dB)
0
-10
-20
-30
-40
-50
-2
-1
0
1
2
DISTANCE (FEET)

FIGURE 6

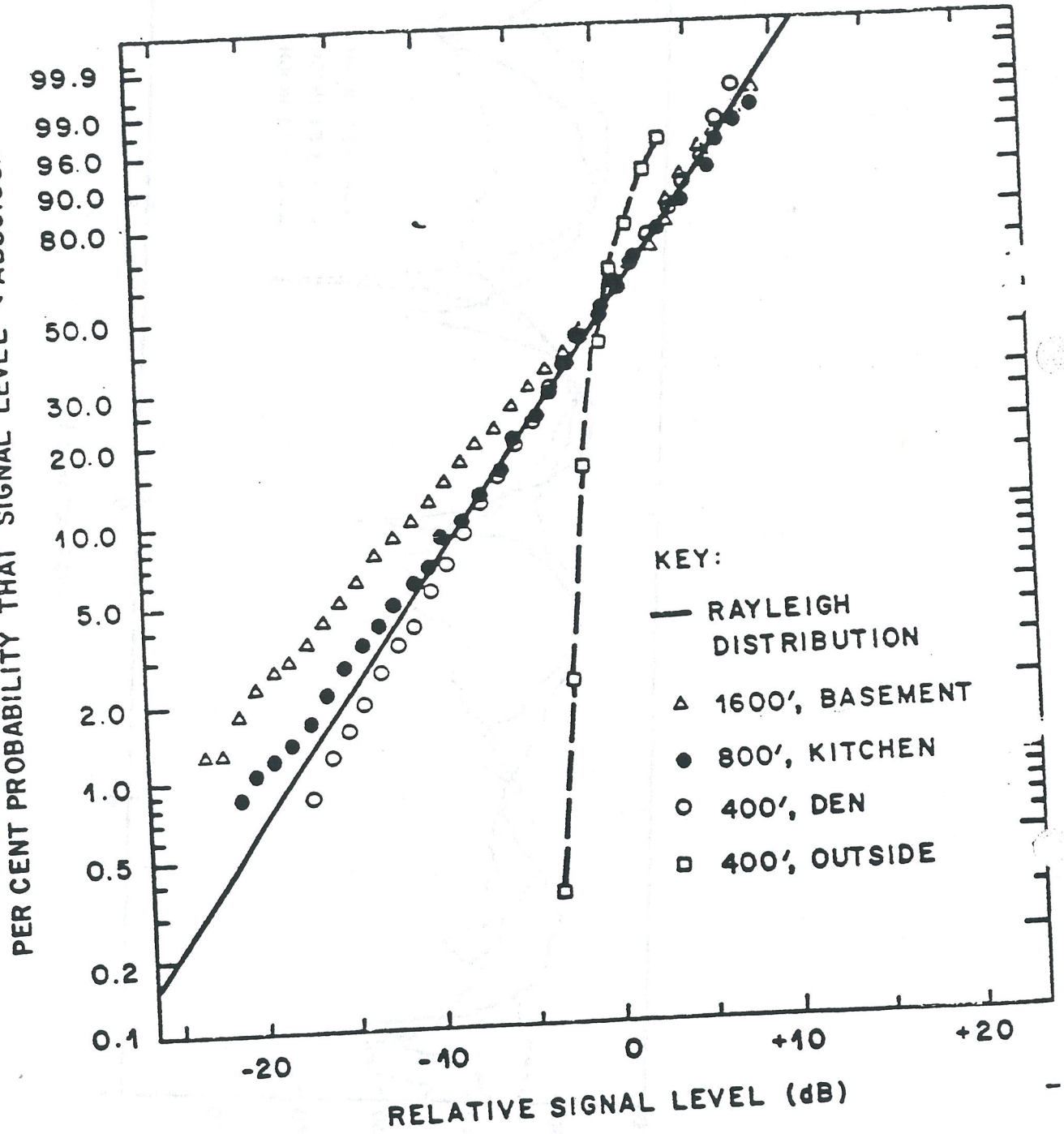
PER CENT PROBABILITY THAT SIGNAL LEVEL < ABSCISSA
99.9
99.0
96.0
90.0
80.0
50.0
30.0
20.0
10.0
5.0
2.0
1.0
0.5
0.2
0.1
-20
-10
0
+10
+20
RELATIVE SIGNAL LEVEL (dB)
KEY:
RAYLEIGH DISTRIBUTION
1600', BASEMENT
800', KITCHEN
400', DEN
400', OUTSIDE

FIGURE 7

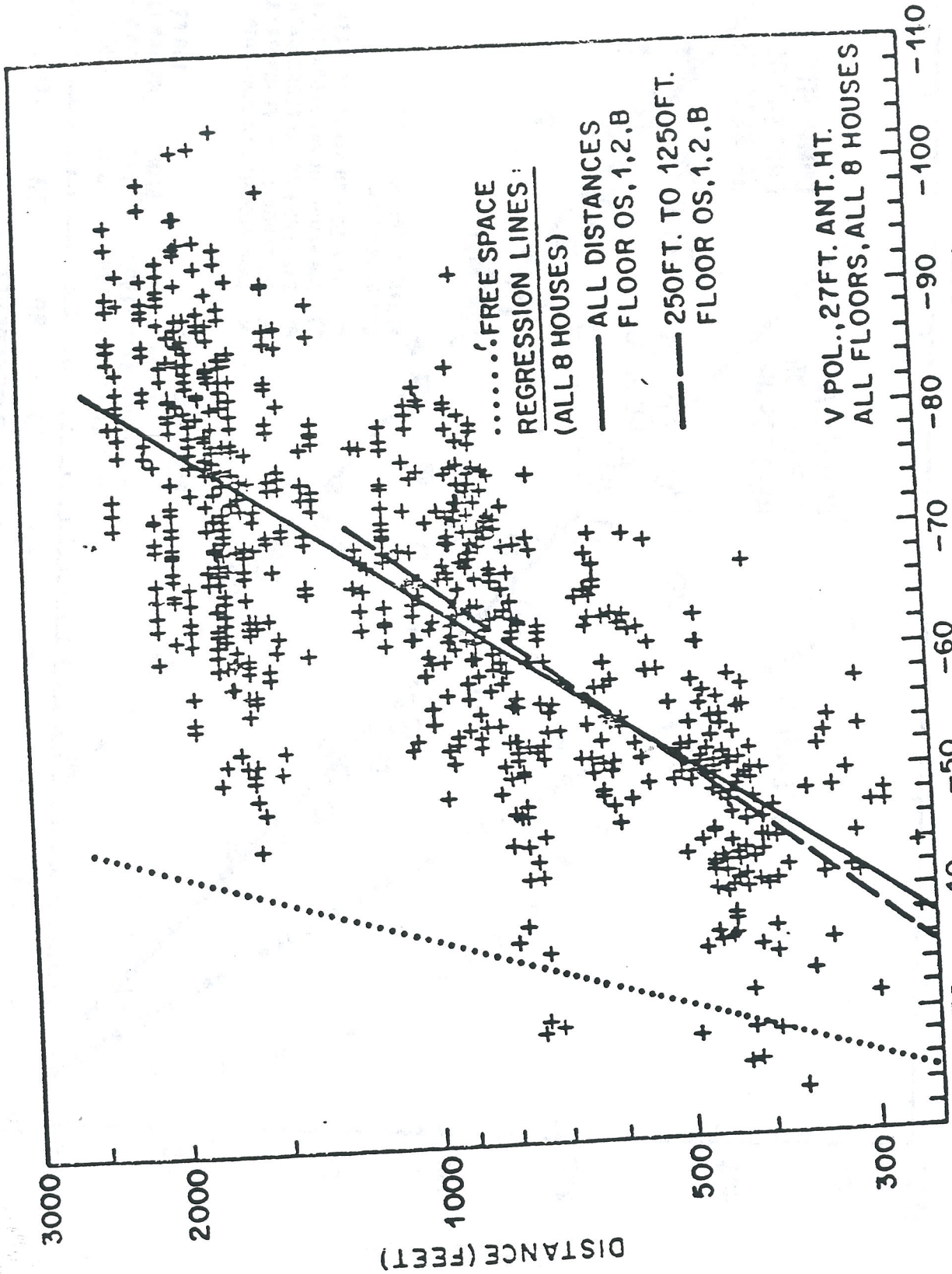
DISTANCE (FEET)
3000
2000
1000
500
300
SIGNAL LEVEL RELATIVE TO REFERENCE (dB)
-20
-30
-40
-50
-60
-70
-80
-90
-100
-110
V POL.,27FT. ANT.HT.
ALL FLOORS, ALL 8 HOUSES
250FT. TO 1250FT.
FLOOR OS,1,2,B
ALL DISTANCES
FLOOR OS,1,2,B
REGRESSION LINES:
(ALL 8 HOUSES)
FREE SPACE

FIGURE 8

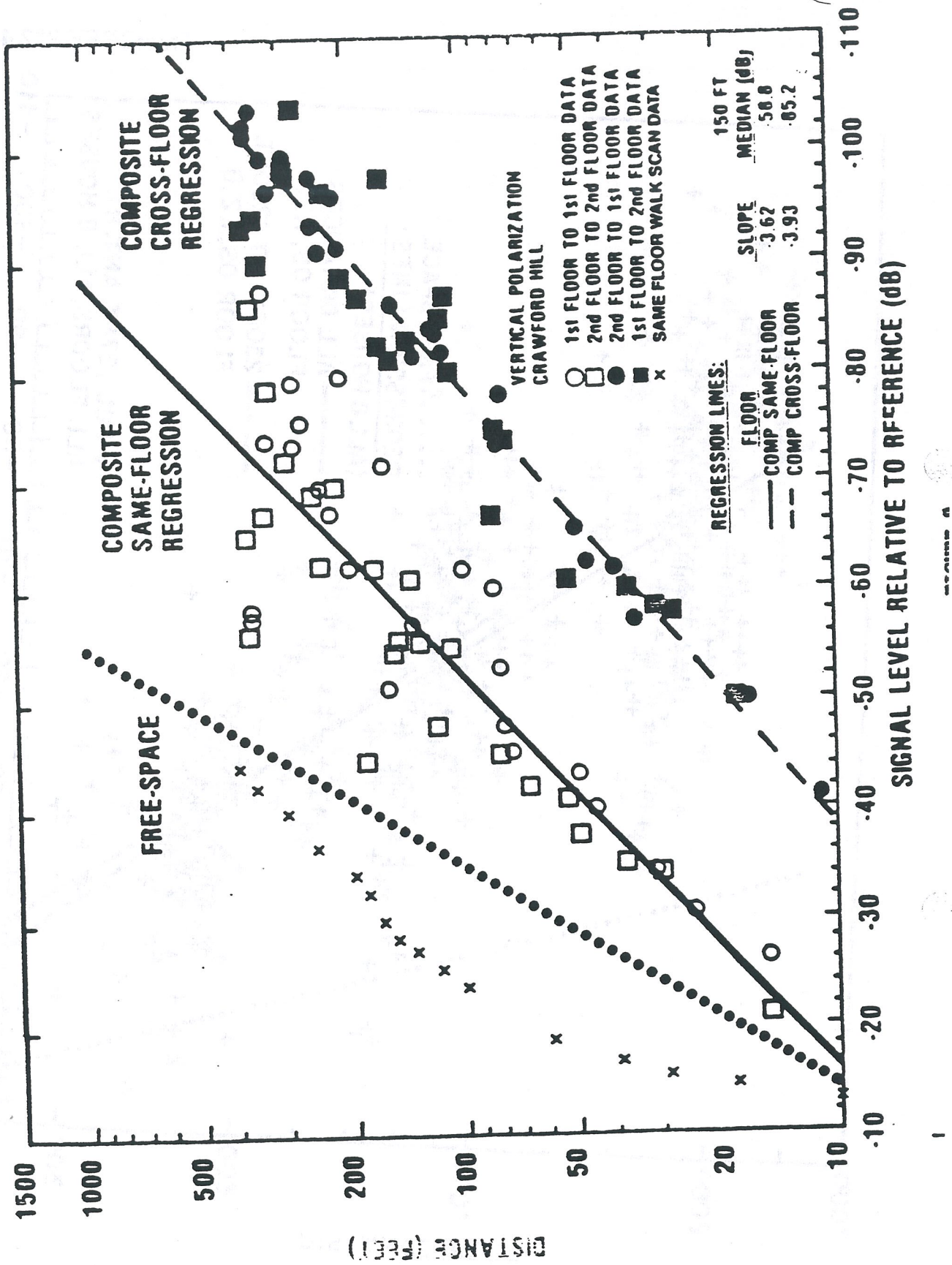
COMPOSITE
CROSS-FLOOR
REGRESSION
COMPOSITE
SAME-FLOOR
REGRESSION
FREE-SPACE
VERTICAL POLARIZATION
CRAWFORD HILL
1st FLOOR TO 1st FLOOR DATA
2nd FLOOR TO 2nd FLOOR DATA
2nd FLOOR TO 1st FLOOR DATA
1st FLOOR TO 2nd FLOOR DATA
SAME FLOOR WALK SCAN DATA
REGRESSION LINES:
FLOOR
SLOPE
150 FT MEDIAN (dB)
COMP SAME-FLOOR
3.62
58.8
COMP CROSS-FLOOR
3.93
65.2
DISTANCE (FEET)
1500
1000
500
200
100
50
20
10
·10
·20
·30
·40
·50
·60
·70
·80
·90
·100
·110
SIGNAL LEVEL RELATIVE TO REFERENCE (dB)

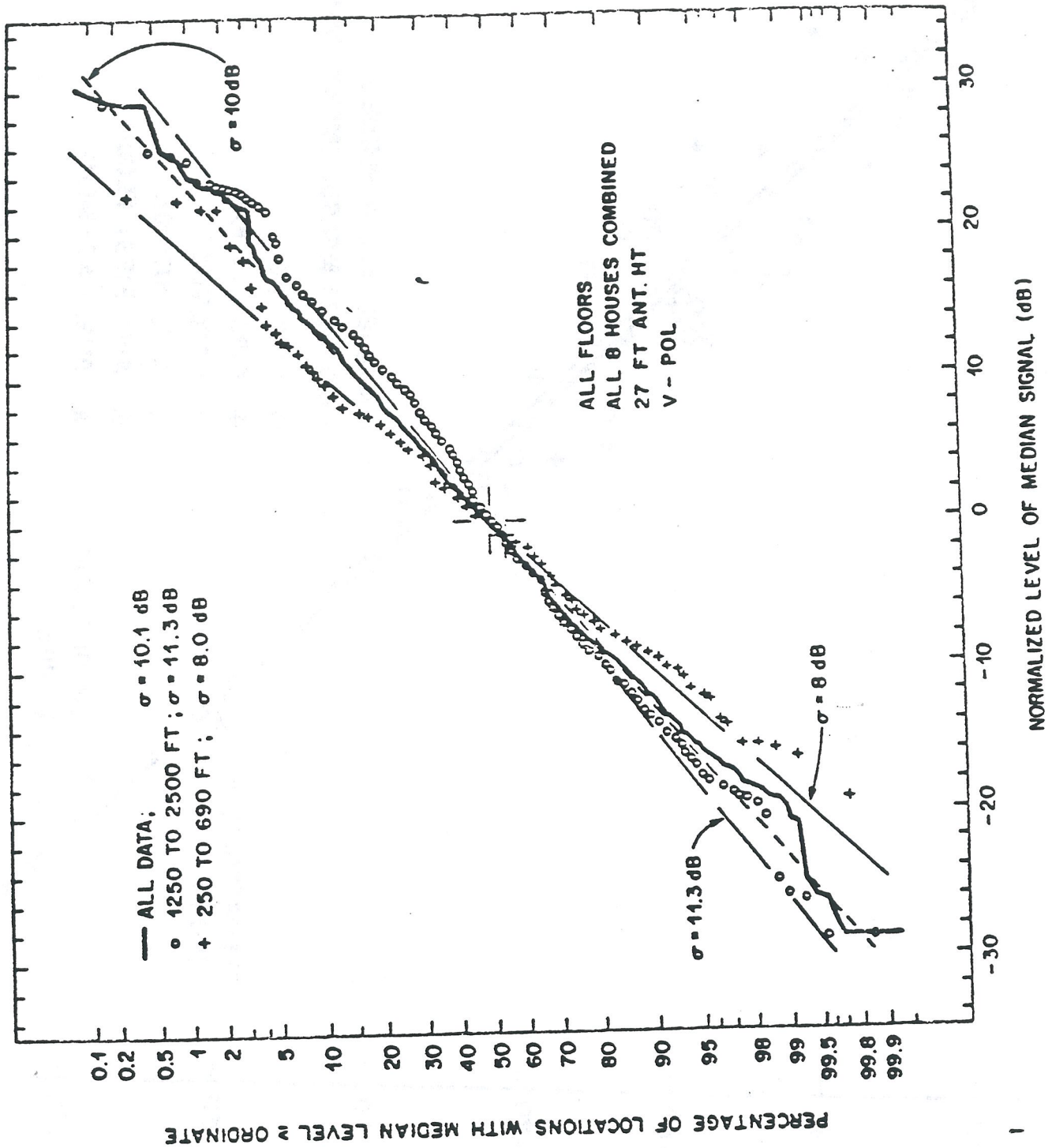
ALL DATA; σ = 10.1 dB
o 1250 TO 2500 FT ; σ = 11.3 dB
+ 250 TO 690 FT ; σ = 8.0 dB
ALL FLOORS
ALL 8 HOUSES COMBINED
27 FT ANT. HT
V - POL
σ = 10 dB
σ = 11.3 dB
σ = 8 dB
0.1
0.2
0.5
1
2
5
10
20
30
40
50
60
70
80
90
95
98
99
99.5
99.8
99.9
30
20
10
0
-10
-20
-30
PERCENTAGE OF LOCATIONS WITH MEDIAN LEVEL ≥ ORDINATE
NORMALIZED LEVEL OF MEDIAN SIGNAL (dB)

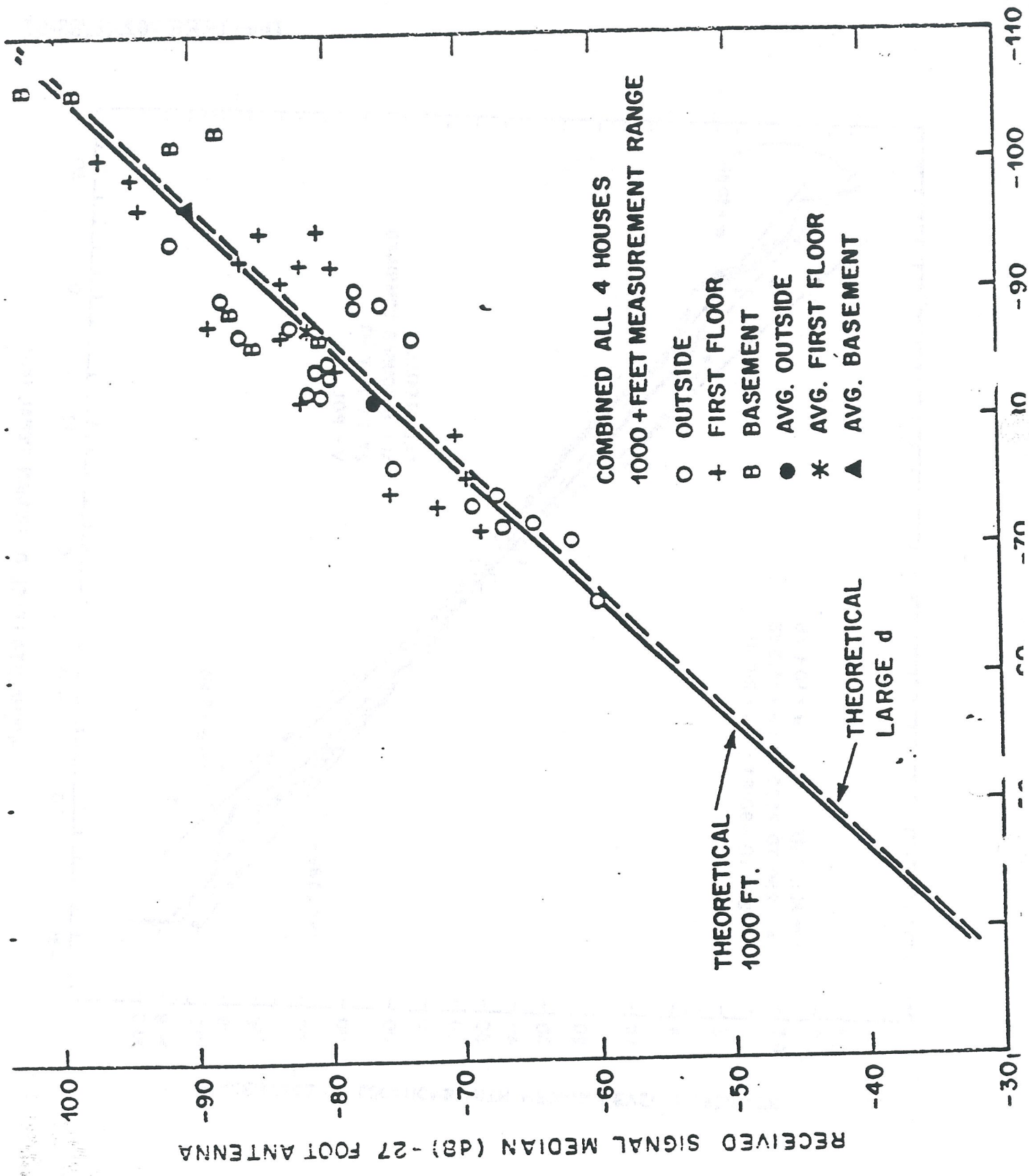
COMBINED ALL 4 HOUSES
1000+FEET MEASUREMENT RANGE
O OUTSIDE
+ FIRST FLOOR
B BASEMENT
● AVG. OUTSIDE
* AVG. FIRST FLOOR
▲ AVG. BASEMENT
THEORETICAL
1000 FT.
THEORETICAL
LARGE d
RECEIVED SIGNAL MEDIAN (dB) -27 FOOT ANTENNA
-30
-40
-50
-60
-70
-80
-90
100
-110

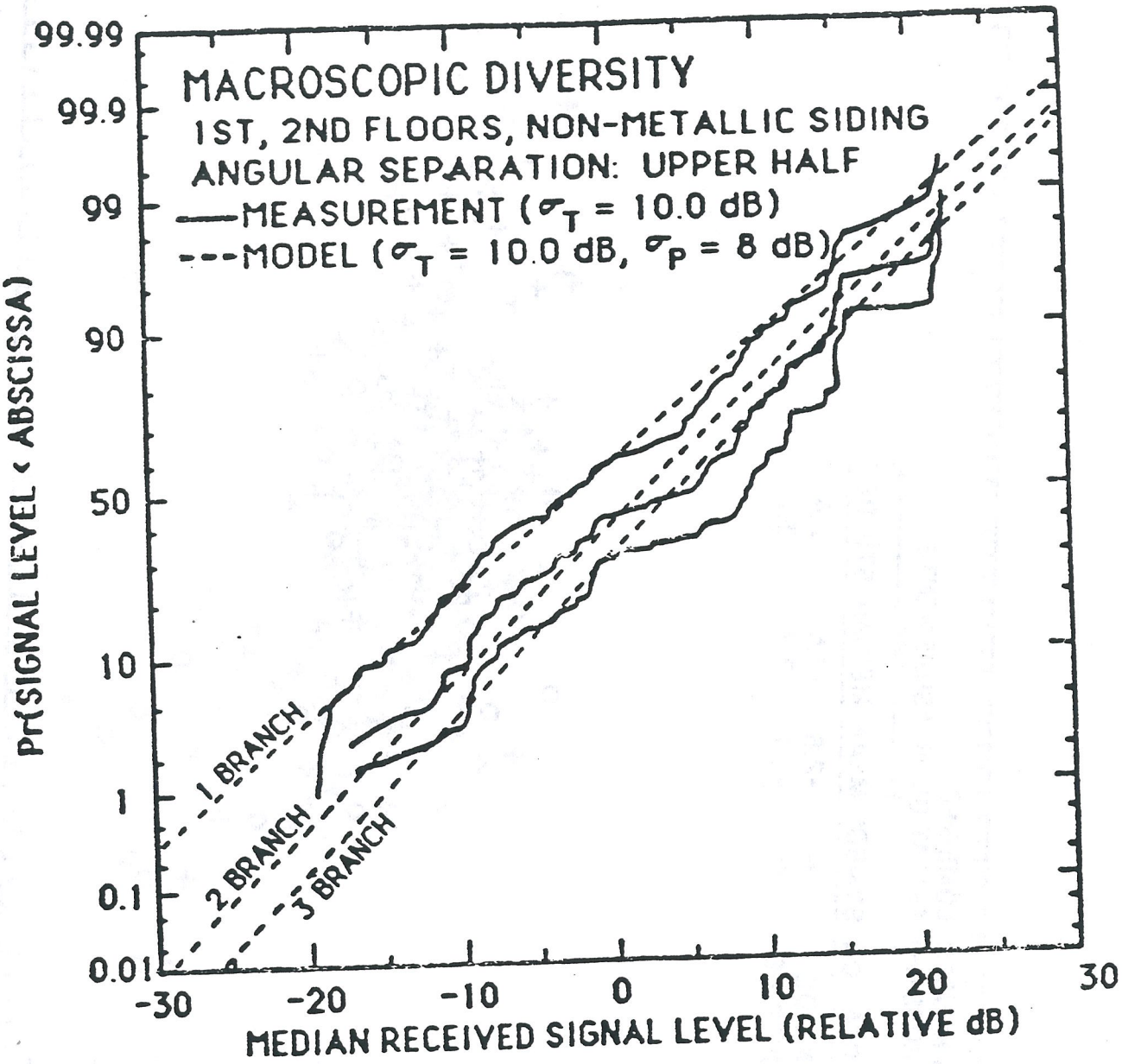
MACROSCOPIC DIVERSITY
1ST, 2ND FLOORS, NON-METALLIC SIDING
ANGULAR SEPARATION: UPPER HALF
—MEASUREMENT (σ_T = 10.0 dB)
---MODEL (σ_T = 10.0 dB, σ_P = 8 dB)
Pr(SIGNAL LEVEL < ABSCISSA)
99.99
99.9
99
90
50
10
1
0.1
0.01
1 BRANCH
2 BRANCH
3 BRANCH
-30
-20
-10
0
10
20
30
MEDIAN RECEIVED SIGNAL LEVEL (RELATIVE dB)

FIGURE 12

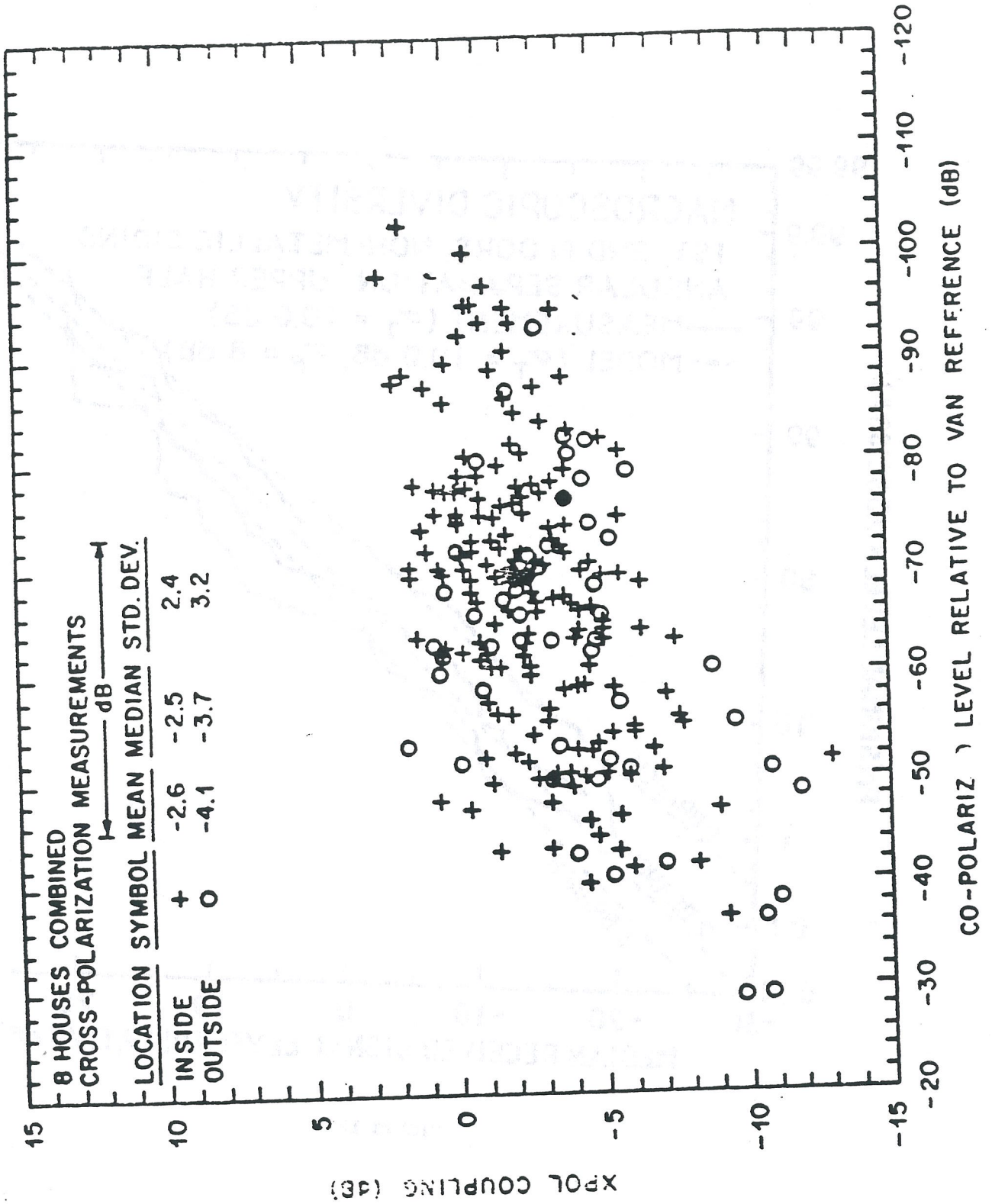
8 HOUSES COMBINED
CROSS-POLARIZATION MEASUREMENTS
dB
LOCATION SYMBOL MEAN MEDIAN STD. DEV.
INSIDE + -2.6 -2.5 2.4
OUTSIDE O -4.1 -3.7 3.2
XPOL COUPLING (dB)
15
10
5
0
-5
-10
-15
-120
-110
-100
-90
-80
-70
-60
-50
-40
-30
-20
CO-POLARIZ) LEVEL RELATIVE TO VAN REFFRENCE (dB)

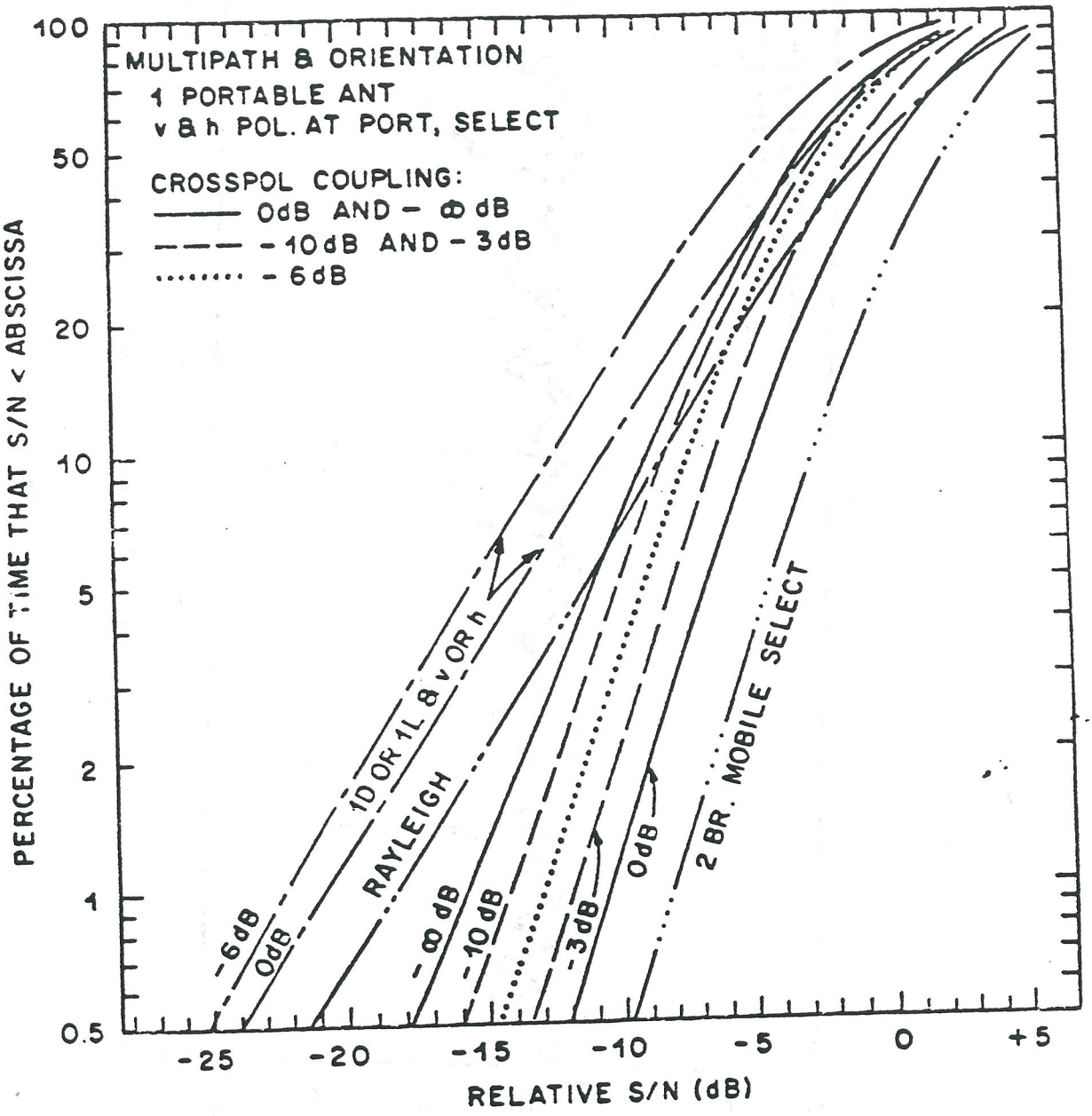
MULTIPATH & ORIENTATION
1 PORTABLE ANT
v & h POL. AT PORT, SELECT
CROSSPOL COUPLING:
0dB AND - ∞ dB
-10dB AND -3dB
-6dB
PERCENTAGE OF TIME THAT S/N < ABSCISSA
100
50
20
10
5
2
1
0.5
-25
-20
-15
-10
-5
0
+5
RELATIVE S/N (dB)
1D OR 1L & v OR h
RAYLEIGH
-6dB
0dB
-∞dB
-10dB
-3dB
0dB
2 BR. MOBILE SELECT

FIGURE 14

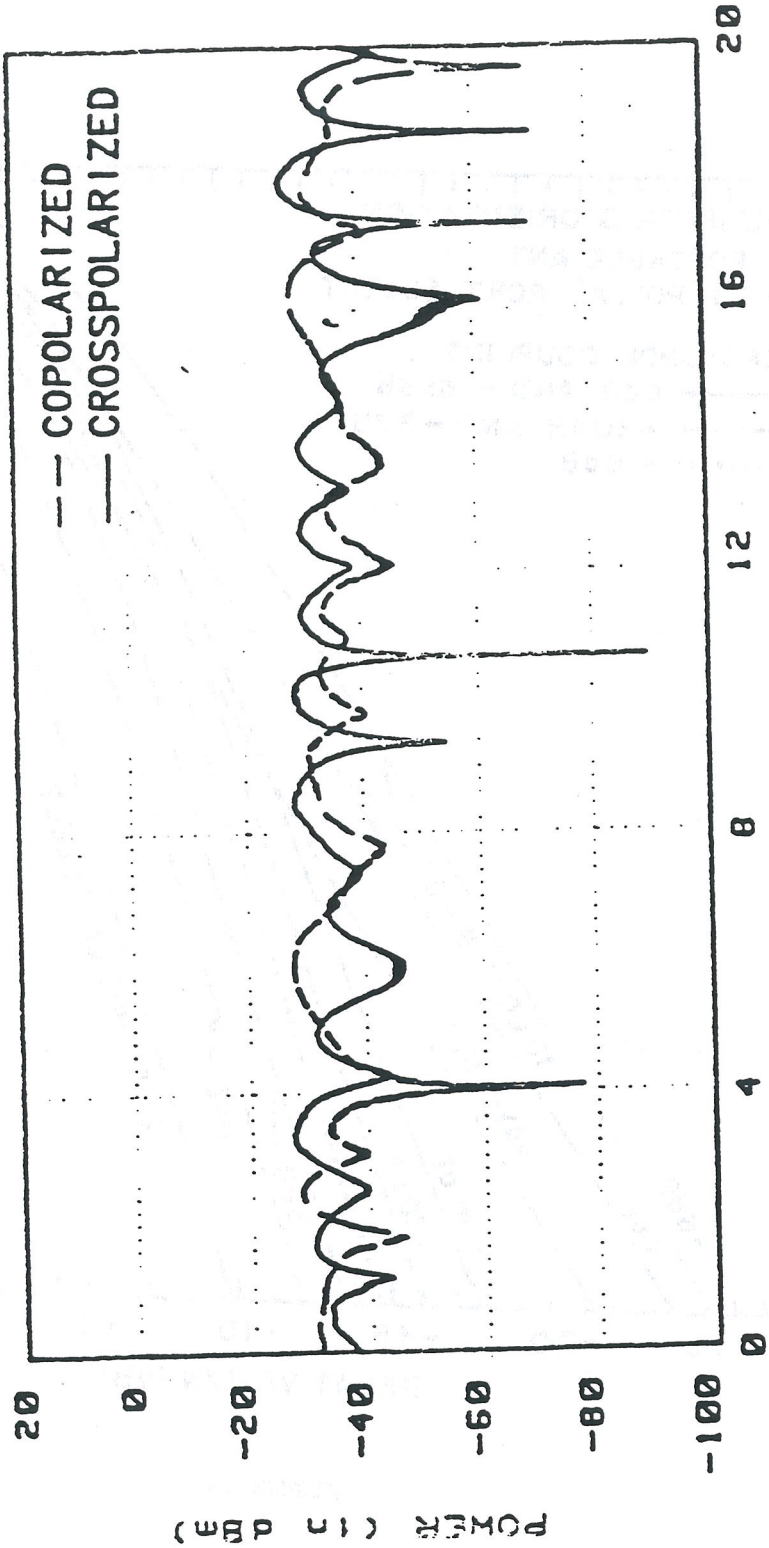
COPOLARIZED
CROSSPOLARIZED
20
0
-20
-40
-60
-80
-100
0
4
8
12
16
20
TIME (in secs)
POWER (in dBm)

FIGURE 15

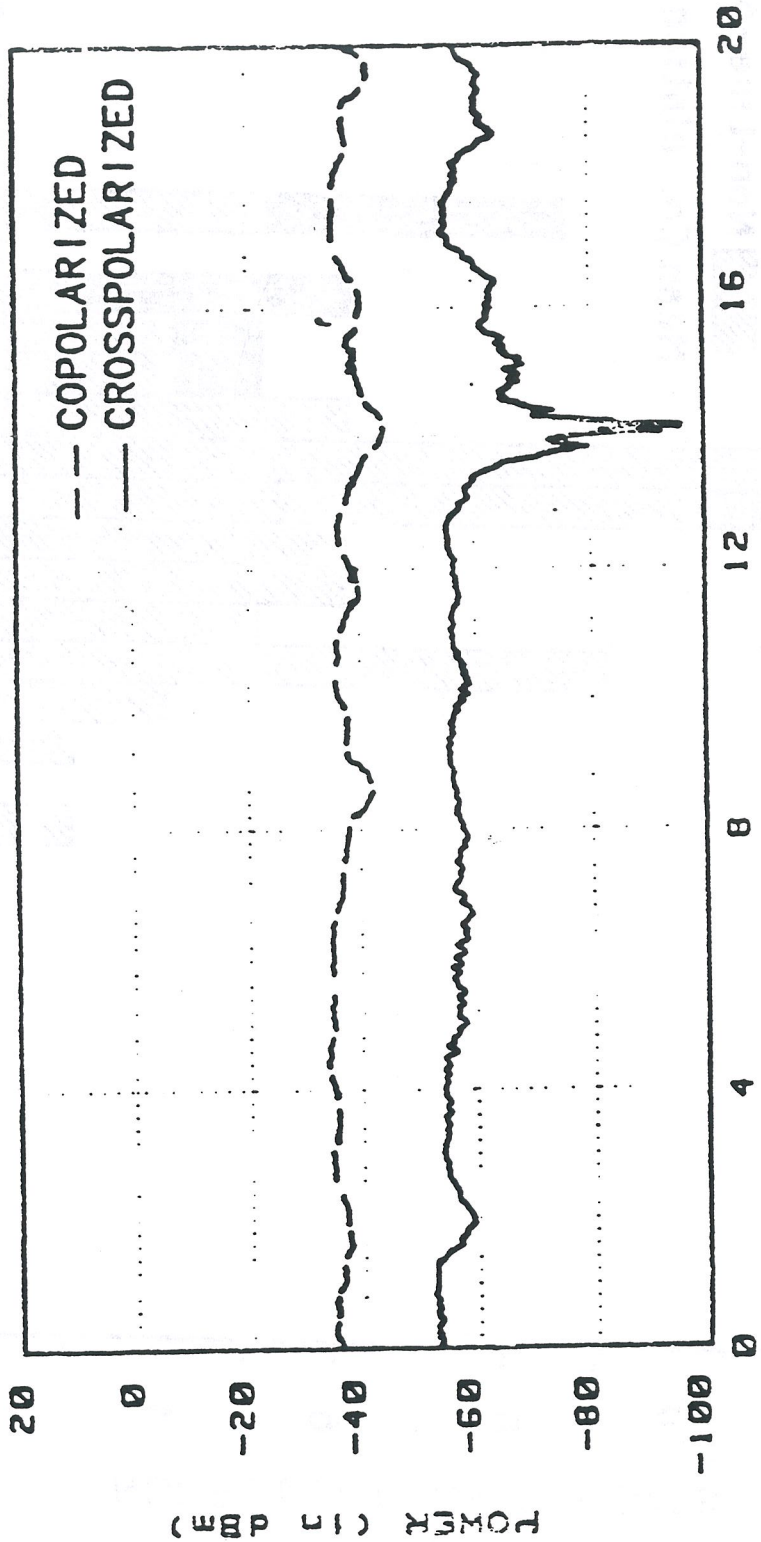
COPOLARIZED
CROSSPOLARIZED
POWER (in dBm)
20
0
-20
-40
-60
-80
-100
0
4
8
12
16
20
TIME (in secs)

FIGURE 16

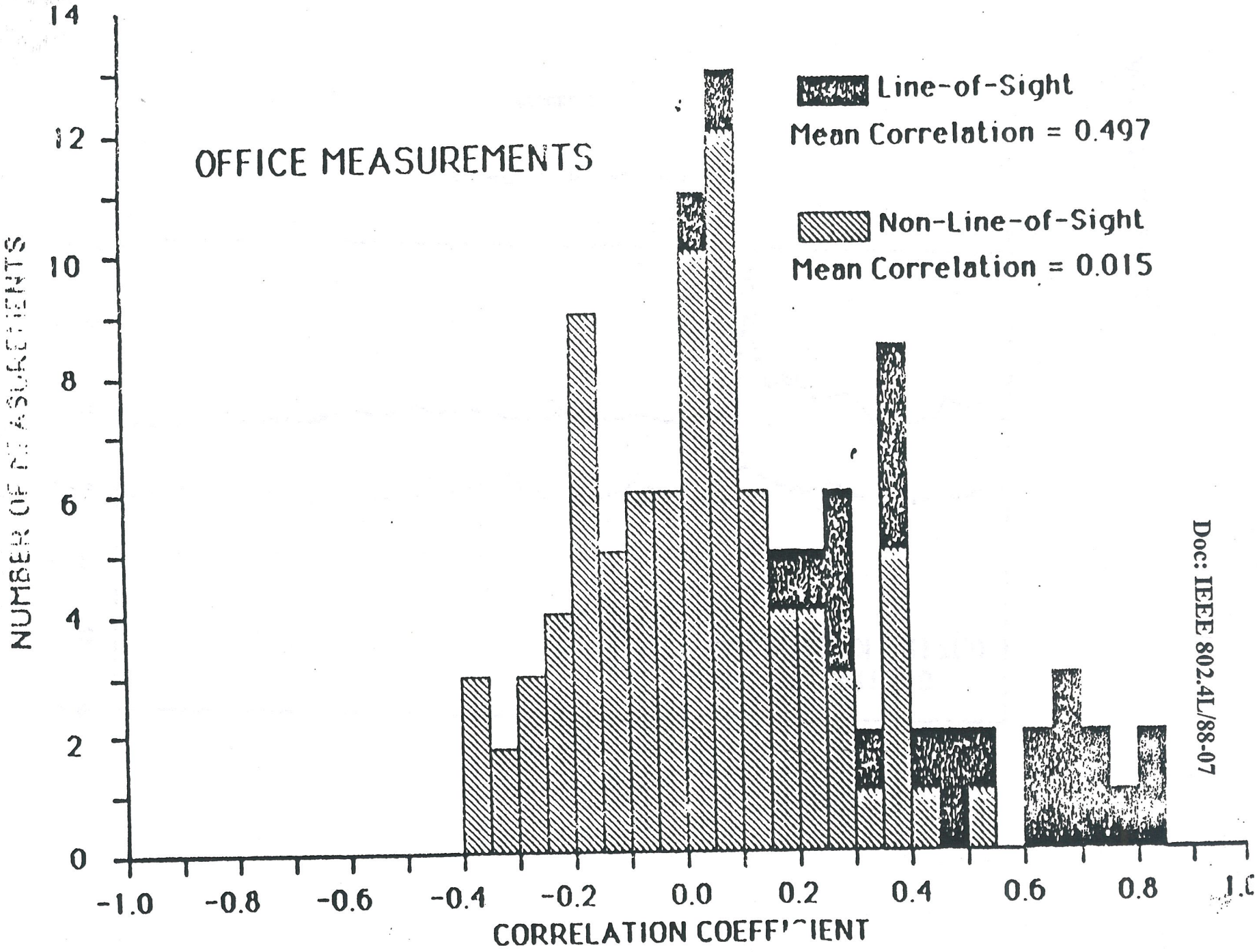

Doc: IEEE 802.4L/88-07